REPORT DOCUMENTATION PAGE

Form Approved
OMB No. 0704-0188

1. REPORT DATE *(DD-MM-YYYY)*	2. REPORT TYPE	3. DATES COVERED *(From - To)*
10-08-06	Final Report	July 21, 2003 to July 10, 2006

4. TITLE AND SUBTITLE

Multiple Strategy Bio-Detection Sensor Platforms Made from Carbon and Polymer Materials

5a. CONTRACT NUMBER

N/A

5b. GRANT NUMBER

N00014-03-1-0893

5c. PROGRAM ELEMENT NUMBER

N/A

6. AUTHOR(S)

Dr. Ryan Giedd, PI
Dr. Kartik Ghosh, Co-PI
Mr. Matt Curry, Co-PI
Mr. Rishi Patel, Co-PI
Dr. Paul Durham, Co-PI
Dr. Xuliang Han, PI of Brewer Science, Inc. Subaward
Dr. Pat Kinlen, PI of Crosslink, Inc. Subaward

5d. PROJECT NUMBER

N/A

5e. TASK NUMBER

I, II, III, IV

5f. WORK UNIT NUMBER

N/A

7. PERFORMING ORGANIZATION NAME(S) AND ADDRESS(ES)

Center for Applied Science & Engineering
Missouri State University
901 South National Avenue
Springfield, MO 65897

8. PERFORMING ORGANIZATION REPORT NUMBER

#6

9. SPONSORING/MONITORING AGENCY NAME(S) AND ADDRESS(ES)

Office of Naval Research
230 South Dearborn, Room 380
Chicago, IL 60604-1595

10. SPONSOR/MONITOR'S ACRONYM(S)

ONR

11. SPONSOR/MONITOR'S REPORT NUMBER(S)

N/A

12. DISTRIBUTION/AVAILABILITY STATEMENT

Approved for Public Release, Distribution is Unlimited

13. SUPPLEMENTARY NOTES

Research in collaboration with Brewer Science, Inc. (Rolla, MO) and Crosslink, Inc. (St. Louis, MO)

14. ABSTRACT

This project involved the development of a biosensor based on a carbon and polymer micro-electromechanical system (CPMEMS) array comprised of micro-bridges to allow multiple bio-detection strategies. It would have the advantages of being autonomous, with quick response and high selectivity, as well as low cost. The multiple-strategy bio-detection platform will include systems that were developed by the Missouri State University and systems that were developed by our corporate partners and collaborators; Brewer Science, Inc. and Crosslink, Inc. One platform strategy is the use of a chemical release electro-active polymer to perform sense and release experiments. In conjunction to a broad-band biological/chemical detection system, a bio-collection system was also developed. The focus of this project was to produce a generalized system or substrate of transducers that can be applied to many emerging bio-detection strategies. We will demonstrate feasibility with well known methods of detection as well as many other new detection strategies that can be accommodated on this platform.

15. SUBJECT TERMS

CPMEMS, Ion Implantation, Active Sense and Release (conducting polymer), Antibodies, Oligonucleotides, Bio-collection.

16. SECURITY CLASSIFICATION OF:			17. LIMITATION OF ABSTRACT	18. NUMBER OF PAGES	19a. NAME OF RESPONSIBLE PERSON
a. REPORT	b. ABSTRACT	c. THIS PAGE			Ryan Giedd, Ph.D.
N/A	N/A	N/A	UU	82	19b. TELEPHONE NUMBER *(Include area code)* (417) 836-5279

Multiple Strategy Bio-Detection Sensor Platforms

Made from Carbon and Polymer Materials

Final Report

ONR Award No. N00014-03-1-0893

for the work performed an July 21, 2003 – July 10, 2006

Dr. Ryan Giedd, PI
Dr. Kartik Ghosh, Co-PI
Mr. Matt Curry, Co-PI
Mr. Rishi Patel, Co-PI
Dr. Paul Durham, Co-PI
Dr. Xuliang Han, PI of Brewer Science Inc. Subaward
Dr. Pat Kinlen, PI of Crosslink Polymer Research Inc. Subaward

Center for Applied Science & Engineering
Missouri State University
901 South National Avenue
Springfield MO, 65897

Biosensors made from Carbon and Polymer Composite Micro-electromechanical Systems

Table of Contents

1.3 Statement of Work

1.3.1 Abstract

This project involved the development of a biosensor based on a carbon and polymer micro-electromechanical system (CPMEMS). The design of the system allowed for incorporation of multiple bio-detection strategies with a number of different biological detection elements such as proteins, antibodies, or oligonucleotides. The system was designed such that an array of CPMEMS structures would serve as the multiple strategy bio-detection sensor platform comprised of micro-bridges. It would have the advantages of being autonomous, with quick response and high selectivity, as well as low cost.

The CPMEMS pixels that are incorporated in this broadband platform have piezoresistive properties that are used as the transducer, which offers label free detection of biological or chemical reactions. For instance, a biochemical reaction on the piezoresistive (pixel) surface can be monitored as a surface deformation change or a change in the vibrational properties. The change in surface properties is then converted into an electrical signal through the piezoresistive material. This electrical signal is analyzed by underlying CMOS circuits and monitored by simple instrumentation. The change in surface stress of the CPMEMS structure is related to the change of Gibbs' free energy during the molecular interaction between the target antigen and the 'detector film' [1]. Therefore the pixels can be used for detection of a wide variety of bacterial, viral, and toxic agents.

The multiple-strategy bio-detection platform will include systems that were developed by the Missouri State University and systems that were developed by our corporate partners and collaborators; Brewer Science, Inc (BSI), located in Rolla, MO and Crosslink, Inc located in St. Louis, MO. One platform strategy is the use of a chemical release electro-active polymer to perform sense and release experiments. For example, if a certain experiment yields a positive result that is not sufficiently selective, a polymer element may be electrically biased to release a specific drug or chemical (e.g. fluorescein tags) to bind with the antigen for increased selectivity. Multiple experiments can be accommodated on the same bio-detection sensor platform. In conjunction to a broad-band biological/chemical detection system, a bio-collection system was also developed. A unique collection system was designed to capture antigens in the air or water, and perform sample particle size separation and concentration using an ultrasonic cracking technique.

This biosensor broadband platform approach can serve as a foundation for further development, and as a starting point for new technologies. The focus of this project was to produce a generalized system or substrate of transducers that can be applied to many emerging bio-detection strategies. We will demonstrate feasibility with well known methods of detection as well as many other new detection strategies that can be accommodated on this platform.

1.3.2 Discussion

1.3.2.1 General Passive Technology

To create the link between the biological world and the MEMS electronics world to develop a novel biosensor, a metal and carbon/polymer-based material was utilized to develop the carbon and polymer MEMS or CPMEMS devices that would bridge the two worlds. The significant advantage of using CPMEMS structures instead of traditional Si based MEMS structures is the known biocompatibility of the CPMEMS surface [2]. These CPMEMS structures can be easily fabricated using standard microlithography techniques.

The CPMEMS devices were fabricated using a carbon/polymer/metal cluster composition with electronic properties that are critically dependent on vibrations [3] or surface acoustic waves (SAW) [4]. A study was performed using the polymer poly(styrene-co-acrylonitrile) (PSA) and the metal gold (Au). A set of varying-thickness Au-films were thermally evaporated onto poly(styrene-co-acrylonitrile) thin film surfaces. The Au/PSA bi-layer targets were then implanted with 50 keV N+ ions to a dose of $1x10^{16}$ ions/cm^2. The electrical conductivity, film microstructure, and elemental diffusion/mixing within the Au/PSA interface were then evaluated. Electrical conductivity measurements of the implanted Au/PSA thin films show a sharp percolation behavior versus the pre-implant Au-film thickness with a percolation threshold near a nominal Au thickness of 44 Å.

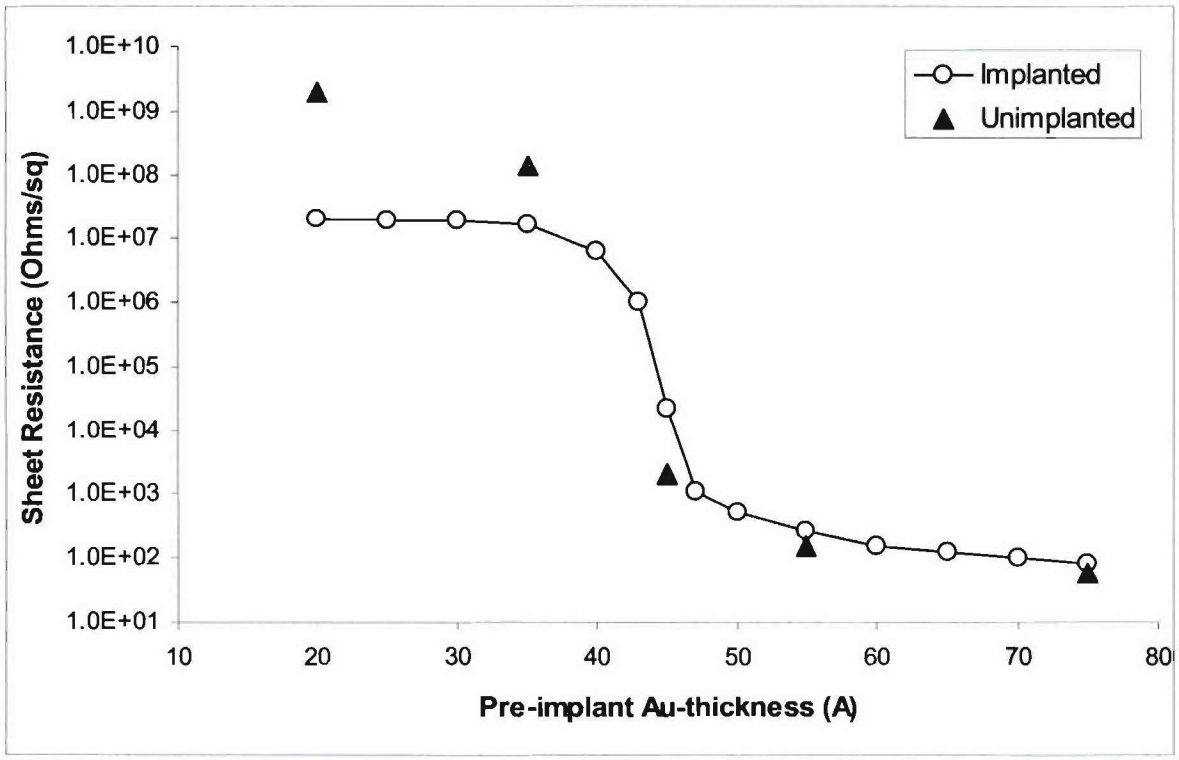

Figure 1: Sheet resistance vs. pre-implant Au-thickness

Figure 1 above, is a comparison of sheet resistance (Ω/sq) as a function of the pre-implant Au-thickness before and after ion implantation. The sharp transition between 40 Å and 50 Å of Au pre-implant where the sheet resistance decreases over four orders of magnitude is significant because, it is here in the sharp percolation region where the material has the appropriate microstructure that is ideal for sensitivity to vibration and will be useful for SAW devices.

Figure 2 shows the relative resistance change as a function of temperature for the implanted Au/PSA bi-layer thin films. The thicknesses below the transition exhibit semiconductor-like curves and the thicknesses above the transition have metallic curves, which again reinforce that the material is moving through a critical transition as the pre-implant thickness of gold is increased. Because of the microstructure and hopping conduction mechanism, that is highly sensitive to the relative proximity of the hop sites [3], these materials are sensitive to vibration and look very promising for sensors using surface acoustic waves.

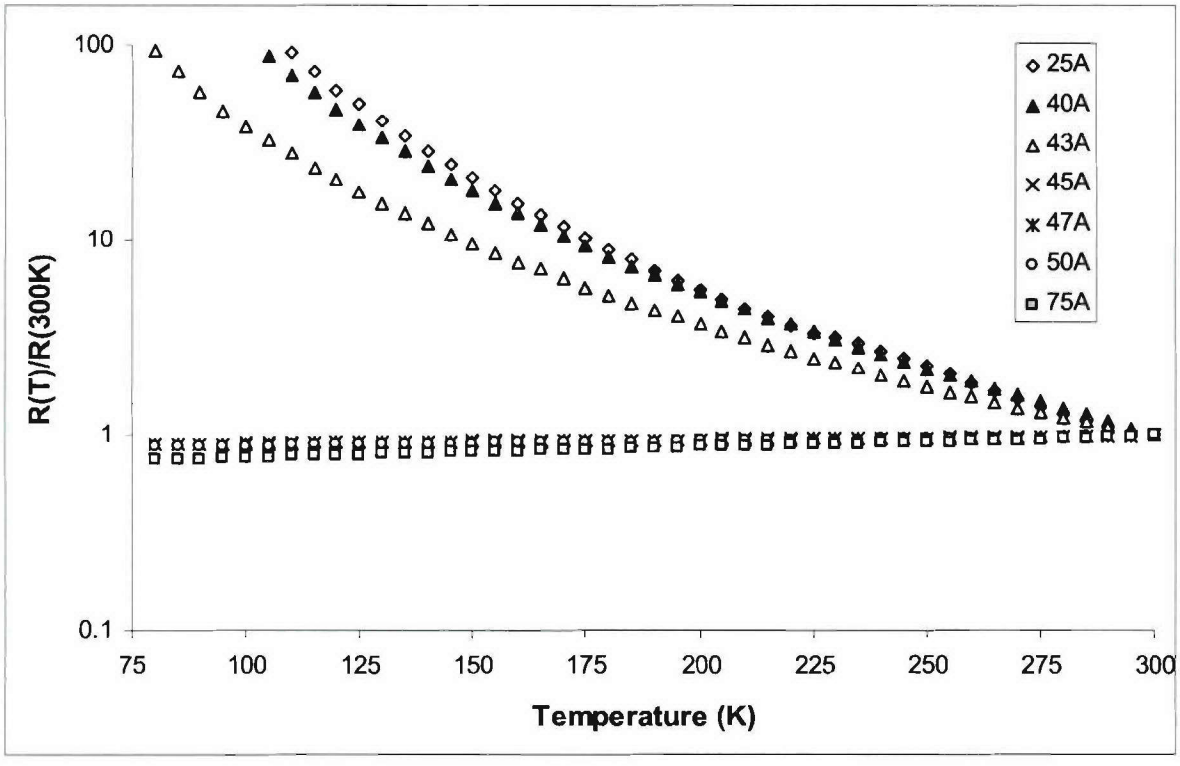

Figure 2: Relative resistance change as a function of temperature

Two ion beam analysis techniques; Rutherford Backscattering Spectrometry (RBS) and Elastic Recoil Detection (ERD) were used to measure Au and H-content, respectively, in the targets. Figure 3 (top), shows the measured H-content in the Au/PSA films as a function of the pre-implant Au-thickness. The results show that ion implantation liberated H-content in the PSA ($C_{11}H_{11}N$) films by approximately 30% thereby creating the C-rich network. Figure 3 (bottom),

shows the measured Au-content in the Au/PSA films as a function of the pre-implant Au-thickness. The plot depicts an approximate 20% loss of Au during the implant process. This indicates that not the entire pre-implant Au layer is embedded into the PSA; some is sputtered off during ion implantation.

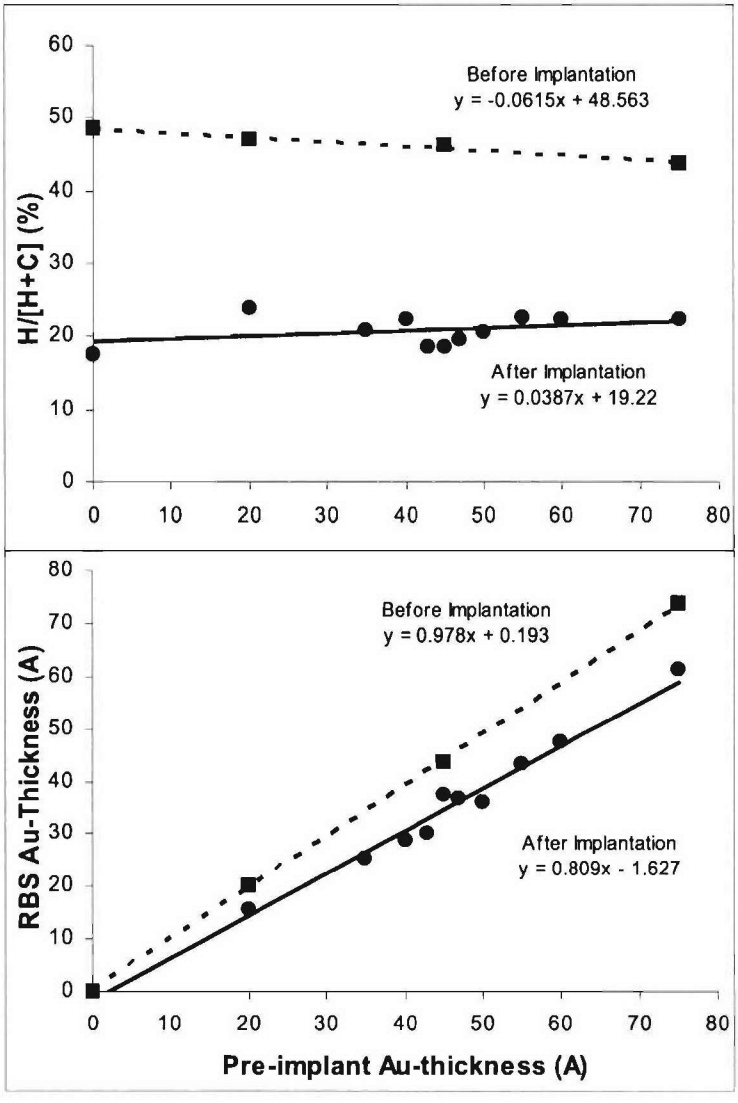

Figure 3: RBS data (top) and ERD Data (bottom)

Figure 4 shows, pictorially utilizing a scanning electron microscope (SEM), the microstructure evolution as the gold pre-implant thickness increases. When no Au is present the implanted polymer is a consistent hydrogen-depleted carbon network. It is this carbon network that is believed to make the polymer harder, more conductive, and more resistive to mechanical wear and chemicals. When the Au film is very thin (20 Å) the implanted Au-particles are isolated from each other (~100 nm apart) and the resistivity is high (semiconductive-like material). Au particles are light colored and the implanted PSA regions are dark.

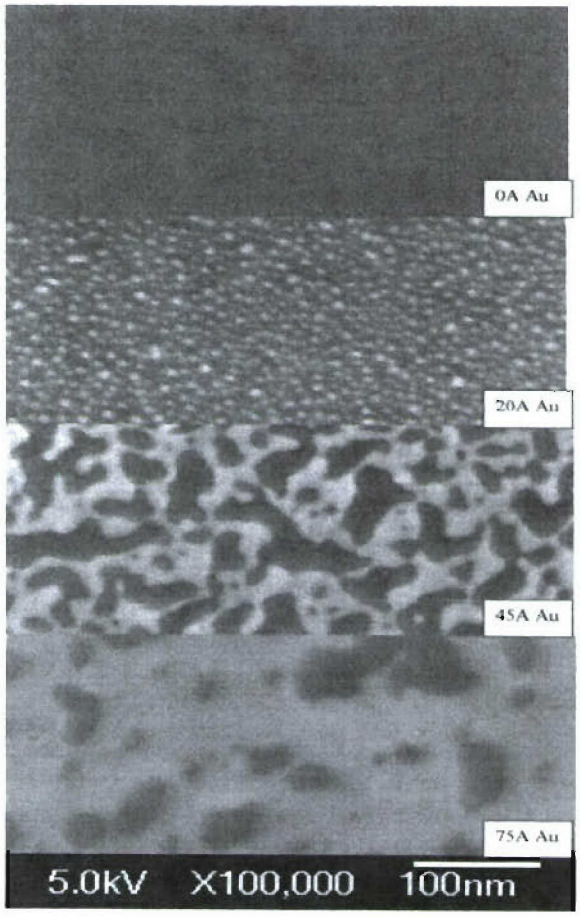

Figure 4: SEM images of microstructure evolution

As the pre-implant Au-film grows thicker (45 Å), the initially separated Au-particles start to form Au-islands (clusters) and the distance between these conducting clusters gets smaller and smaller. This is the transition region or steep portion of Figure 1. The electrical conduction behavior is moving through a semiconductive to metallic transition. As the Au-thickness continues to increase, these conducting islands start to overlap and finally form a nearly continuous Au-film (75 Å). As a result, the electrons are free to move within the continuous Au-film (metallic conduction).

Below in Figure 5 are some images taken of the Au/PSA composite material at 45 Å of pre-implanted Au. The first image shows a 2D representation of the topographical data of the implanted Au-45Å/PSA sample surface. While the image at the bottom shows a 3D representation of the surface topography of the same sample. This helps us to better understand the microstructural evolution of the Au/PSA composite materials as the pre-implant gold thickness is increased through the transition region. It also helps verify that what we are seeing with the SEM micrographs are consistent with a different form of imaging micron and sub-micron surfaces. The ion implantation of the surface actually smoothes the surface and thus allows for clean biological and chemical element binding sites.

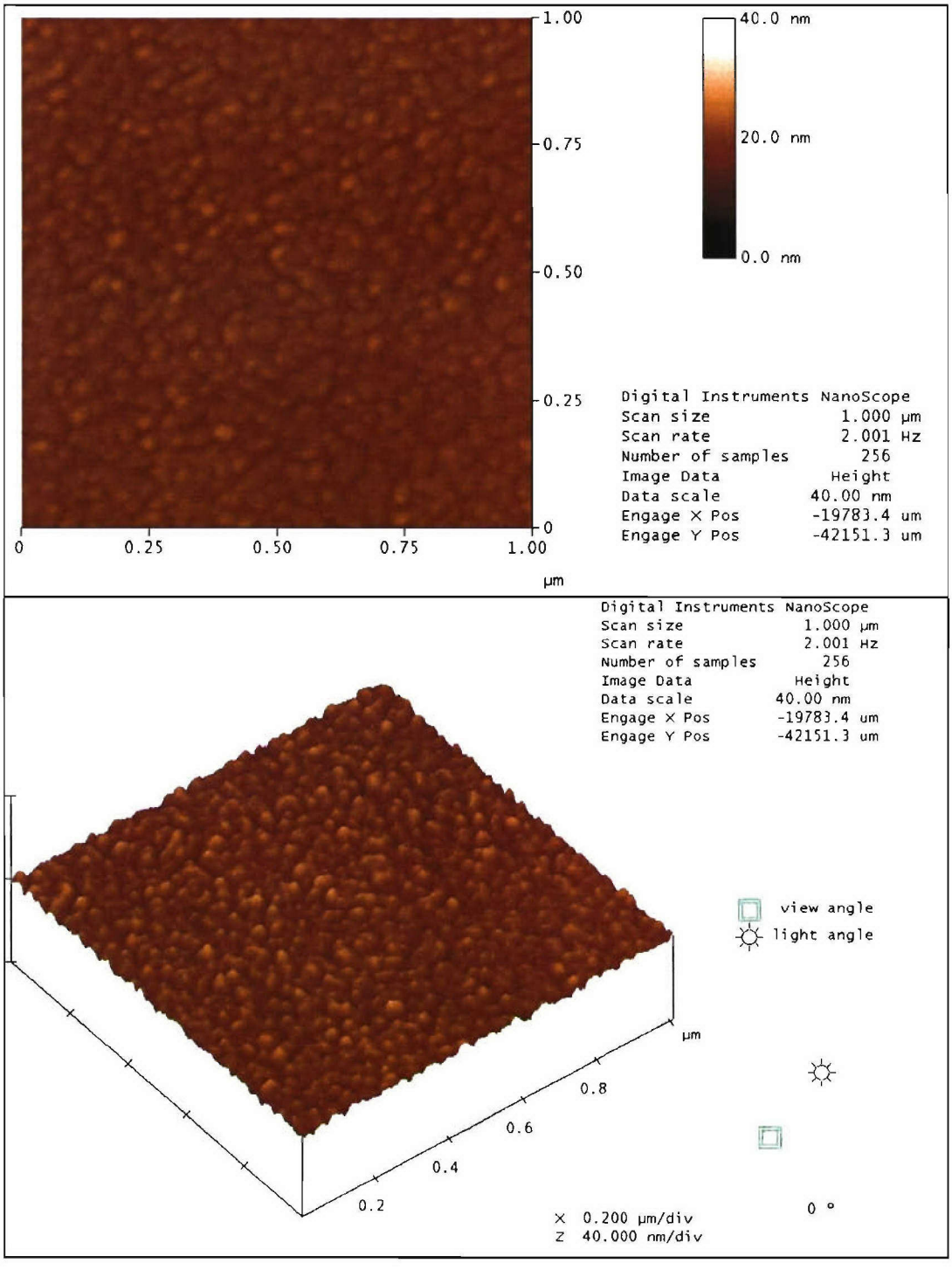

Figure 5: AFM images of Au/PSA composite material

1.3.2.2 Device Fabrication

The device fabrication process for the CPMEMS structures involved engineering of the appropriate carbon/polymer/metal cluster composition on the surface of the CPMEMS to have electronic properties that are critically dependent on vibrations [5] or surface acoustic waves (SAW) [6], and optimizing of the process to generate the appropriate microstruture of the CPMEMS [6]. The completed CPMEMS microstructures consists of carbon polymer-based freestanding bridge 25 μm square, which will serve as the bio-compatible material upon which biological detection elements such as proteins, antibodies, or oligonucleotides could be attached.

The CPMEMS structure shown in Figure 6 was one of the original demonstrations of the collaborative effort between University and BSI to fabricate a carbon polymer-based, ion implanted freestanding bridge with pixel sizes of 10-20 microns square [7,8]. This CPMEMS platform would then serve as a foundation for a broadband array of sensors where pixels may have proteins, antibodies, oligonucleotides, or other biological/chemical sensing systems attached to the surface.

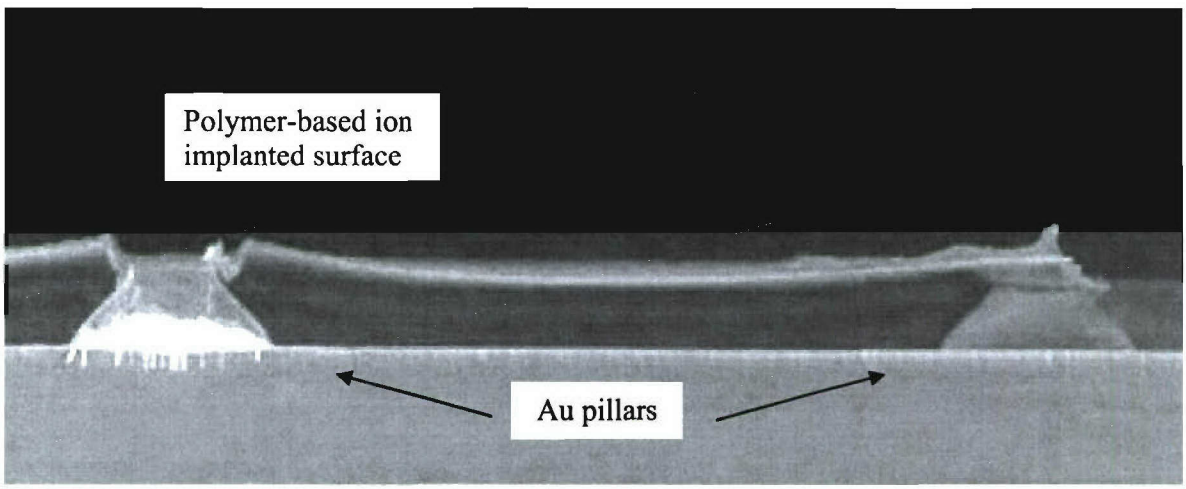

Figure 6: SEM image of a free standing carbon and polymer bridge

a. CPMEMS layer fabrication procedure

To create the CPMEMS freestanding bridge structures, a microlithography process was developed. The following schematic steps depict the process that was developed and refined to create the CPMEMS structures. A number of different strategies were employed and tested to develop the bridge structures as was stated in previous interim reports, but it was the following set of microlithography steps that was found to exhibit the best results.

Steps one through six depict the procedures required to create the free-standing bridges. Step one consisted of a 76 mm [Si + Si_3N_4(~2,000 Å thick)] wafer that had a tri-layer deposited onto it which consisted of 300 Å Cr, 2000 Å Au and 2.5μm of SiO_2. The Cr acts as an adhesion

layer between the Si + Si_3N_4 surface and the Au. The SiO_2 used in the fabrication of the CPMEMS structures was deposited via an e-beam deposition system that was set up for the specific purpose of depositing greater thicknesses of SiO_2 in shorter periods of time compared to other deposition techniques such as RF magnetron sputtering. The deposition of the SiO_2 layer was to act as an insulating and sacrificial layer. The insulating nature of SiO_2 prevents Au from being deposited in certain unwanted areas during electroplating. Step 2 comprised of patterning the SiO_2 to create the wells where the Au pillars would be grown, and step 3 correspondingly was where the 2.5μm Au pillars were electroplated. In step 4, once the Au pillars were electroplated up to the plain of the SiO_2, the polymer material was spin coated onto the surface and then patterned such that a bridge lay across the two electroplated Au pillars. In step 5 the remaining SiO_2 layer is removed such that an air cavity is created under a free standing polymer bridge. Lastly, in step 6 the Cr and Au seed layers are removed to isolate the bridge structures from each other.

Step 1: Deposit 300 Å Cr and 2000 Å Au and 2.5μm of SiO_2 on silicon wafers purchased with silicon nitride deposited on them (~2,000 Å thick)

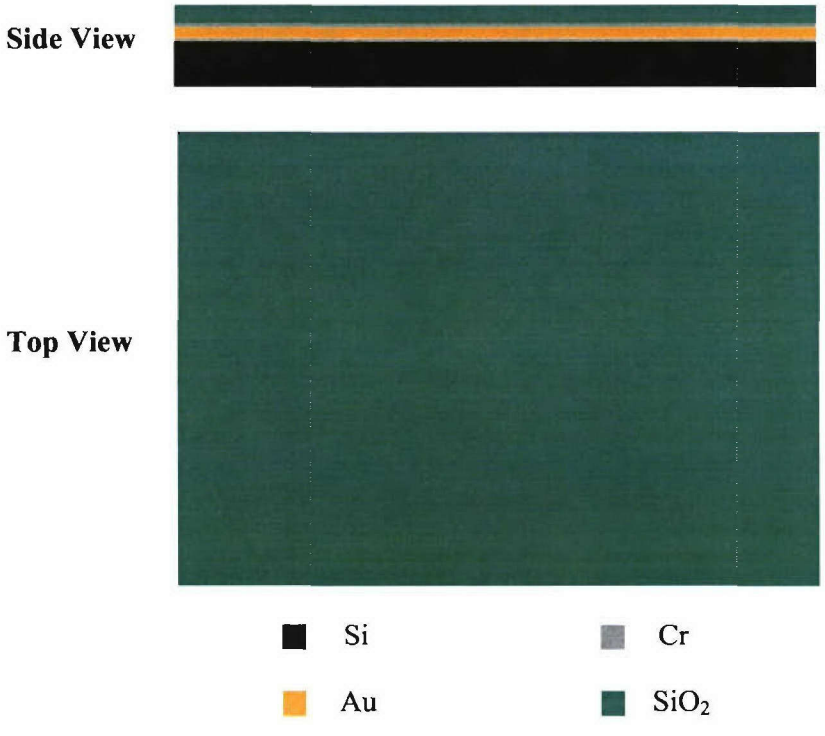

Step 2: Selective wet etch of the SiO_2 down to the Au seed layer to create the wells for electroplating the 2.5 μm Au pillars

Side View

Top View

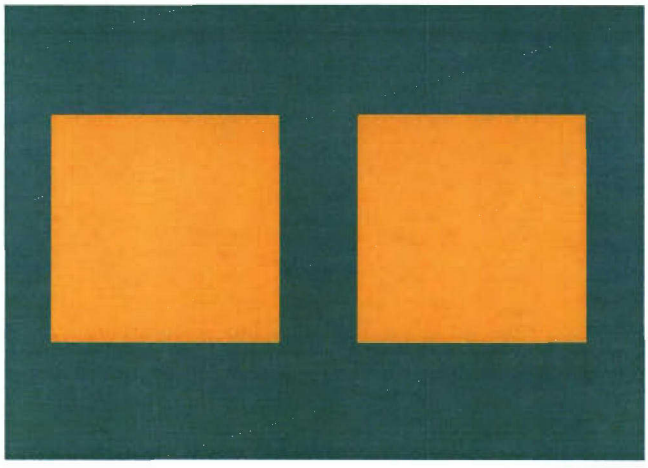

Step 3: Electroplate the Au pillars up to 2.5 μm such that they are in the plane with the SiO_2

Side View

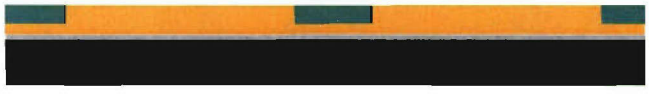

Top View

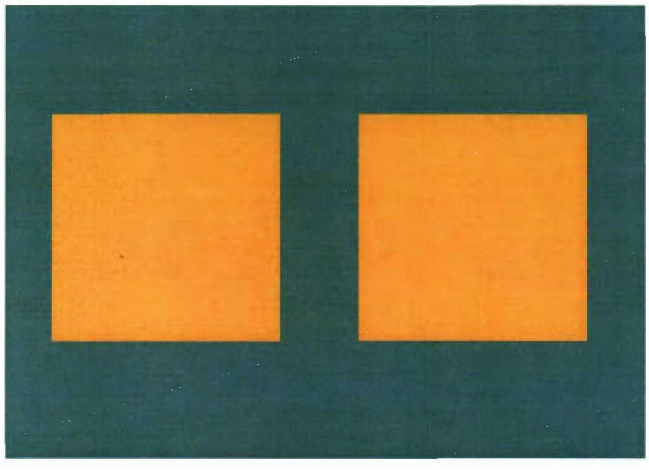

Step 4: Patterning of the carbon polymer material between the Au pillars

Side View

Top View

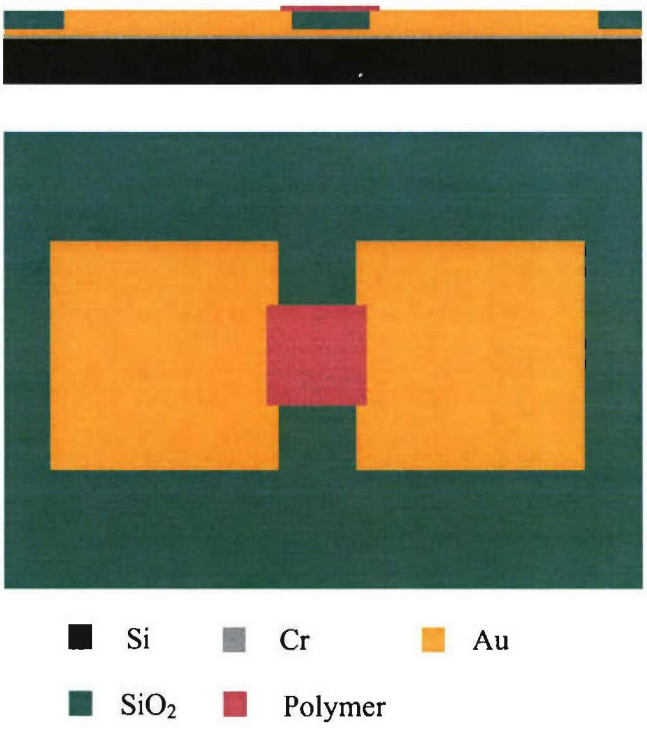

Step 5: Wet etch SiO_2 layer for to create freestanding CPMEMS structure

Side View

Top View

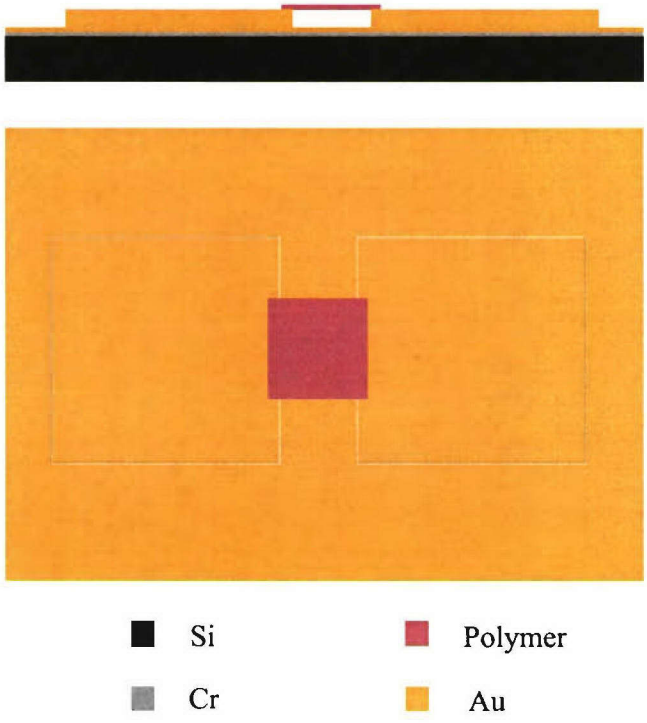

Step 6: Selective wet Au and Cr etch to create individually accessible CPMEMS devices

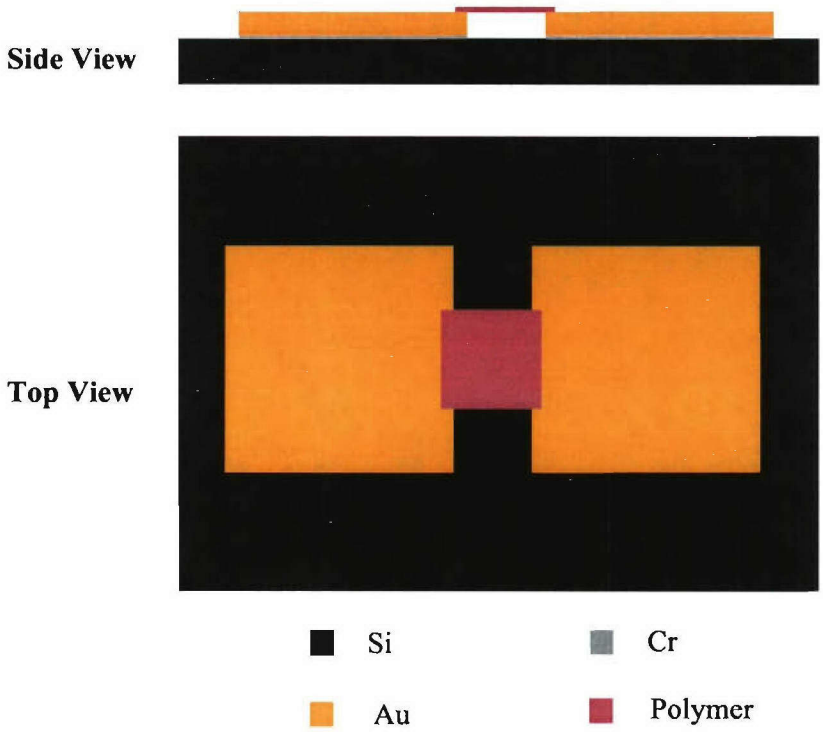

b. Fabricated CPMEMS structures

Below are some a series of SEM micrographs of the fabrication steps for developing the CPMEMS bridge structures that were outlined above. Figures (7-10) show the generalized steps from creating the wells in SiO_2 to allow for the building up of the Au pillars, to actually building up the Au pillars via electroplating, to patterning the carbon polymer bridge material, to finally removing the SiO_2 to create a freestanding CPMEMS bridge structure. Figure 11 shows dimensional information regarding the CPMEMS structures. These dimensions were optimized for the CPMEMS' merit to be utilized in an aqueous solution with vibrational or ultrasonic stimulation, as well as for metal cluster content, and carbon concentration of the carbon polymer material to maximize vibrational responsivity, and finally for composition so that bio-sensitivity and bonding with a variety of bio-detection elements would be maximized.

A cross-sectional view as shown in Figure 12 gives a visual of a CPMEMS bridge structure. It is this unique bridge design that will serve as a broadband detection platform upon which different biological detection schemes can be built upon. Figure 13 gives an example of creating CPMEMS structures of different sizes. The Au pillars in this scheme are 125 μm square. This helps to optimize the broadband detection platform such that it would provide the most feasible conditions for bio-compatibility.

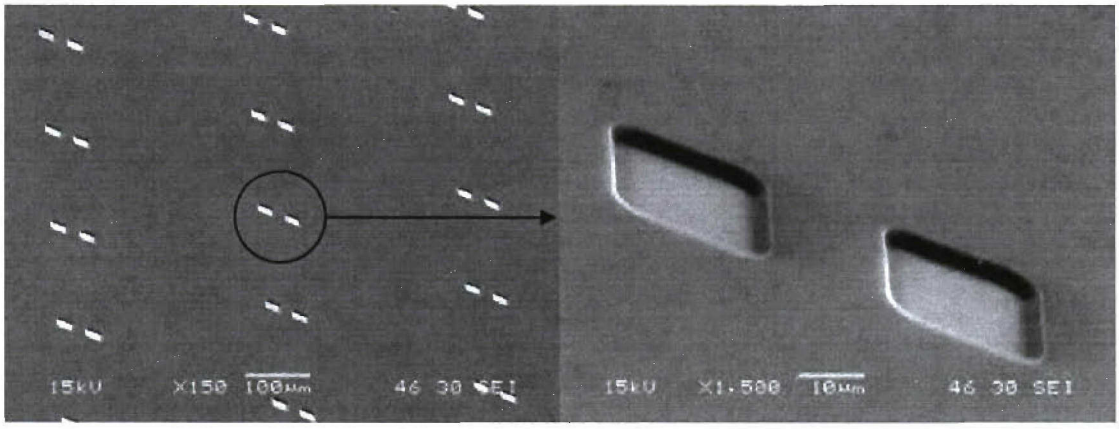

Figure 7: SiO_2 wells created prior to electroplating Au pillars

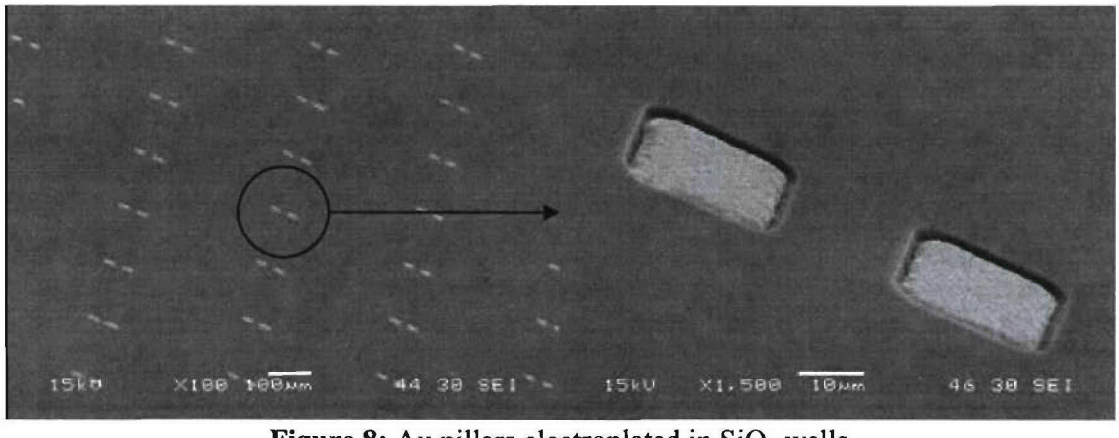

Figure 8: Au pillars electroplated in SiO_2 wells

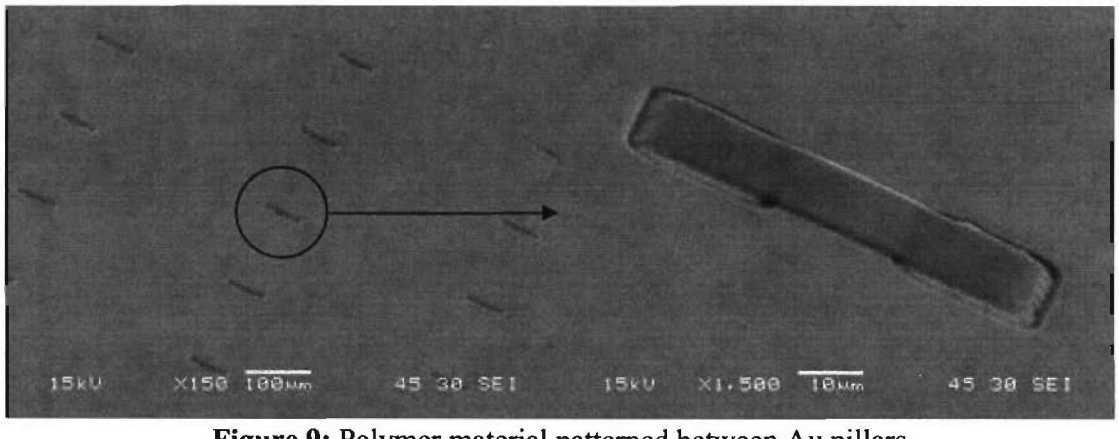

Figure 9: Polymer material patterned between Au pillars

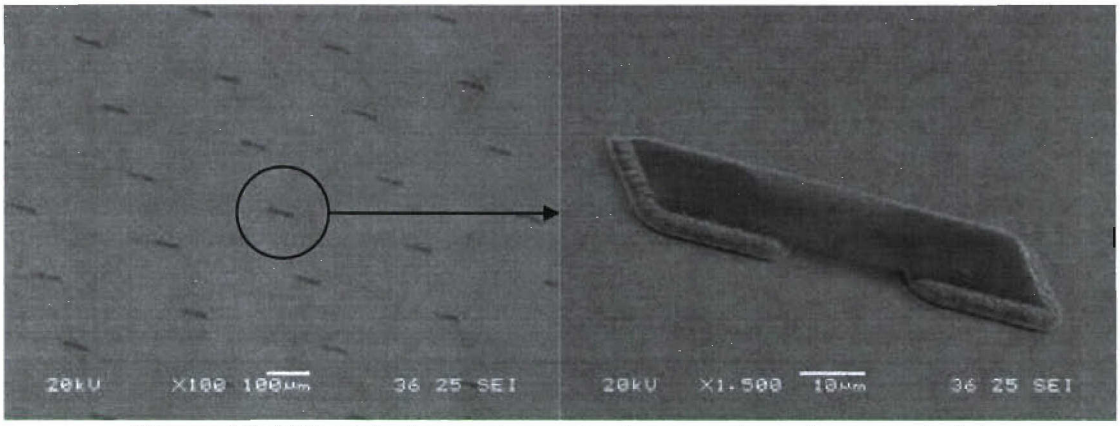

Figure 10. SiO_2 etched away to create air gap under polymer material

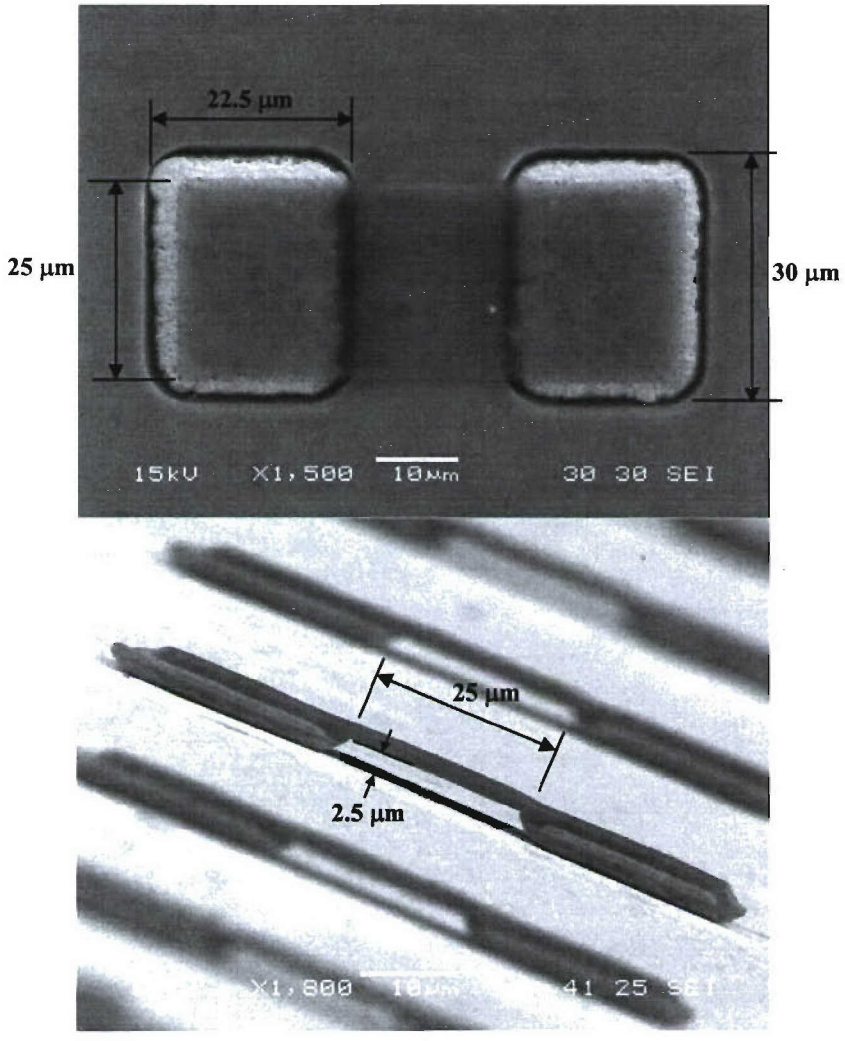

Figure 11: CPMEMS structural dimensions

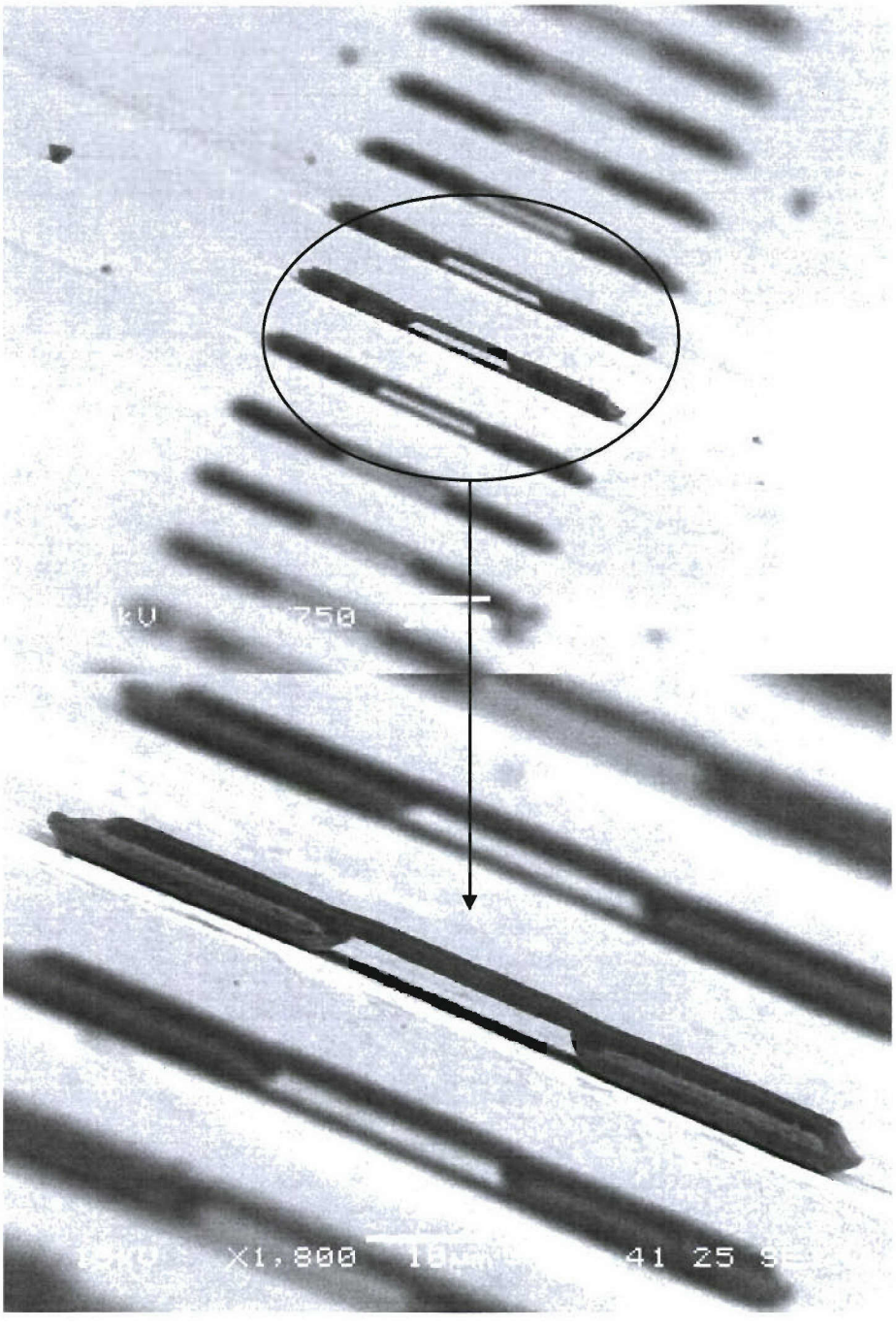

Figure 12: Cross-sectional view of free-standing CPMEMS structure

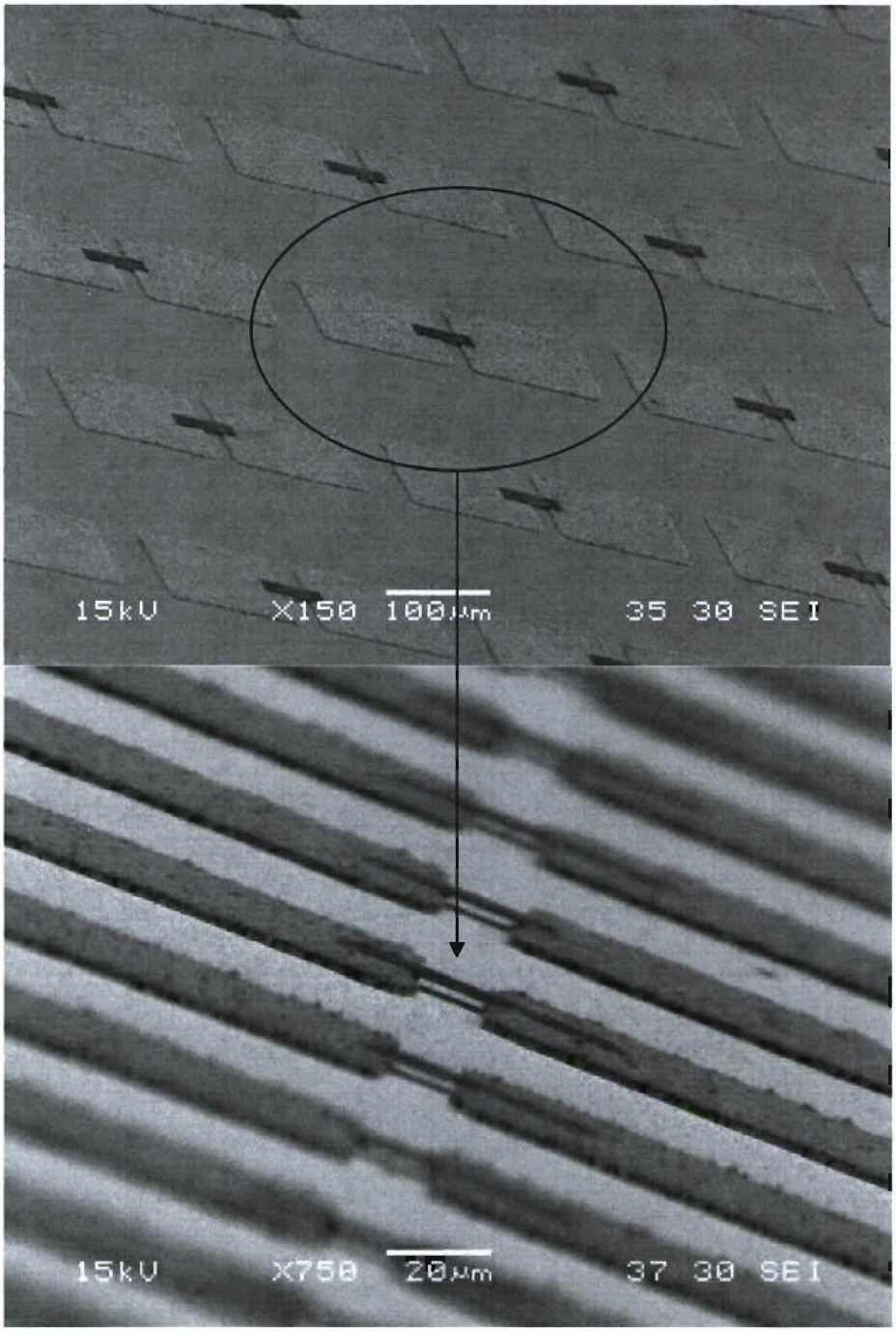

Figure 13: CPMEMS structures with larger Au pillars (125µm x 125µm Au pillars)

c. Unity 400

Initial studies revealed that the wet etching process to remove the SiO_2 layer to create the freestanding polymer bridges had shown to cause stresses on the carbon and polymer material, and thus making it bow a little. Therefore a study was conducted on alternative methods/materials in partnership with BSI who specializes in developing processes for unique microlithography patterning materials. As an alternative to SiO_2, a heat dissolvable polymer from Promerus LLC was investigated by BSI in parallel to further work on optimizing the development of the CPMEMS structures using SiO_2. As was shown in the previous section, an optimized process was successfully developed using SiO_2 to create a polymer bridge that did not bow, but work with Unity 400 still continued.

The Unity 400 would have the same function in the process steps of developing the CPMEMS bridge structures as the SiO_2, except that the processing of the material to create the wells for electroplating the Au pillars as well as the removal process to create the freestanding polymer bridges would be different. Instead of e-beam depositing SiO_2, the Unity 400 heat dissolvable polymer would be put down via spin coating. To create the wells for building up the Au pillars would require a Reactive Ion Etch (RIE) process instead of wet etching. Once the wells are made and the Au pillars are electroplated up, and the polymer bridge is patterned between the Au pillars, the Unity 400 polymer is heated to 425°C, which will cause it to cleanly decompose and hence create a residue-free air cavity.

The thermal decomposition kinetics of Unity 400 was studied by using dynamic TGA (Thermal Gravimetric Analysis). The Unity 400 sample was heated to and held at 425 °C for 120 minutes. The dynamic TGA result shown in figure 14 verified that the Unity 400 completely decomposed at 425 °C, and there was only a negligible amount of residue left in the sample chamber. Another advantageous property of Unity 400 is its good thermal stability up to 300 °C. This ensures a sufficient processing window subsequent device fabrication steps.

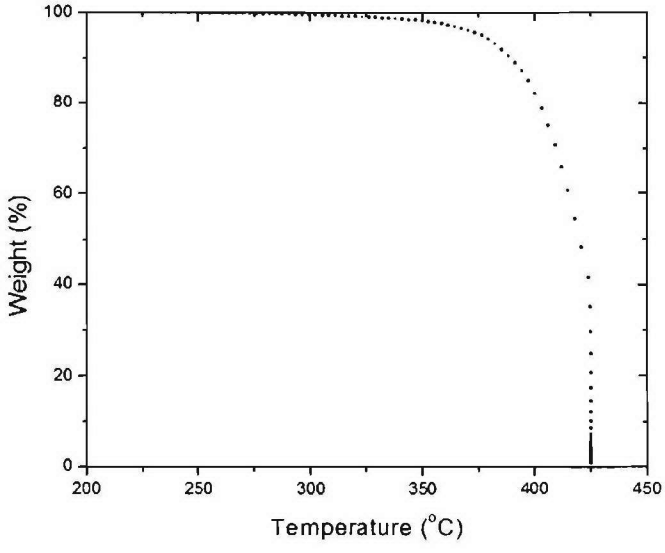

Figure 14: Dynamic TGA of Unity 400

The compatibility of the cured Unity 400 film in the Au electroplating bath (Aurall 305) was also tested. Several silicon wafers were coated with 2.5 μm thick Unity 400 films. After Unity 400 being cured, these wafers were respectively immersed in the Au electroplating bath at 60 °C for as long as 65 minutes. No dissolution of these cured Unity 400 films or change of the Au electroplating bath were observed. These soaked wafers were rinsed with DI water, baked at 115 °C for 2 minutes, and then loaded into the tube furnace for the thermal decomposition test. No residue could be visually noticed after the thermal decomposition process. The results herein verified the compatibility of the cured Unity 400 film in the Aurall 305 bath.

RIE was used as the etching process, where an etch recipe was optimized for patterning the Unity 400. The etch rate of Unity 400 was first measured by conducting a series of timed RIE runs. At the end of each run, the thickness of the Unity 400 layer left on the wafer was measured using a profilometer. The results were plotted with the RIE time with a linear fit as shown in figure 15, which indicated that the etch rate was approximately 3.6 nm/second. A SEM micrograph of the resulting pattern in the Unity 400 layer with an Al hard mask is shown in figure 16. For the purpose of studying undercut and sidewall profile, an Al hard mask was left on top of the Unity 400 during the SEM inspection. The major issue encountered in patterning a Unity 400 film by RIE was considerable undercut due to the dominance of the isotropic etching. Continued work still needs to be conducted to refine the process.

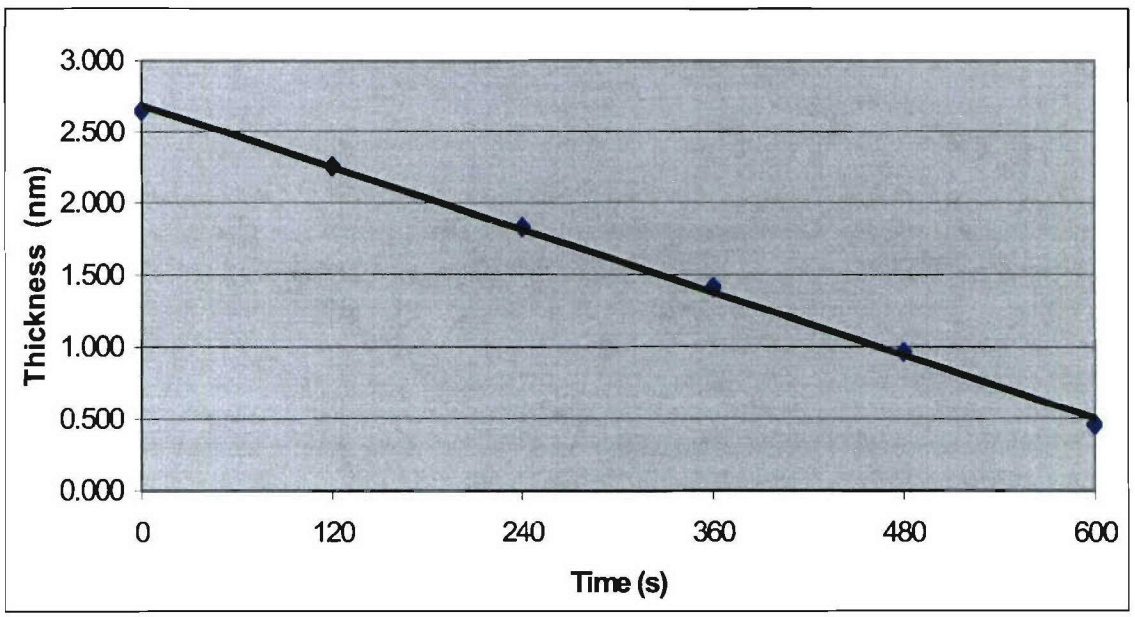

Figure 15: Etch rate of Unity 400

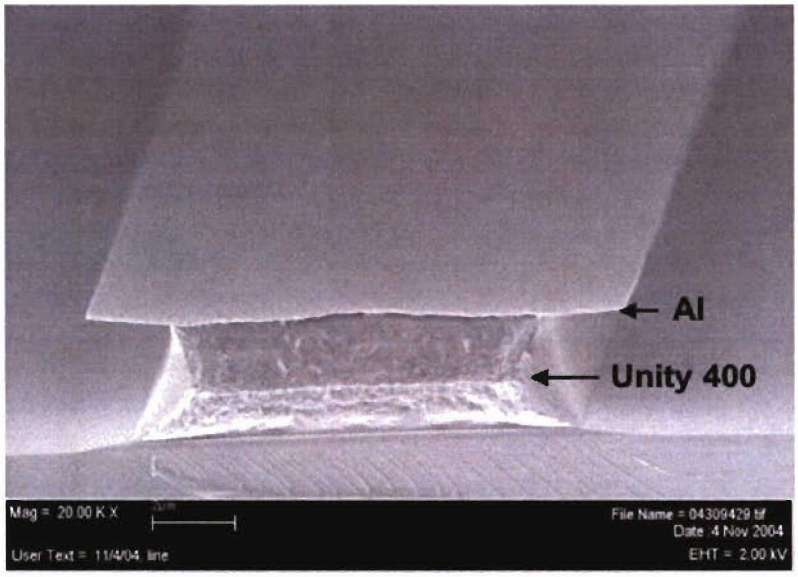

Figure 16: Unity 400 pattern after RIE

1.3.2.3 Antigen Platform, Self-Assembled Protein Layers

a. Antibody-antigen scheme

The primary objective of this task was to determine antigen platform feasibility to develop the appropriate process to bind proteins, antibodies, or oligonucleotides to the carbon and polymer bridge material such that it would function as a sensing element. Initial work was conducted on binding antibodies to the Au/PSA surface to determine their compatibility. Studies revealed that the antibodies themselves could not be attached directly to the carbon polymer material but rather intermediate layers were required to obtain binding. Three different methodologies were investigated to attach antibodies to the surface of the Au/PSA mixed carbon-rich surface that would make up the bridge material of the CPMEMS structure. These methodologies included poly-d-lysine and protein A, nitrocellulose and a chemical functionalization of the Au/PSA surface for binding of the antibodies to occur. Lastly, studies were conducted using oligonucleotides as the biological sensing system instead of the antibody-antigen system.

Figure 17 shows a multi-layer system that is required for the attachment of the antibodies to the carbon and polymer substrate. A thin poly-D-lysine coating is applied to the substrate, which provides a positively charged surface. Next, a layer of protein A, which has a high affinity for the IgG class of antibodies, is added. The advantage of using protein A is that any IgG antibody will readily attach to the protein A and thus, a large number of antibodies can be bound in this manner. Many of the antibodies will bind to protein A in an orientation that favors binding of a particular ligand or molecule (i.e. antigen). In traditional microarrays, the ligand or binding molecule needs to be fluorescently-labeled in order to detect its binding to the antibodies. For the purpose of feasibility, fluorescence-labeling was utilized to determine whether or not a binding event had occurred.

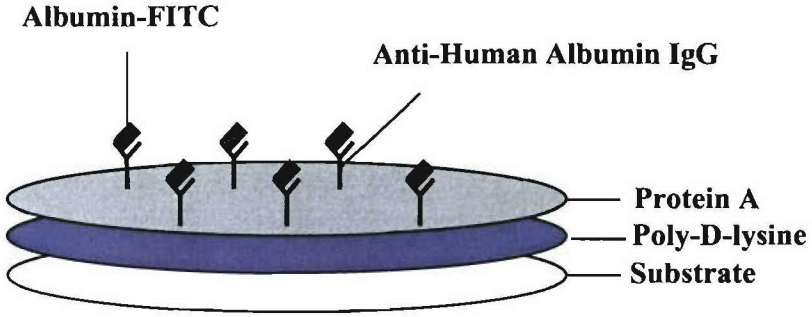

Figure 17: Side view of antibody array

It was demonstrated that the design of our antibody microarray allows for the detection of a specific binding molecule to the antibodies. Anti-human Albumin IgG was immobilized onto Protein A, and then a fluorescently-labeled molecule (Albumin-FITC) at different concentrations was allowed to bind to the immobilized antibodies. It was noted that the intensity of the fluorescence signal, which corresponds to the amount of fluorescent molecule bound by the antibody, is proportional to the amount of binding molecule presented to the antibodies (figure 18 a & b). For lower concentrations of antigen binding to antibodies attached to the Protein A layer, there was a significant decrease in the fluorescence signal.

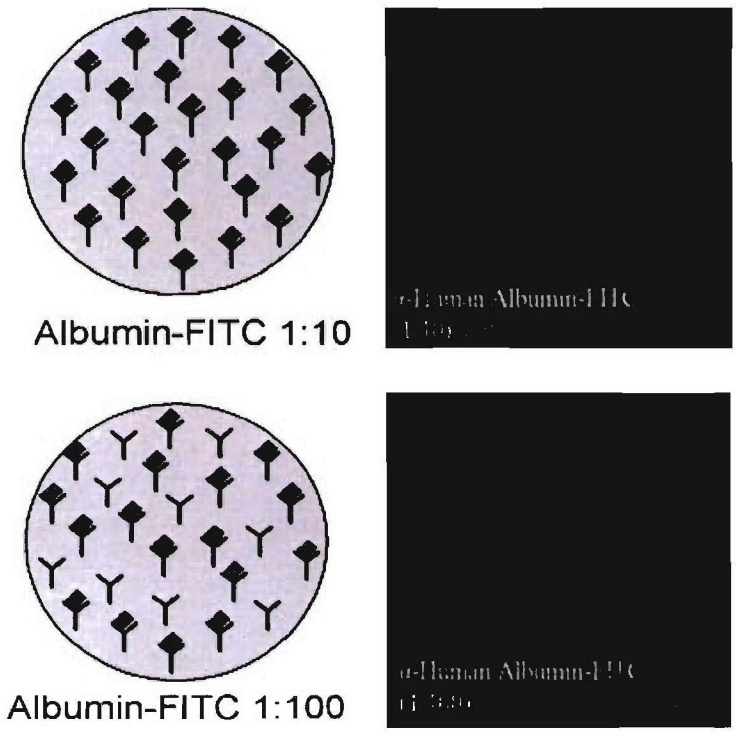

Figure 18: a) 1:10 Concentration of IgG antibody & b) 1-100 concentration of IgG antibody

Although this methodology proved to have been viable, there was an issue with non-specific binding of the antigen to the poly-D-lysine that was used to anchor the antibodies to the carbon and polymer bridge material. Further analysis revealed that the concentration of poly-D-lysine used to coat the surface of the carbon and polymer material was deposited not as a monolayer of the substrate as intended. The thickness of poly-D-lysine would likely increase the amount of background. Tests to lower the concentration of poly-D-lysine to determine the minimum amount required for bridge assembly was conducted but this still exhibited non-specific binding.

b. Nitrocellulose study

The next methodology that was investigated in light of determining that the methodology of using poly-D-lysine resulted in non-specific binding was the use of nitrocellulose as an immobilization substrate. Nitrocellulose has been shown to provide a near-quantitative surface, allows for long-term storage of the immobilized antibodies, and allows for proteins (antigens) in solution to interact with the immobilized antibodies. Initial studies were conducted on glass slides where optimized spin coating conditions were established to create a thin, uniform and nearly flat surface for immobilizing antibodies with just only layer. It was found that fluorescent antibodies would bind in a uniform manner to the nitrocellulose-coated slides. In addition it was also demonstrated that antibodies specific to the recognition of E. coli bacteria were immobilized onto nitrocellulose and did capture these bacteria with controlled experiments (see figure 19).

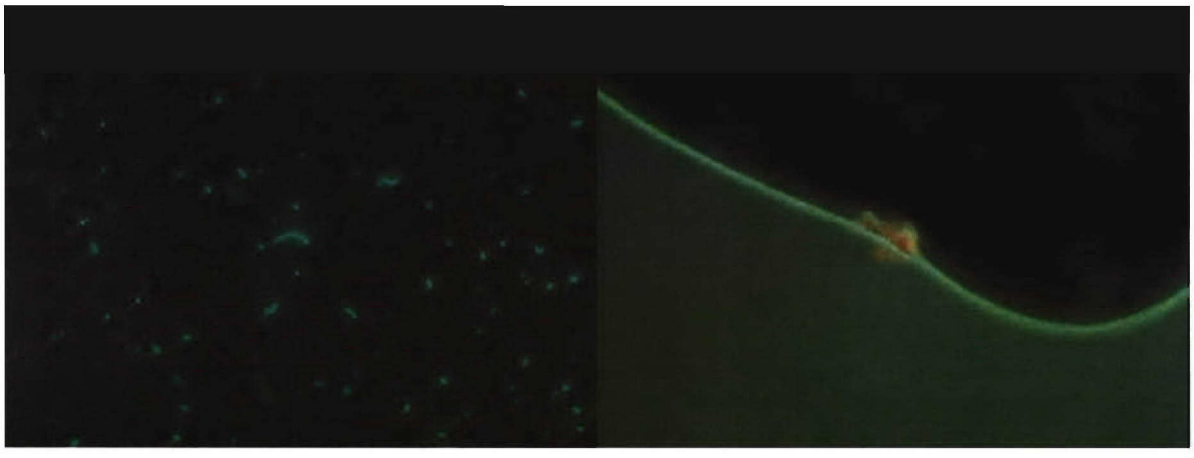

Figure 19: The fluorescence microscope image on the left is of E. coli bacteria captured by antibodies and the image on the right is of Primary antibody IgG binding on a nitrocellulose coated membrane

c. Functionalizing of Au/PSA

The last methodology that was investigated to bind antibodies to the carbon and polymer bridge material was the use of a functionalization technique. This would allow for antibodies to be directly immobilized onto the carbon and polymer material without any intermediate layer. Initial studies for functionalizing the surface of a material to allow for antibody binding was conducted on silicon (si). Aldehyde silane was used as a precursor to bind onto a si surface to form one silane monolayer. This silane monolayer is designed for further immobilization procedures. With the reaction between the aldehyde group and the amine group of an antibody, antibodies can be immobilized onto si through chemical covalent bonding. Fluorescently tagged antibodies were then immobilized onto the functionalized si surface. This is evident in figure 20 where antibodies did bind to the functionalized si surface where as there was no binding to the non-functionalized si surface.

Figure 20: Left: fluorescence microscope image of antibodies immobilized to functionalized si surface, Right: fluorescence microscope image of no antibodies being immobilized to non-functionalized si surface

Once it was determined that immobilization did in fact occur on a functionalized si surface, the procedure then was repeated, but this time using the Au/PSA bridge material. The Au/PSA surface is rich of hydroxyl (-OH) groups and can be used to form a uniform silane monolayer. The aldehyde silane monolayer is formed on the Au/PSA surface through the reaction between the –OH groups of the Au/PSA surface and silane. Aldehyde groups again as before react with the amine groups of antibodies which causes immobilization on Au/PSA. Figure 21 below shows a schematic illustration of the binding of the hydroxyl groups that are formed on the Au/PSA surface with the amine groups of the antibodies. Figure 22 shows a fluorescent microscope image of antibodies on the surface of a functionalized Au/PSA material. We have demonstrated that it is possible to immobilize antibodies on Au/PSA surface with covalent bonding, and these immobilized antibodies on the Au/PSA surface show a high stability, thus suitable for use on the CPMEMS bridge structure.

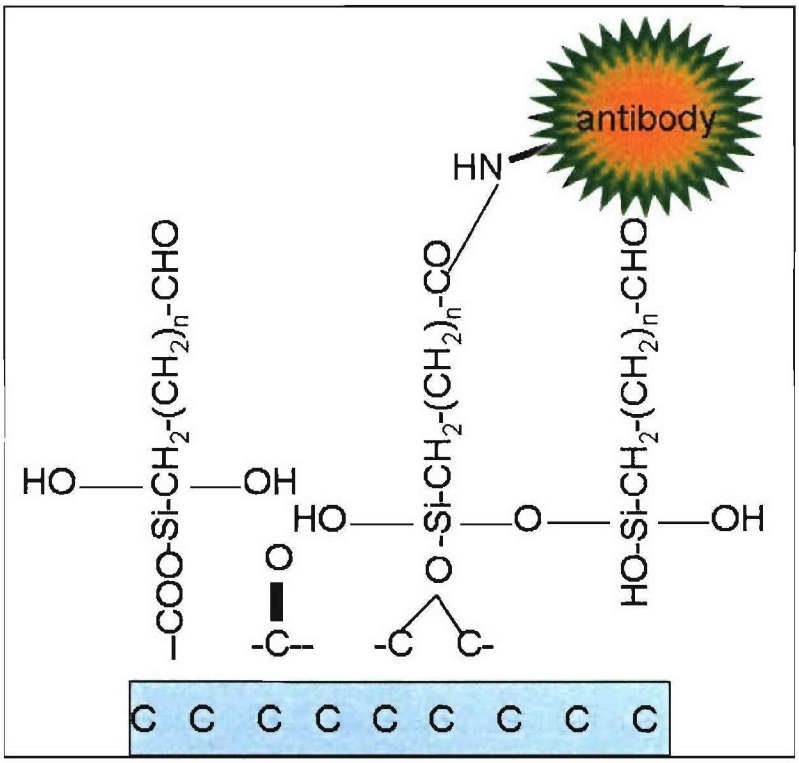

Figure 21: Immobilized antibody to Au/PSA surface by silanization

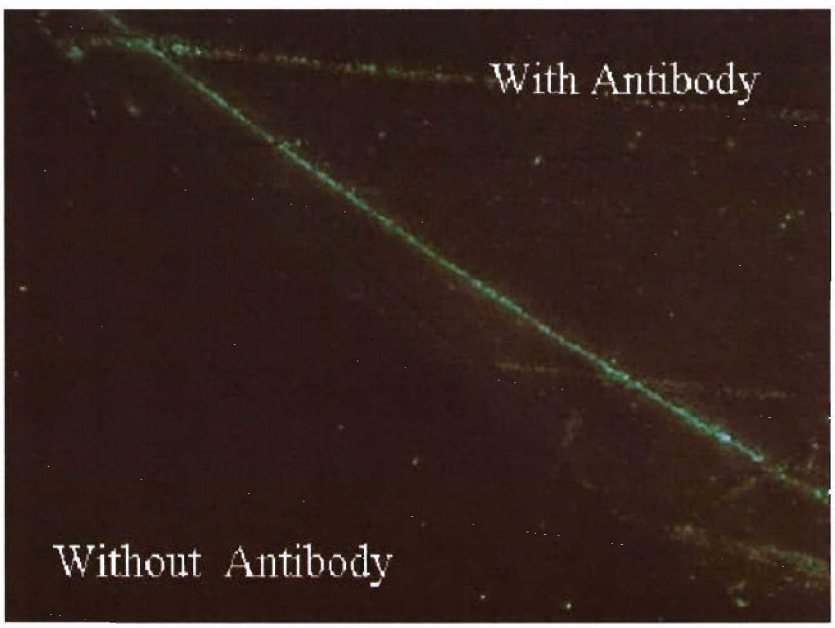

Figure 22: Fluorescence microscopy image of antibody on Au/PSA surface

d. Conclusions of antibody study

With the three different methodologies that were investigated to immobilize antibodies to the bridge material of the CPMEMS structure, it has been shown that a link between a biological detection system and the CPMEMS electronic system has been established. In the development stages of this type of biological (antibody-antigen) detection system a couple of drawbacks were noted. The first being background noise, which would hinder accurate detection signals; from the first immobilization method that was investigated (Au/PSA + poly-D-lysine + protein A + antibodies) the background noise would be high due to the multiple layers required to immobilize the antibodies. With this methodology it was also noted that non-specific binding of antigens did also occur due to the protein A. With the second methodology (Au/PSA + nitrocellulose + antibodies) the issue of non-specific binding was overcome, but background noise would still be an issue due to a thick layer of nitrocellulose. The last methodology (Au/PSA + silane + Antibodies) shows the most promise for being an immobilization technique because it would provide the least background noise due to the silane layer being only a monolayer, and that their would be less non-specific binding of antigens.

Further investigations were conducted on the antibody-antigen detection scheme using known test antigens (i.e. bacteria). While this method worked in preliminary studies, the use of antibodies was determined not to be feasible for detecting many different types of bacteria in solution. Also, as the number of bacteria in a solution increased, it became necessary to wash the detection surface more extensively to favor specific antibody-bacteria interactions. Unfortunately, the number of captured bacteria decreased dramatically as a result of the more stringent wash procedure. Thus, by trying to minimize nonspecific binding of bacteria to the antibodies, it resulted in greatly reducing the number of captured bacteria. As a result, a decrease in detection signal would occur. To circumvent this problem that is characteristic of antibody arrays, the study was then focused on a biological detection scheme that utilizes oligonulceotides as the capture molecule for the detection of antigens.

e. Oligonucleotides

i. Feasibility study

The first study in determining the feasibility of using oligonucleotides (short pieces of DNA) as a biological detection method was immobilization onto a known substrate and subsequent monitoring of binding using fluorescent microscopy. Studies were conducted to attach oligos to a gold (Au) substrate and establish a method to monitor the binding event. The use of oligos will allow for the design of multiple probes to specifically detect fungi, bacteria, or viruses from a given environment.

Oligonucleotide (DNA) hybridization involves the joining of two complementary single-stranded DNA (ssDNA) with high efficiency and extremely high specificity, even in the presence of a mixture of many different, non-complementary oligos. It should be noted that some non-complementary oligos that have some matching base pairs may hybridize, but will have a weak bond. This methodology of detection will increase the likelihood of positively identifying a particular organism or class of organisms. A model of the DNA sensor is shown in figure 23.

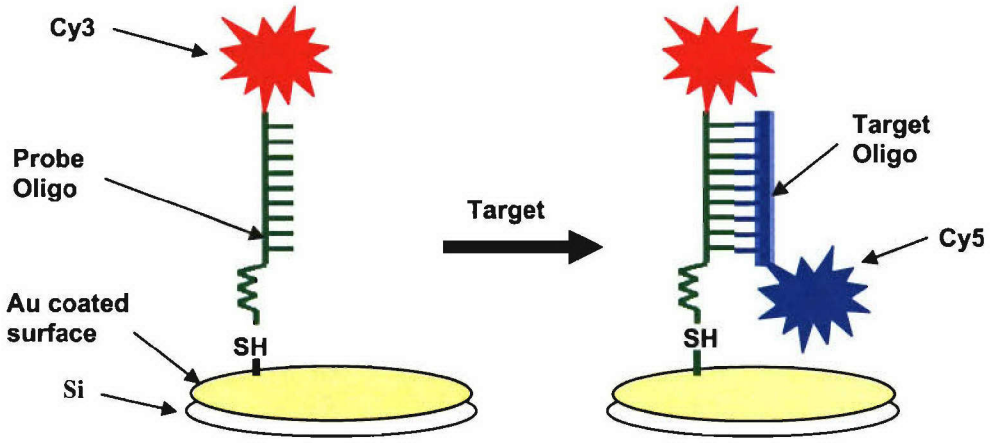

Figure 23: Model of DNA Biosensor

Initially, a chemically modified piece of ssDNA (Cy3-labeled oligo) that contains a thiol (SH) group, along with a hydrophilic linker between the thiol group and DNA is immobilized onto a Au surface. A hydrophilic linker is used to minimize non-specific absorption events, where as the SH group facilitates uniform binding of the DNA to the Au surface and also helps to orient the DNA on the surface so as to increase the likelihood of binding with the target DNA as shown in figure 24. In addition, the Cy3 label allows for monitoring the density of oligo binding using fluorescent microscopy. The probe of a DNA biosensor most frequently consists of an oligonucleotide, 15-50 base pairs in length. The target DNA which has a Cy5 label is then allowed to bind to the probe DNA for proof of concept simulations. The resulting hybridization can be detected using fluorescence microscopy.

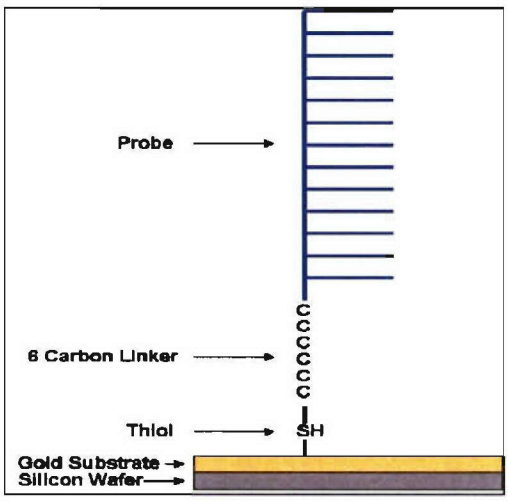

Figure 24: Modified Probe Attached to Gold Substrate

In order to detect organisms of interest; they have to captured and isolated such that they can be broken down into their basic DNA structure. A bio-collection system that was developed is able to concentrate the amount of biological material found in the air using a water capture method. To be able to gain access to the DNA in the biological material, it is necessary to break up the material where a number of techniques such as heating, addition of detergents, or sonication can be used. Sonication was chosen because it has the advantage of not only breaking open the biological material but also shears the DNA into small fragments that can be used for more efficient oligo hybridization. As shown in figure 25, sonication of a biological material such as bacteria for 5 mins (left lanes) yields DNA that is only several hundred base pairs in length, which is optimal for conducting these test experiments.

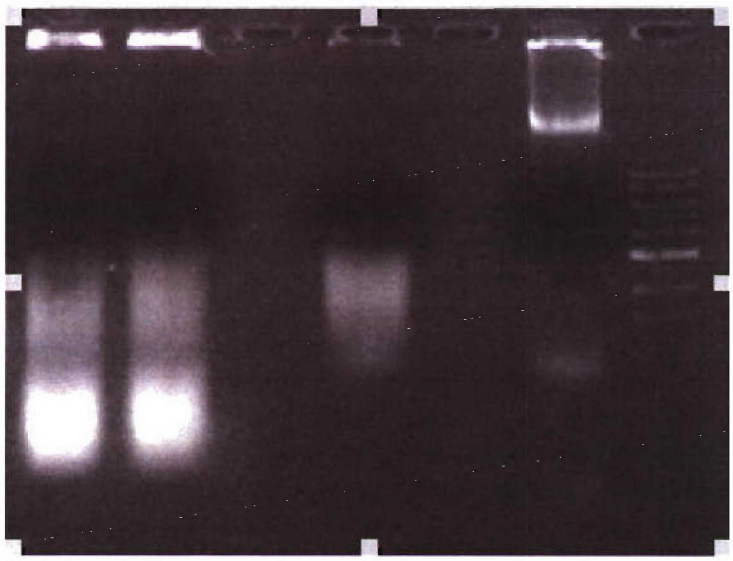

Figure 25: Sonicated bacteria E.coli DNA on agarose gel

ii. Oligonucleotide hybridization using fluorescence detection

Several variables affect the hybridization event such as salt concentration, temperature, contact time, and length of the probe sequence. Increasing salt concentrations can enhance the analytical signal; however, non-specific absorption can also increase. The rate of hybridization is strongly affected by temperature, where maximum kinetics is observed at 20-25°C below the duplex melting temperature. Longer probe and target length can reduce sensitivity due to steric hindrance. The hybridization event is generally carried out at a neutral pH, thereby allowing hybridization to remain independent of pH, and incubation times range from 2 minutes to 1 hour.

Simple model single-stranded DNA (ssDNA) probe sequences (20-mer) were used for this study, providing the basis for future detection of pathogen recognizing probes. Fluorescence microscopy was initially utilized to establish experimental parameters, such as incubation time, washing conditions, concentrations of probes, blocker conditions, and surface characterization to create an optimized DNA hybridization event. Conditions optimized using the fluorescence method of detection will be applied to other detection methods for hybridization detection. The

signal produced will differentiate between complementary and non-complementary sequences providing the groundwork for future, specific biosensors to be used in clinical and environmental diagnostics.

As was mentioned earlier, oligonucleotides are short sequences of nucleotides (RNA or DNA), typically with fifty or fewer bases, which can be used as probes for detecting complementary DNA or RNA because they bind readily to their complements. Antisense or complementary oligonucleotides are single strands of DNA or RNA that are complementary to a chosen sequence. For the fluorescent research studies, 20-mer oligonucleotides were purchased with the probe strands being synthesized with a SH group and 6 chain carbon linker on the 5' end and labeled with a Cy3 marker on the 3' end. The antisense, or complementary, target strand and the non-complementary control strand were labeled with Cy5 dye. The sequences of the oligonucleotides are as follows (see figure 26):

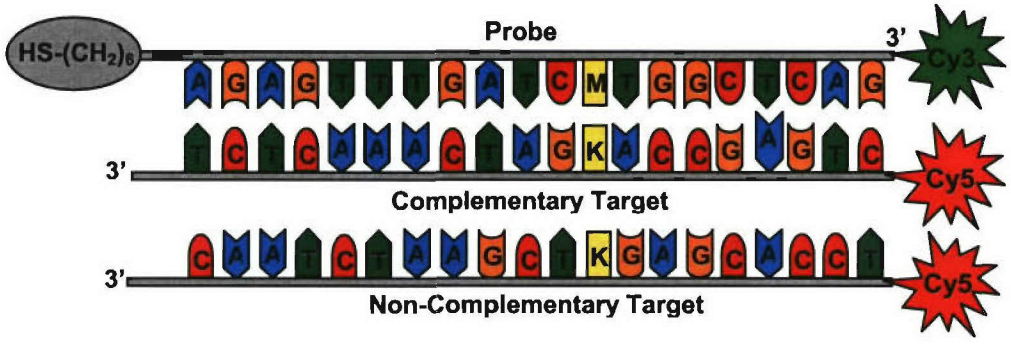

Probe: (5') HS-$(CH_2)_6$-AGAGTTTGATCMTGGCTCAG-Cy3
Complementary target: (5') Cy5-CTGAGCCAKGATCAAACTCT
Non-complementary target: (5') Cy5-TCCACGAGKTCGAATCTAAC

Figure 26: Schematic diagram of fluorescently tagged probe, along with fluorescently tagged complementary target and non-complementary target oligonucleotides

Au was used as a substrate for fabricating the self-assembled monolayers of oligonucleotides, where for all experiments 1000Å of Au was evaporated onto a silicon (Si) wafer or glass slide using a mask to create a pattern of choice. 100Å of chrome (Cr) was deposited first to promote good adhesion between Au and either Si or glass. To verify the selectivity of the thiol for Au versus other substrates, 10 μl of thiolated oligonucleotide solution with a Cy3 label (0.100 μM) was deposited onto Au and Si portions of an electrode. The probe was then incubated at 37°C for 20 minutes to increase the binding rate of DNA to the Au surface. The thiolated DNA solution was then removed from the Au, and washed three times with a Tris-HCL solution (0.1 mM, pH 7.2). The substrate with the immobilized probe was then analyzed by a fluorescence microscope. As seen in Figure 27 the signal (indicated by the red color) of the probe DNA immobilization is more intense in the regions with Au compared to the regions with Si. This indicates that very minimal binding of the SH group does occur on Si, and simultaneously validated the use of a Au substrate with a thiol-modified ssDNA probe for the

baseline DNA sensor scheme. Further studies were conducted replacing Si with glass slides, where it was determined that it was more favorable to use the glass slides because they are less conductive than Si. It was also determined that more binding occurred on the glass slides as compared to Si, however this was shown not to be a concern for investigating other methods of oligo hybridization detection using electrical techniques.

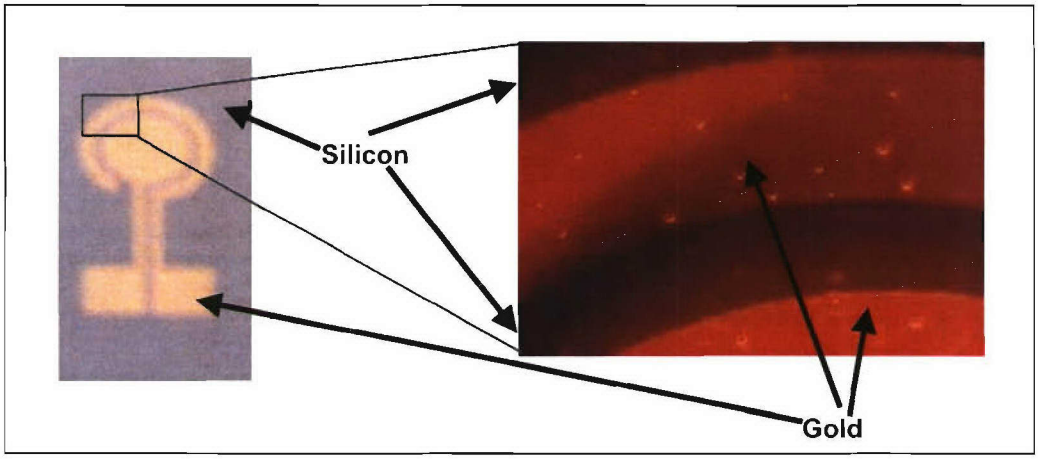

Figure 27: Image of Au electrode on left with corresponding fluorescence microscopy image on right of region where thiolated Cy3 tagged probe oligos were bound to the substrate

Studies were conducted to determine the most viable probe concentration due to the selectivity, which is constrained in part by the physical properties of the environment of the ssDNA at the surface. The location and speed of signal development will be dependent on the stability of the hybrid, which is dependent on the density, sequence, and availability of the immobilized ssDNA. Probe density can be a controlling factor for efficiency of target capture as well as for the kinetics of target-probe hybridization, due to the accessibility of the surface-immobilized probe [9].

To immobilize the probe, 10 µl of thiolated oligonucleotide solution (0.100 µM) was deposited onto the center of the Au electrodes. The probe was then incubated at 37°C for 20 minutes to increase the binding rate of DNA to the Au surface. The thiolated DNA solution was then removed from the Au, and washed three times with a Tris-HCL solution (0.1 mM, pH 7.2). After washing, 10 µl of the Tris buffer was added back to the center of the electrode. Following the probe immobilization, the Tris buffer was removed and 10µl of the target oligo (complementary or non-complementary; 0.100 µM) was placed on the Au substrate (Figure 28). This solution was incubated again at 37°C for 20 minutes to increase hybridization time and specificity of the probe for the target. The target DNA solution was again removed from the Au electrodes, and washed three times with a Tris-HCL solution (0.1 mM, pH 7.2). After washing, 10 µl of the Tris buffer was added back to the electrode and analyzed by fluorescent microscopy.

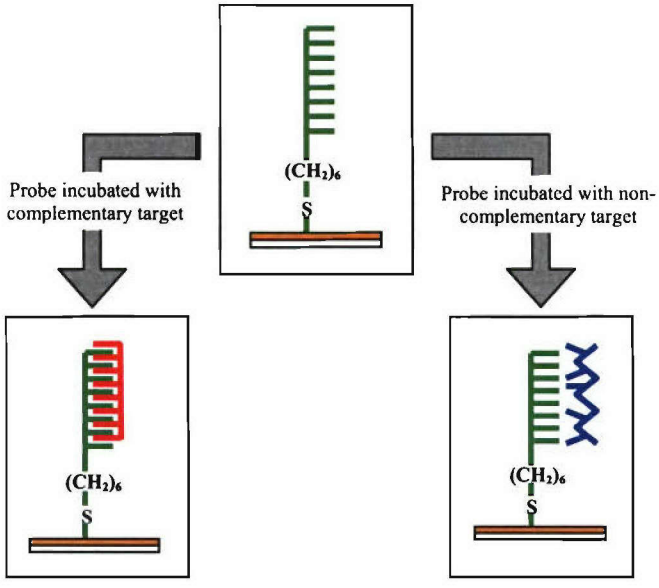

Figure 28: Schematic representation of fluorescent oligonucleotides hybridization

Fluorescently-tagged oligonucleotides were used initially, to show feasibility of the process by which all further experimental conditions would be kept constant. On four separate Au substrates, four different setups were used. On the first substrate, the Cy3 labeled, thiolated probe was immobilized and viewed for surface binding on Au with a fluorescence microscope. The oligonucleotide binding of the probe can be seen as the bright red color in Figure 29 (a). Once probe immobilization had been established, non-fluorescent tagged thiolated probes were immobilized on the next three Au substrates, so that a constant baseline experimental setup could be established. On the second Au substrate, free Cy5 dye (not tagged to an oligonucleotide) was added to the non-fluorescent tagged thiolated probed bound to Au as a control or background to ensure that only the oligonucleotides were binding and not the dye itself. The free Cy5 dye image taken with the fluorescence microscope was basically negative; almost completely black (Figure 29 (b)), thus indicating no binding of the Cy5 dye to the Au surface. The third substrate was used for inspecting the actual hybridization events between the immobilized probe and complementary target. The fluorescent signal (blue color) obtained, indicated that the most binding occurred with the complementary target (Figure 29 (c)). The fourth Au substrate was used the same as the third, except a non-complementary target was used. Some hybridization did occur as indicated by the weak signal seen in Figure 29 (d). Ultimately, these results substantiated the experimental process that would be used for all further experiments.

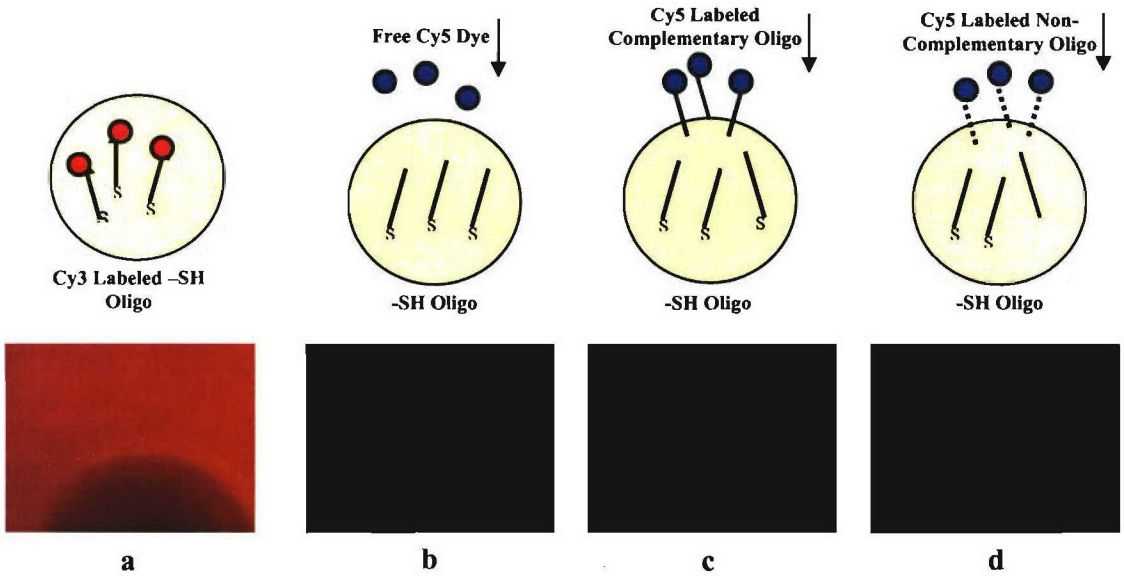

Figure 29: a) Immobilization of Cy3(red) tagged probe oligos; b) Cy5(blue) tag introduced onto non-tagged immobilized probe DNA; c) Hybridization between complementary oligo; d) Hybridization between non-complementary oligo and free dye to immobilized oligo probe

iii. Novel detection method

The DNA sensor method can be easily integrated into the CPMEMS broadband platform which utilizes SAW as the transducer signal output. Initial experiments as was stated earlier used fluorescent microscopy as the transducer output signal, a laboratory standard in detection of a binding or hybridization event. A number of electrical detection methods such as cyclic voltammetry have been used to study hybridization events. In the interest of creating a more versatile detection system, a new approach was investigated in order to detect a hybridization event, where the mode of detection was modeled after a capacitor. Figure 30 below gives an example of the parallel modeling of a capacitor and the DNA detection scheme that was investigated.

The modeling of the DNA sensor detection scheme to a capacitor more closely represents the overall structure of a simple parallel plate capacitor rather than its function as device to store energy. As shown is figure 30, the components of the DNA sensor are analogous to the capacitor where the Tris-HCL solution and the Au electrode act as the parallel metal plates of a capacitor, and the probe oligos are analogous to the dielectric material of a capacitor. The idea is that the baseline condition is where the thiolated oligo probes are immobilized onto the Au electrode and immersed in the Tris-HCL solution. The Tris-HCL solution is slightly ionic and thus allows for conduction from the solution through the oligo probe monolayer down to the Au electrode. When oligonucleotide hybridization occurs, this basically is analogous to a change in the dielectric constant of the capacitor.

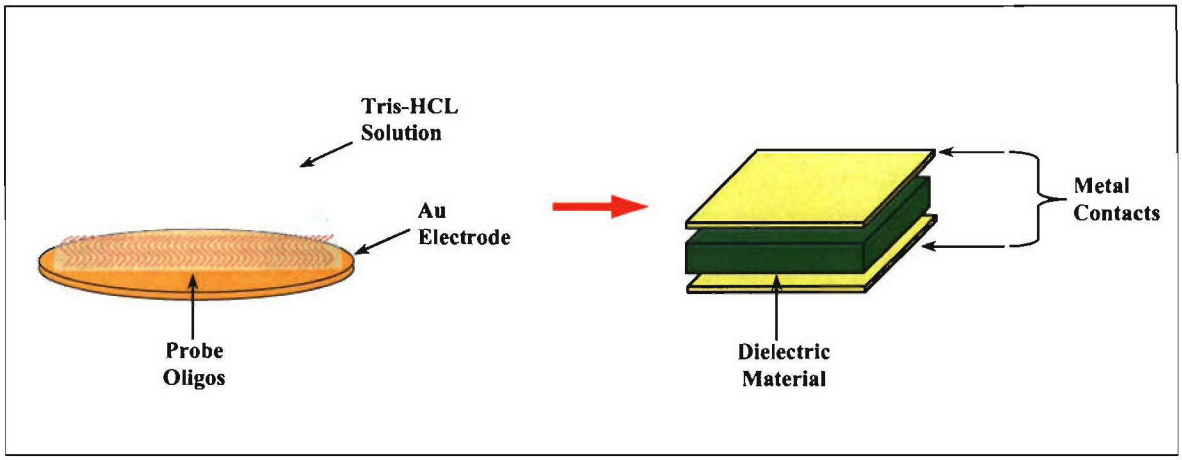

Figure 30: DNA sensor scheme modeled after simple parallel plate capacitor

Capacitors can be measured for their capacitance, impedance, and phase angle. In the case of the DNA sensor scheme, the transducer signal of interest that was measured was impedance (Z). A schematic diagram of the measurement setup is shown in figure 31 where the contact leads probe the Au electrode and the Tris-HCL solution to apply and AC signal as well as measure the impedance (Z). Figure 103 shows the detection process from the baseline detector to actual detection of a control complementary antigen as well as a control non-complementary antigen. The test conditions that were utilized for the proof of concept studies using fluorescence microscopy were repeated with this new impedance measurement scheme. Impedance measurements were taken at each of the four stages shown in figure 32; from just the buffer Tris-HCL solution, to the probes being immobilized on the Au surface, to the final hybridization of both the complementary as well the non-complementary oligos.

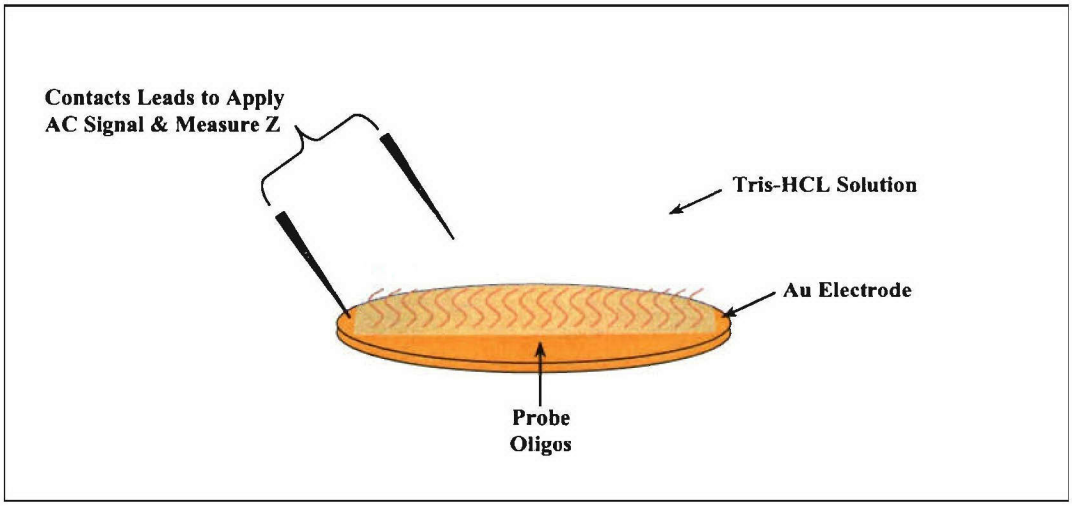

Figure 31: Schematic diagram of measurement setup

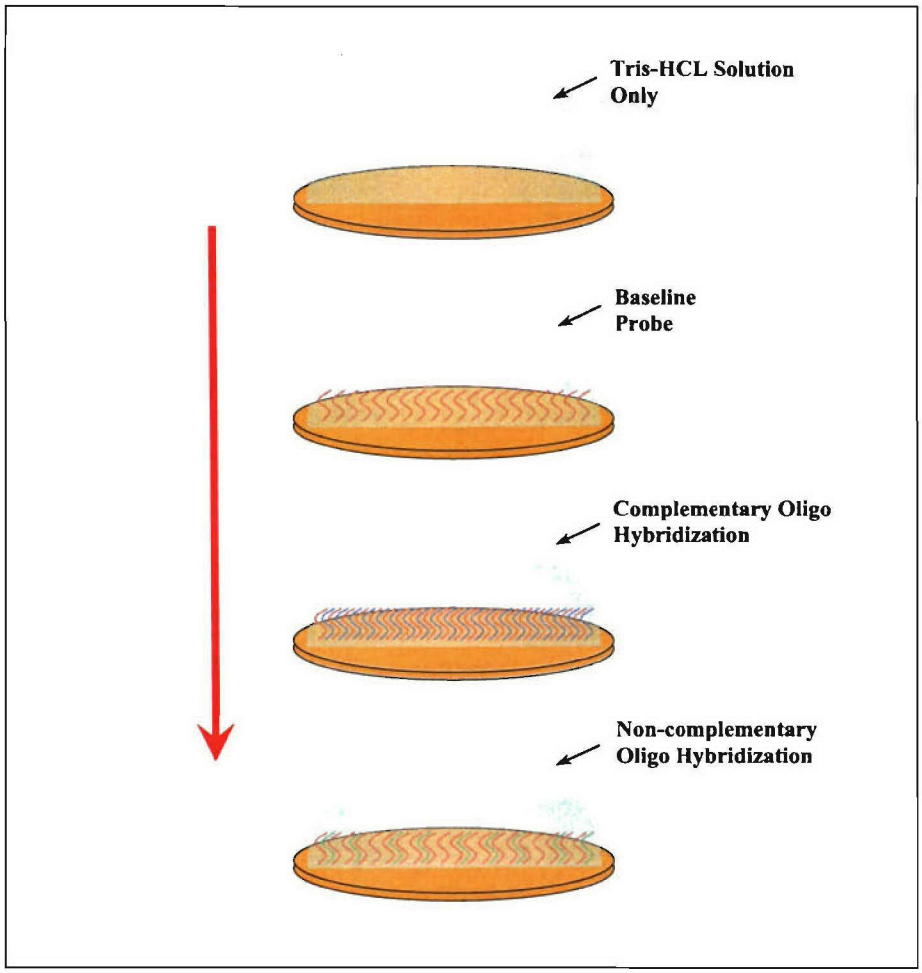

Figure 32: Four stage detection process for obtaining impedance measurements

i. Oligonucleotide hybridization using impedance detection

The instrumentation setup to conduct the impedance measurements included a function generator to produce an AC signal along with a voltage preamplifier and a 100 kΩ resistor in series with the sample test device (DNA sensor). This resistor is used to be the dominant resistor, making the resistance of the sample negligible and thus allowing for the current through the sample to be held constant. An oscilloscope and a spectrum analyzer were also used to measure the output signal of the test device. A schematic diagram of the instrumental setup to conduct the impedance measurements is shown in figure 33. The spectrum analyzer allows for analysis of the amplitude response of the test device against frequency and can measure very low voltage levels at even high frequencies.

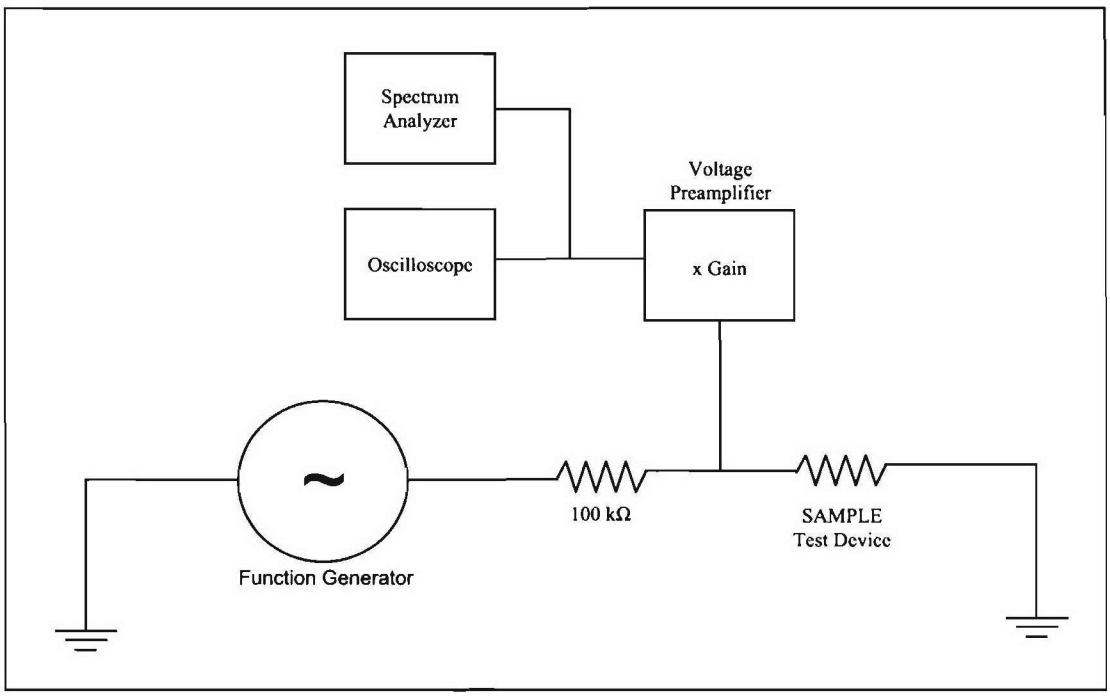

Figure 33: Schematic representation of impedance analysis instrumentation

Initial studies revealed that the electrode setup which consisted of one Au electrode and the other electrode being the Tris Buffer solution did not give much of an impedance signal output. The design of the electrodes was modified slightly to obtain an increased impedance signal as shown in figure 34. In this new design scheme the modeling after a capacitor is still made except that now the two Au electrodes are analogous to the metal plates and the Tris-HCL solution + probe oligo combination would be analogous to the dielectric material. A macro-scale device was designed similar to the existing MEMS structures. This would allow for a more feasible transition into the micro-scale level using the CPMEMS structures.

Prior to immobilization of the probe oligos to the Au electrodes, 10 µl of the Tris buffer was placed at the center of the electrodes and Z measurements were taken. These measurements were taken to subtract any background noise associated with the buffer solution itself. To immobilize the probe, 10 µl of thiolated oligonucleotide solution was deposited onto the center of the Au electrodes. The probe was then incubated at 37°C for 20 minutes to increase the binding rate of DNA to the Au surface. The thiolated DNA solution was then removed from the Au, and washed three times with a Tris-HCl solution (0.1 mM, pH 7.2). After washing, 10 µl of the Tris buffer was added back to the center of the electrode. Impedance measurements were then performed. These impedance measurements signify the base signal before any detection event occurs.

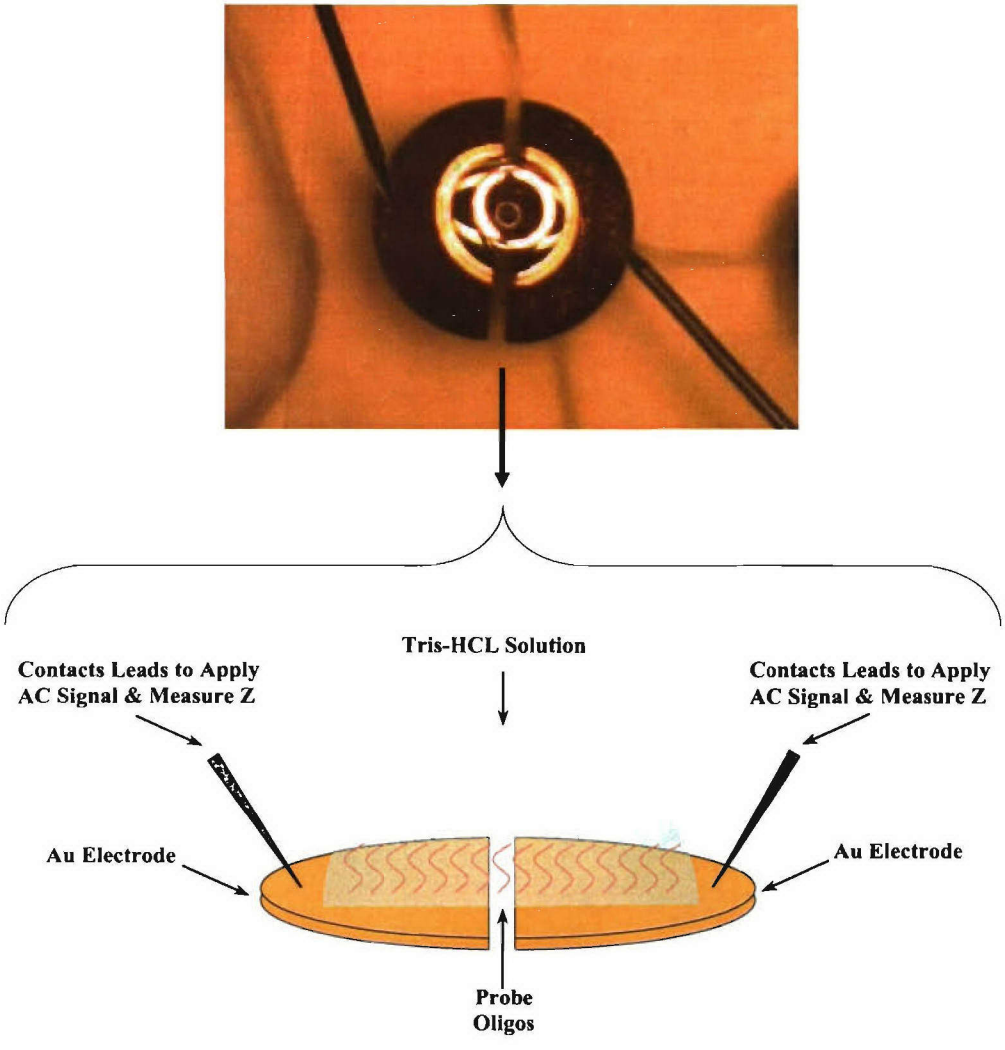

Figure 34: New electrode design to conduct impedance measurements of oligo hybridization

Figure 35 shows the progression of the study to obtain impedance measurements as function of DNA-DNA hybridization. The probe oligos were immobilized onto the Au substrate and Z measurements were taken. Following the immobilized probe analyses, the Tris buffer was removed and 10 µl of the target oligo (complementary or non-complementary) was placed on the electrodes. This solution was incubated again at 37°C for 20 minutes to increase hybridization time and specificity of the probe for the target. The target DNA solution was again removed from the Au electrodes, and washed three times with a Tris-HCl solution (0.1 mM, pH 7.2). After washing, 10 µl of the Tris buffer was added back to the center of the electrode, and impedance trials were once again performed.

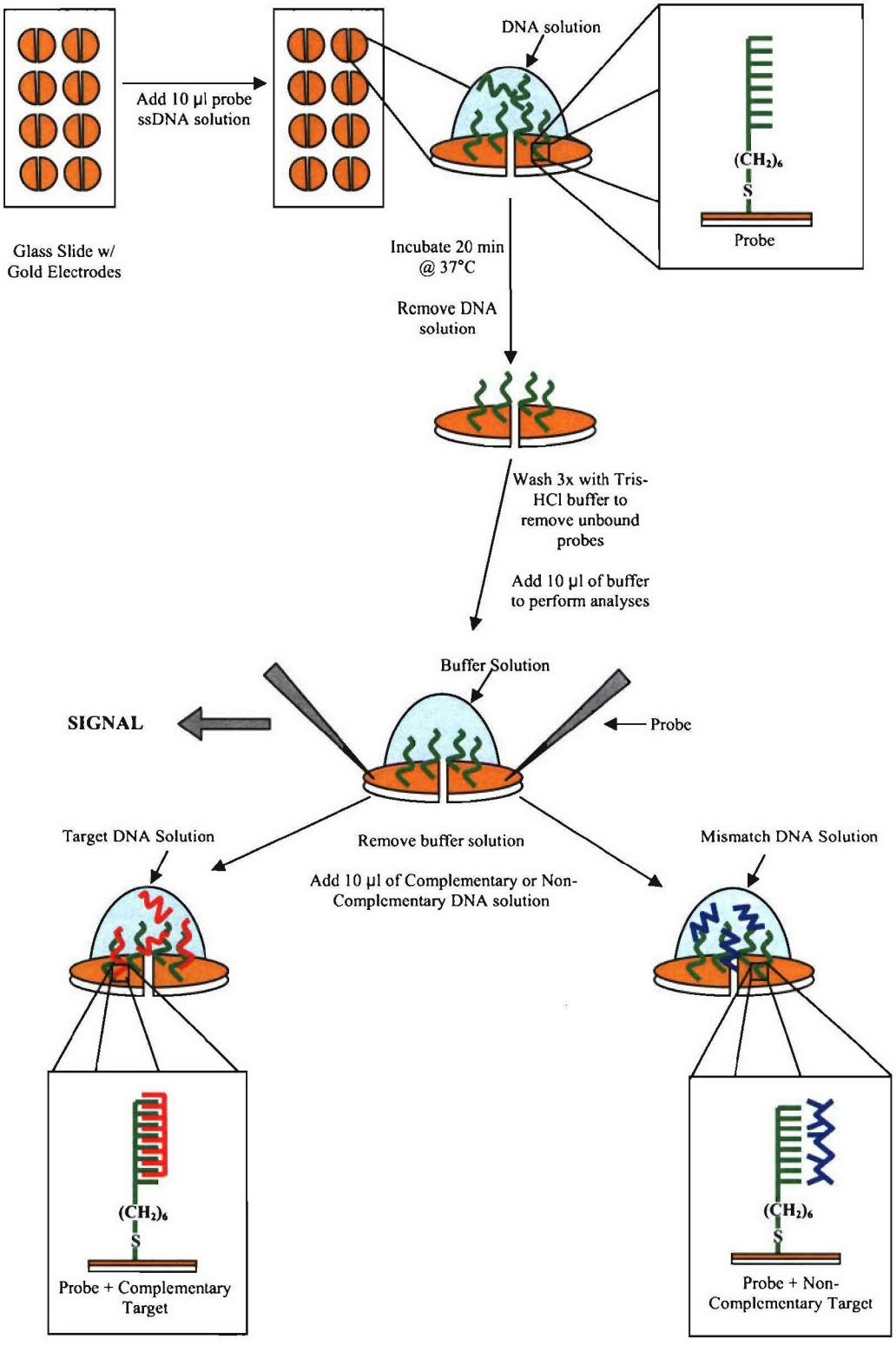
Add 10 µl probe ssDNA solution
DNA solution
Glass Slide w/ Gold Electrodes
Incubate 20 min @ 37°C
Remove DNA solution
Wash 3x with Tris-HCl buffer to remove unbound probes
Add 10 µl of buffer to perform analyses
Buffer Solution
SIGNAL
Probe
Target DNA Solution
Remove buffer solution
Add 10 µl of Complementary or Non-Complementary DNA solution
Mismatch DNA Solution
(CH2)6
S
Probe
Probe + Complementary Target
Probe + Non-Complementary Target

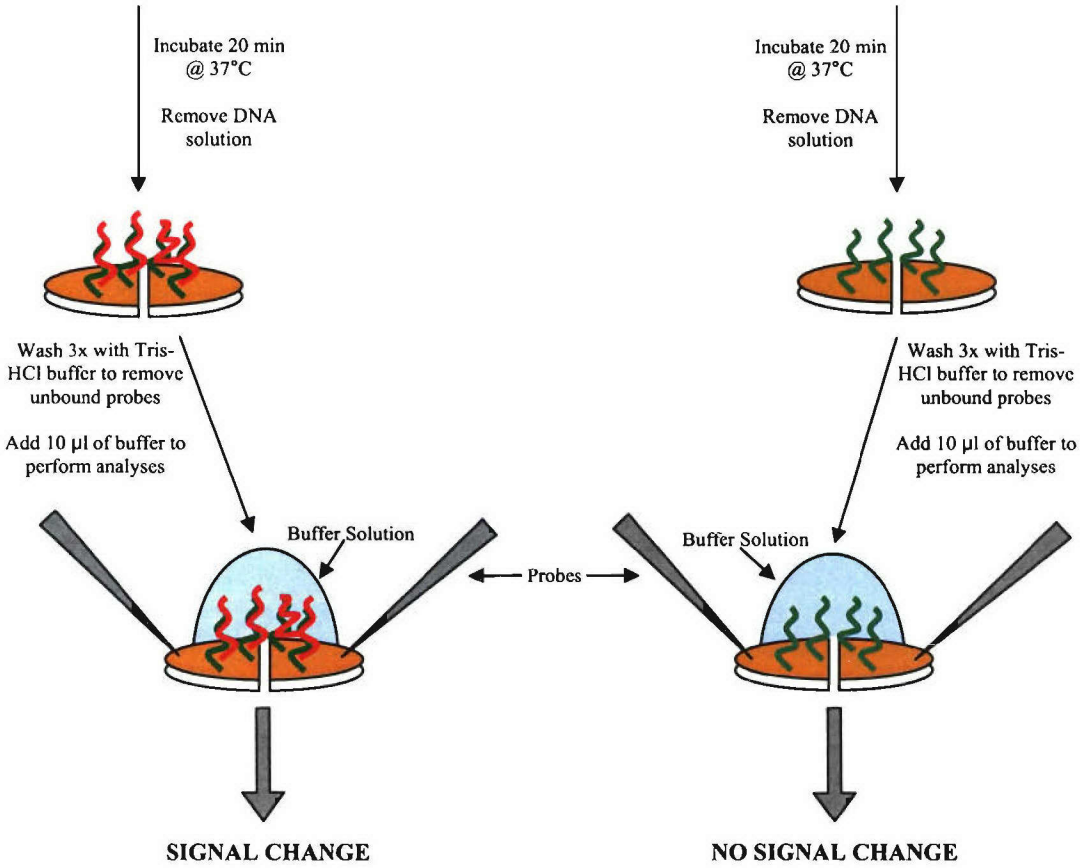

Figure 35: Schematic diagram of experimental procedure

The impedance instrumentation was set with constant parameters for every trial. The current flowing through the sample was fixed at 4 µA. This was accomplished by setting the function generator voltage amplitude to 0.2 V_p, which was read by the oscilloscope as 0.4 V_{pp}. Using Ohm's Law, the current can be calculated by dividing the voltage peak-to-peak (0.4) by the resistance, 100 kΩ, which equals 4 µA. Other parameters of the function generator were established; the frequency sweep range was set from 1 Hz to 300 kHz at a rate of 13 Hz, and the offset and phase stayed at 0_{pp} and 0 degrees, respectively. The gain of the voltage preamplifier was set to 50 V/V. The spectrum analyzer could only sweep the frequency range from 0 kHz to 100 kHz, but averaged the values of 20,000 sweeps for one measurement. For each sweep, 400 data points were collected, starting from 0 kHz to 100 kHz in increments of 0.25 kHz. As mentioned previously, a spectrum analyzer is useful for analyzing the amplitude, or voltage response of a device against frequency. The measurements obtained using the spectrum analyzer was the rms voltage (V_{rms}) and thus was converted to peak to peak voltage (V_{pp}). The voltage gain factor was then divided out of the spectrum analyzer voltage measurement for total voltage

of the sample and then divided by current for the total impedance. The standard calculation for each data point, X, was the following:

$$V_{pp} = \frac{X * 1.414 * 2}{50}$$ where,

X = voltage value obtained from the spectrum analyzer,
1.414 = factor to convert from V_{rms} to V_p,
2 = factor to move from V_p to V_{pp}, and
50 = voltage gain factor (V/V).

Then to calculate total impedance, Ohm's Law was used:

$$Z = \frac{V_{pp}}{I}$$ where,

Z = total impedance (in ohms),
V_{pp} = total voltage peak-to-peak of sample, and
I = total current of sample (constant = 4 μA or 4 * 10^{-6} A)

Total impedances, once calculated, were plotted against frequency, as shown in the following experimental impedance results section.

For the initial set of experiments, the impedances of the buffer, probe, complementary target, and non-complementary target were all compared (figure 36 and figure 37). The first experiments were run in parallel on 4 electrodes on 2 glass slides. The results of the trials were all compiled by averaging (figure 36). The impedance of the buffer had the highest signal and when the probe was added to the electrode, the impedance dropped by approximately 25 Ω. This drop is most likely due to the interface between the Au and the solution that the current that passes through. The probe may form a better interface for the current to travel through than just the buffer alone, thereby causing the impedance decrease. Next, when the actual complementary target was added to the probe oligos, the impedance increased due to the hybridization events. When non-complementary targets were added, no impedance change was detected due to little or no binding. The same experiment was repeated using 7 electrodes from 1 glass slide (figure 36). Since there is high variability between electrodes, the 7 trials were not averaged with the first 8 trials. In the 7 trials, the complementary target changed from the probe by only 8 Ω; the impedance values of the non-complementary target actually dropped by about 2 Ω. This may relate to a random error in more rigorous washing conditions or in electrode surface differences.

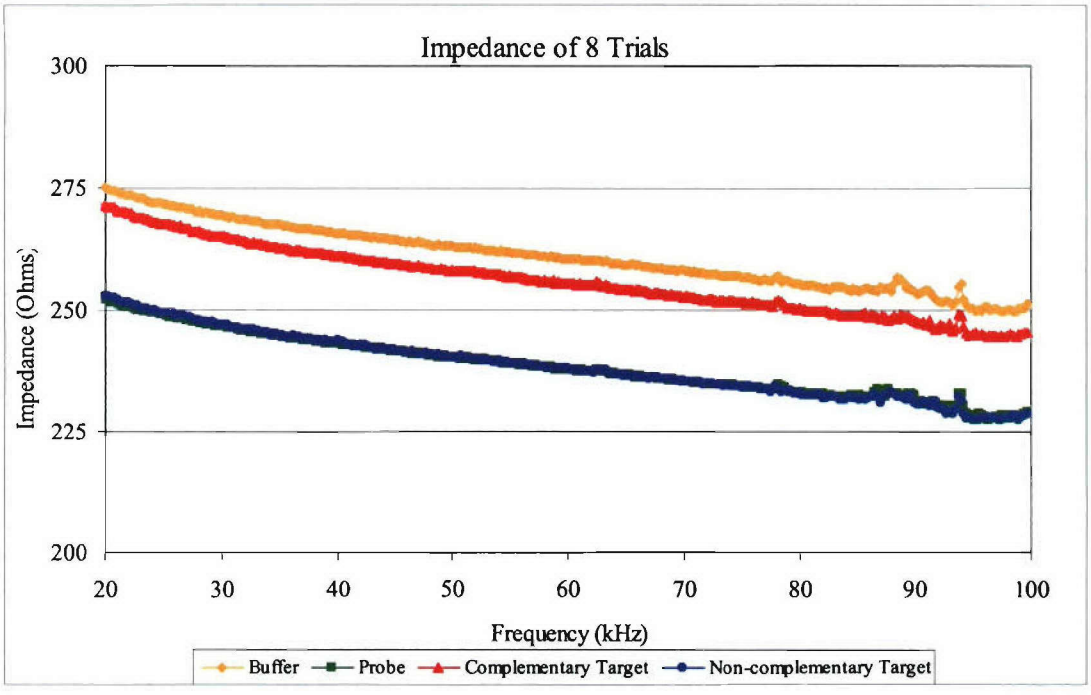

Figure 36: Impedance values of 8 averaged trials of buffer, probe, complementary and non-complementary targets over a range of frequencies

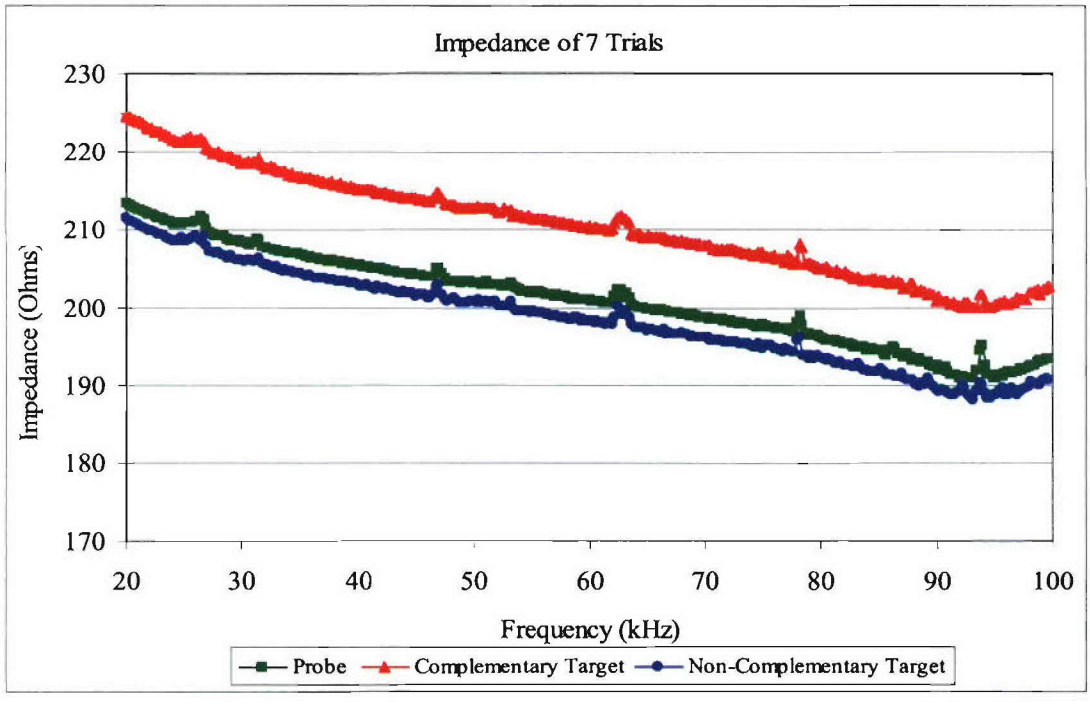

Figure 37: Impedance values of 8 averaged trials of buffer, probe, complementary and non-complementary targets over a range of frequencies

By subtracting the probe values from the target values, the signal change between complementary and non-complementary targets was identified. The difference between the complementary and non-complementary target from the probe (8 trials) was approximately 17 Ω and 0 Ω, respectively (figure 38). The difference between matching and mismatching targets (7 trials) was about 10 Ω and -2 Ω, respectively (figure 39). The percent change was calculated for both the 8 trial experiment and the 7 trial experiment. The result was a signal change of 7% when a complementary target is detected versus a non-complementary target when 8 electrode trials were averaged (figure 40). A signal change between complementary and non-complementary targets of approximately 5% was detected for the 7 electrode trial (figure 41). Whereas the non-complementary target in the 8 electrode trials produced no percent signal change and the non-complementary target in the 7 electrode trial produced a -1% change.

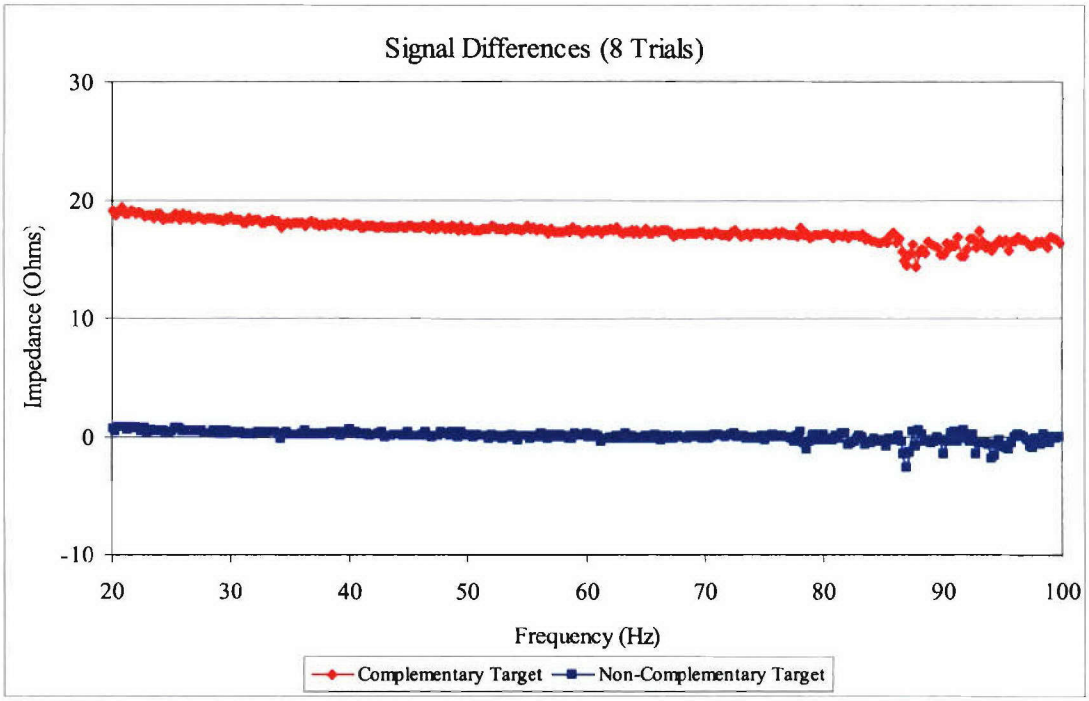

Figure 38: Signal differences (n=8) between complementary and non-complementary targets

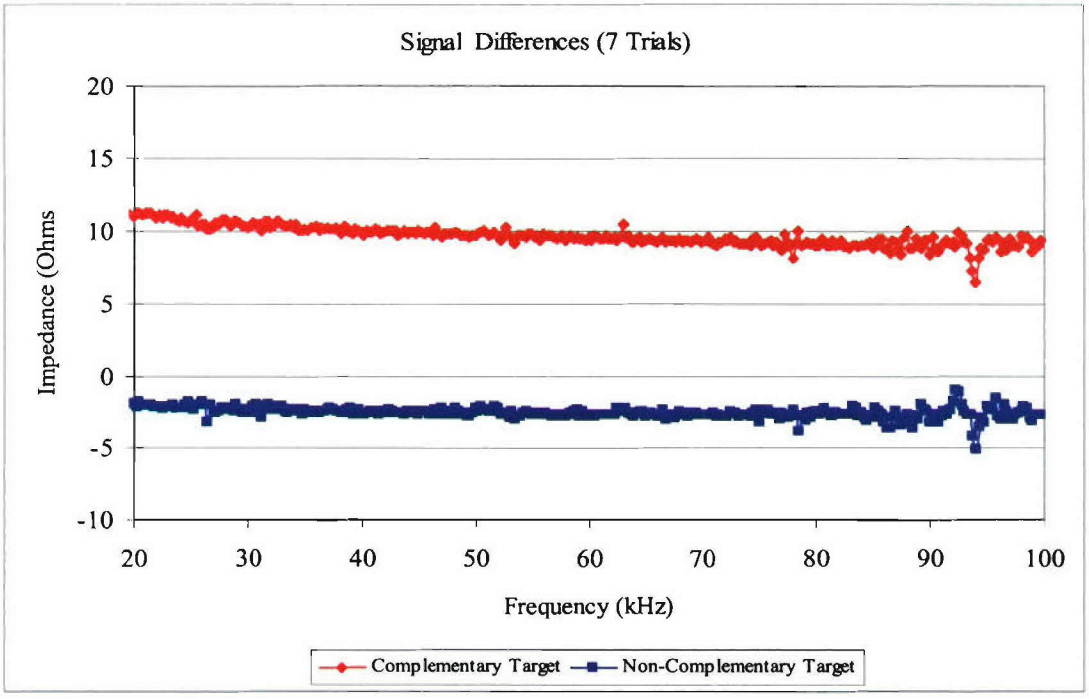

Figure 39: Signal differences (n=8) between complementary and non-complementary targets

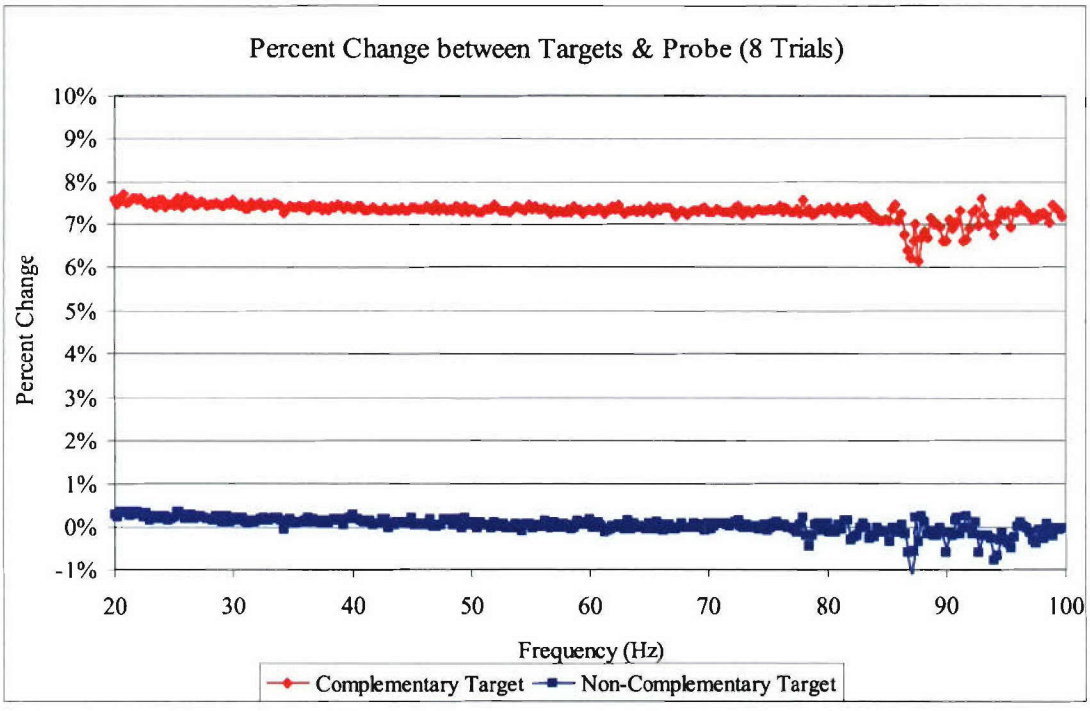

Figure 40: Percent impedance change of the target oligonucleotides from the probe

These results demonstrate the initial feasibility of producing a signal change for detection of DNA hybridization events. For oligonucleotide hybridization detection, it is important to achieve a baseline or threshold for what is considered normal or a "negative" signal. Then, when a certain threshold is crossed, or a signal change is produced of a certain amount, a "positive" hit (hybridization event) can be identified. For instance, in the case of the 8 trials shown in Figure 3.19, 0% would be considered a baseline, while, 7% could be considered as a threshold, and any signal above that would be deduced as a positive hybridization event. However, a threshold of 5% may be more acceptable, as in the case of the 7 trials shown in figure 41, where signals above 5% would be detected as a positive hybridization event.

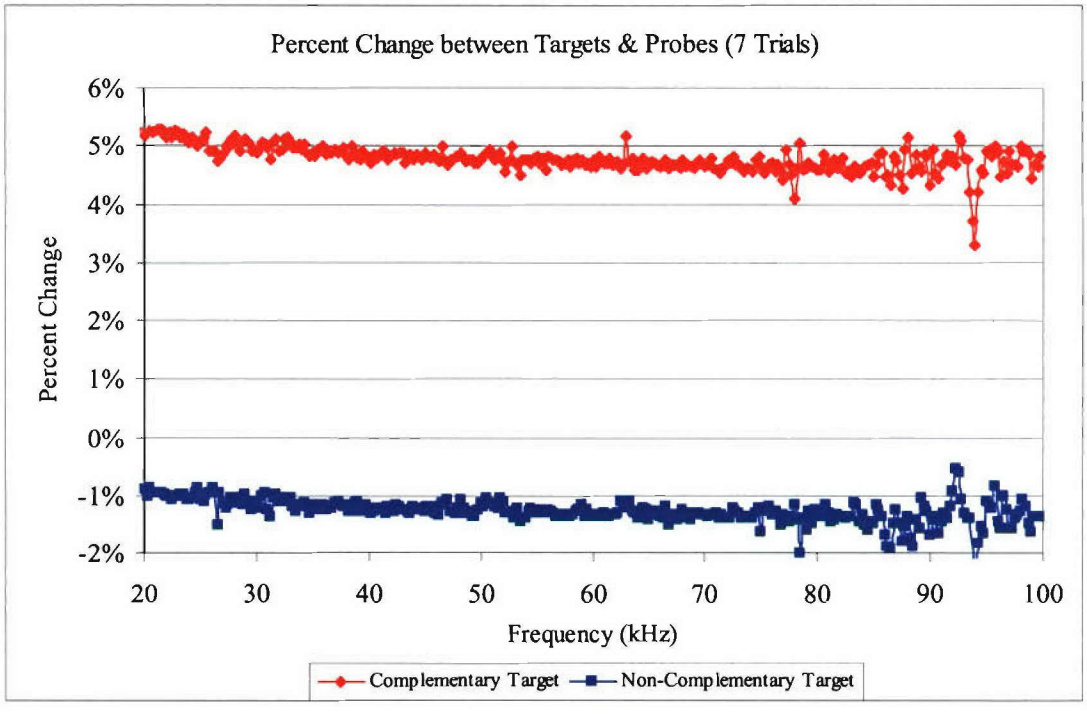

Figure 41: Percent impedance change of the target oligonucleotides from the probe

One concern that must be overcome is the variability of impedance measurements between Au electrodes. The signal trends appear to be similar from electrode to electrode, however, the actual values observed vary from electrode to electrode. This inconsistency is demonstrated by the differing impedance values for identical probes between the 15 different electrodes used. If just the averages of both of the 2 completed trials are compared (8 trials averaged from 4 electrodes on 2 slides and 7 trials averaged from 7 electrodes on 1 slide), the difference between total probe impedance averages is approximately 40 Ω (figure 42). If all probe impedances would have been averaged together, the standard deviation would have been about 20 (figure 43). Thus, fabrication of the Au electrodes must be optimized or each individual trial must be characterized individually.

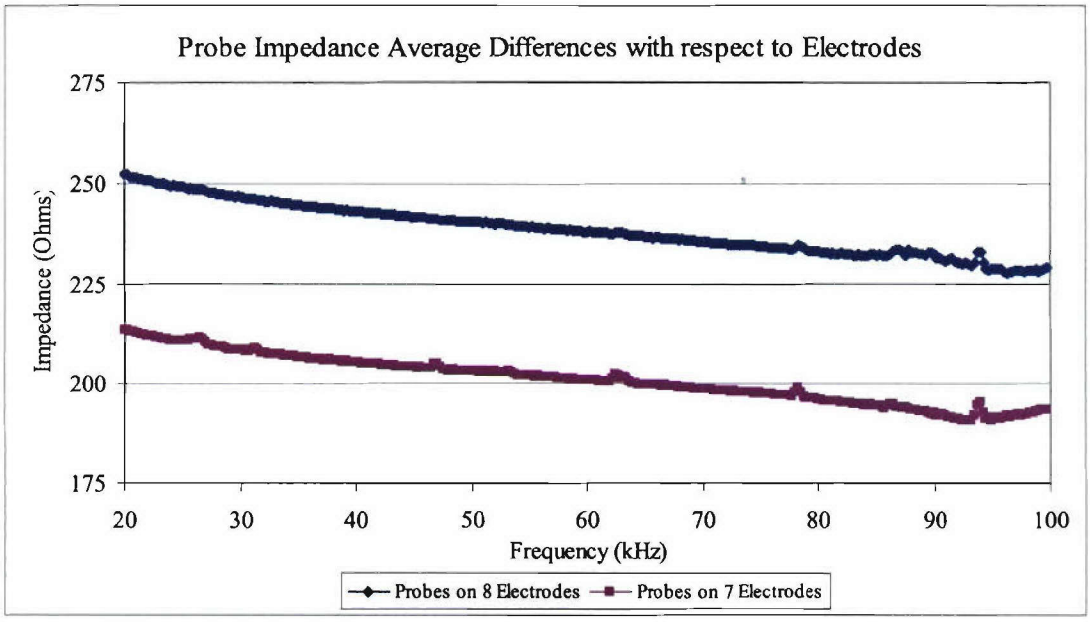

Figure 42: Differences between averages of probe impedances on individual electrodes

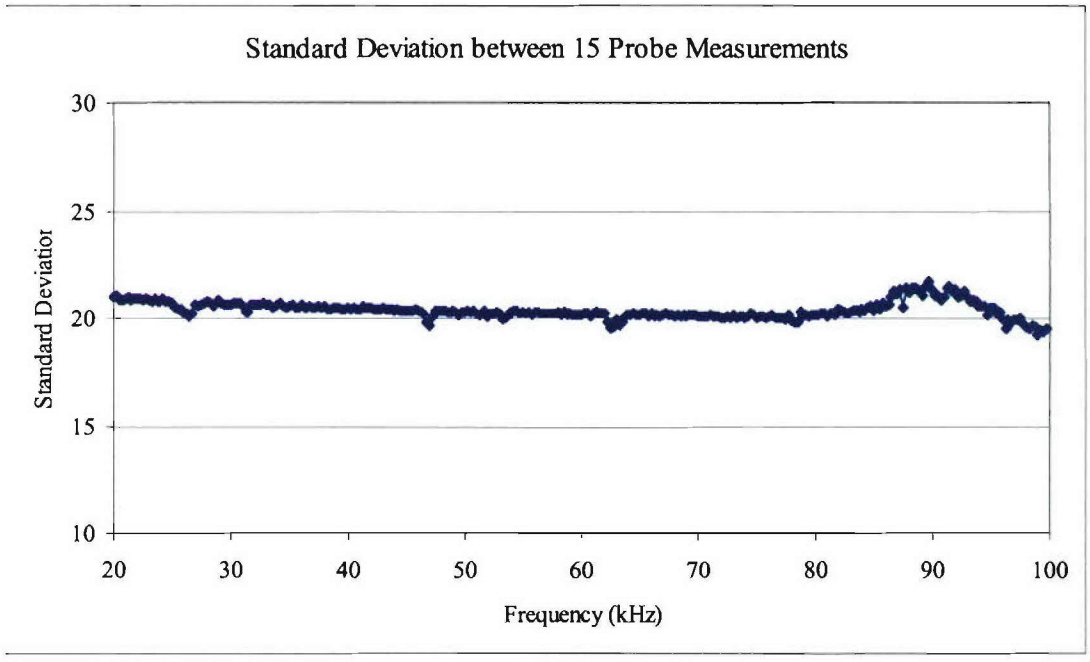

Figure 43: Standard deviation of all 15 probe impedance trials averaged collectively

A study was done to compare the detection of synthesized targets versus actual targets for further feasibility of an actual biosensor. An oligonucleotide probe, EC1-1F (5' - SH – $(CH_2)_6$ – AGCCTCGGTGTAAAGT - 3'), was used to detect the bacteria *Escherichia coli* (*E. coli*). Actual *E. coli* bacterial cells were sonicated to break up the cells into innumerable pieces of DNA. The sonicated material is then ready to be introduced to the impedance electrode system. After the EC1-1F probe was immobilized (see previous experimentation setup procedures), the target sample of *E. coli* was introduced to the electrode. *Psuedomonas aeruginosa* (*P. aeruginosa*) was also sonicated and was added to an adjacent electrode as a non-complementary target control, and impedance measurements were then obtained (figure 44).

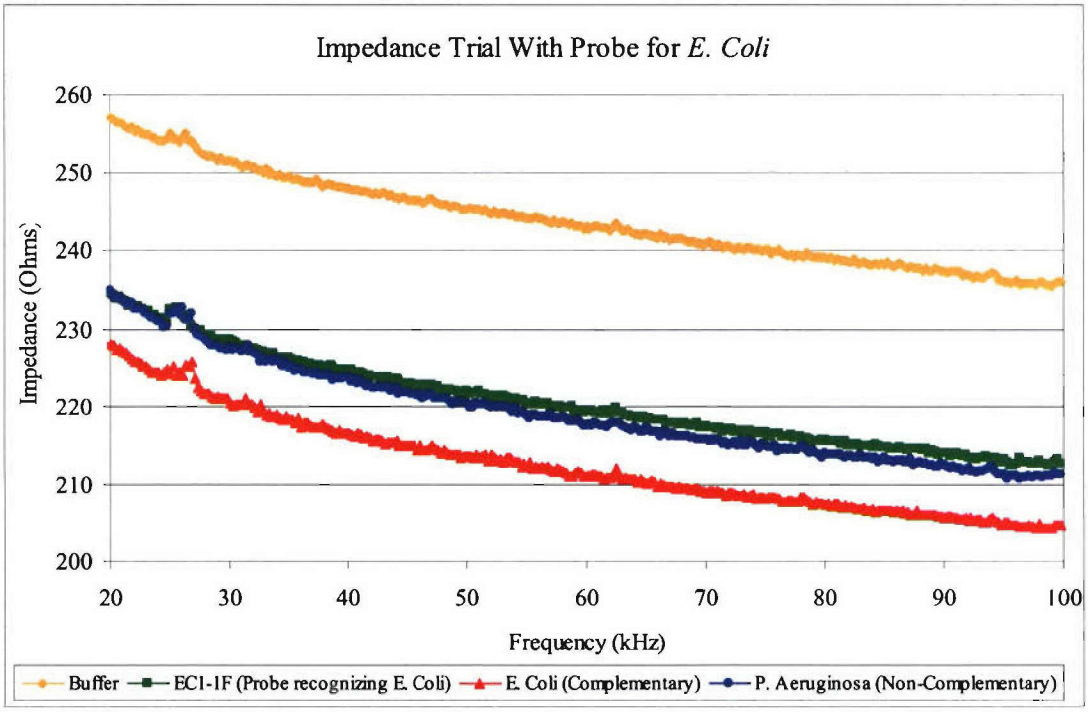

Figure 44: Impedance results for experimental run using an actual probe sequenced for *E. coli* and targets of *E. coli* and *P. aeruginosa* bacterial sonicated cells

For the experiment using the EC1-1F probe, the impedance of the buffer had the highest signal once again, just as the synthesized runs. It was determined that when the probe was immobilized to the Au electrodes, the impedance decreased by approximately 20 Ω. This drop was again most likely due to an increased interface between the Au and the solution. Next, when the actual *E. coli* complementary target was added to the immobilized probe electrode, a signal change in impedance resulted due to the hybridization events. When the non-complementary target of *P. aeruginosa* was added, no impedance change was detected due to minimal binding occurring. The drop in impedance of the complementary target may be attributed to the very specific relationship between probe and target. Further studies must be performed to determine the affects of this relationship on the direction of signal change. By subtracting the probe values

from the target values, the signal change between complementary and non-complementary targets were identified (figure 45).

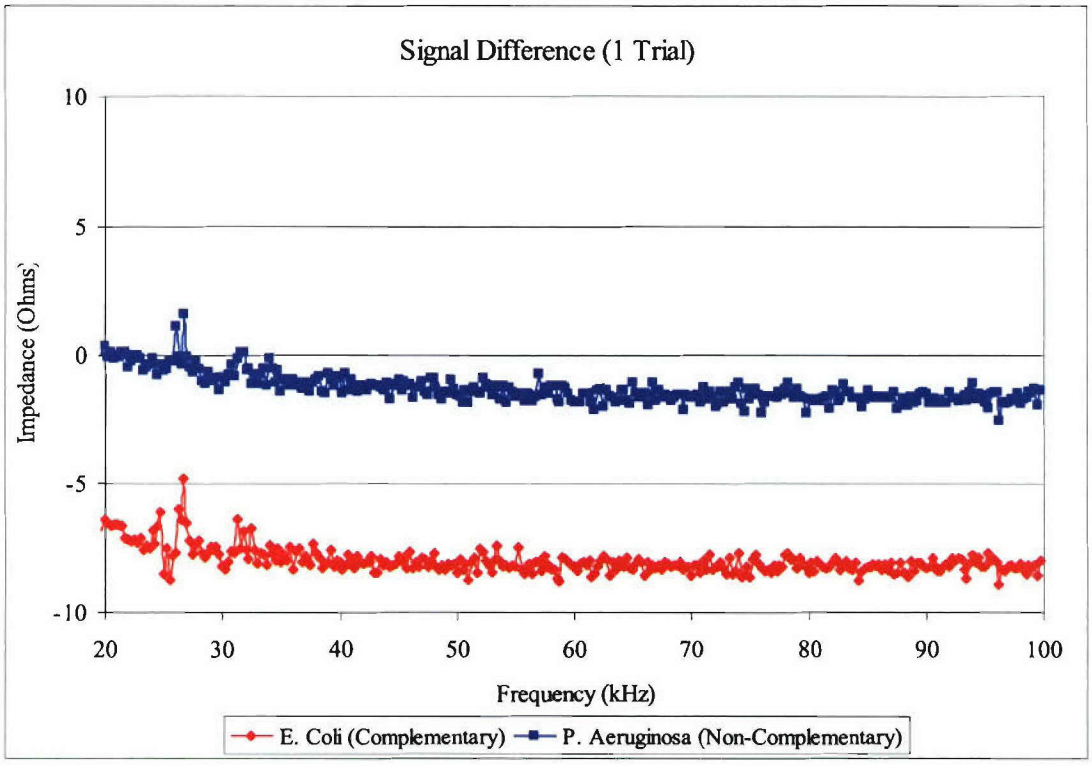

Figure 45: Impedance differences between complementary and non-complementary targets using *E. coli* and *P. aeruginosa*

The difference between the complementary and non-complementary target was only 8 Ω, which is lower than the signal change observed with the synthesized probes and targets. The percent change was calculated, resulting in signal change of 4% when a complementary target was detected versus a non-complementary target (figure 46). As mentioned previously, this signal change must be studied in further detail to characterize specific interactions of impedance changes as hybridization events between varying probes and targets occur.

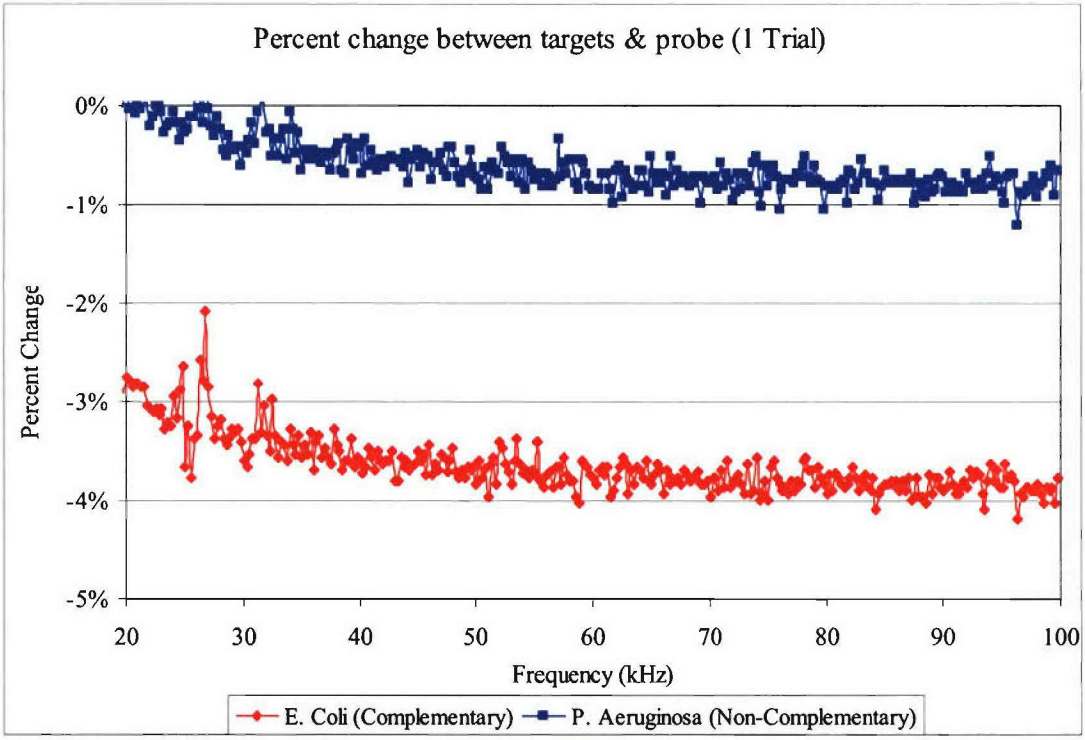

Figure 46: Percent impedance change of the target oligonucleotides from the probe EC1-1F

v. Detection approach of oligonucleotide probes

There are two approaches in oligonucleotide detection. The first is direct detection of pathogens, which involves designing a probe that will hybridize to a segment of DNA that is unique to only that organism. This works well only for cases where the organism of interest is known. In cases where the organism is unknown and potentially hazardous, a second approach is more effective, which entails classification of taxonomical hierarchies. With this approach probes are designed such that they recognize groups of organisms following the groups of a taxonomical tree.

In cases where organisms have been purposely modified, the first direct approach would not reveal a positive signal, however the second approach would look for genomic characteristics that are inherent for certain classes or groups of organisms. A hypothetical example of a taxonomical tree is shown in figure 47.

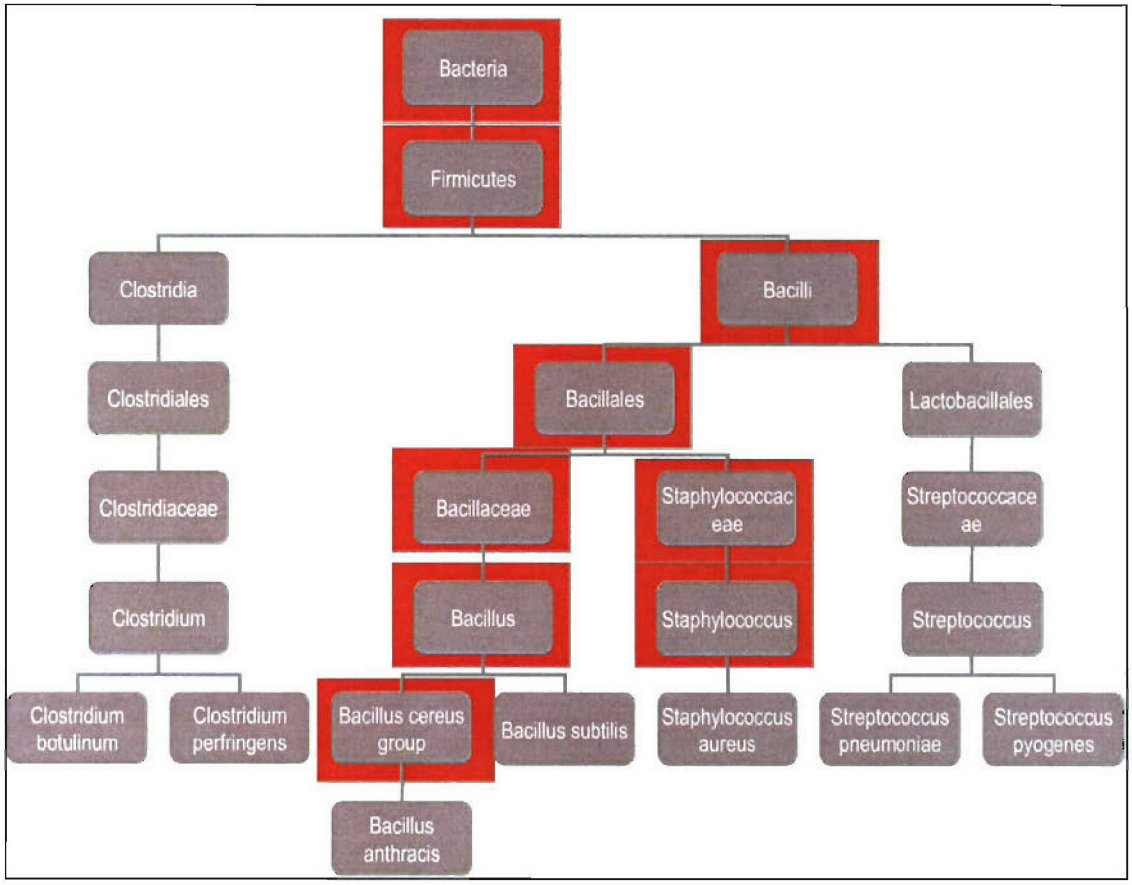

Figure 47: Illustration of detection by taxonomical classification

Figure 47 shows one of the many subtrees within the bacterial taxonomical tree. If for instance two bacteria such as *Bacillus anthracis* and *Staphylococcus aureus* were to be combined to make a superbacteria, it would not be detected by the first direct detection method. Direct detection can be conducted simultaneously in this manner, but would only reveal a positive hit of an actual antigen in the case of a specific hybridization. With taxonomical classification, sensors breaking down the tree would send up red flags so that a more extensive detection procedure can be undertaken to determine what exactly has caused the sensors to send out a warning. Allowing for an early warning of a possible threat would help to quickly alleviate or even avoid a disaster.

Figure 48 shows a simple classification example that was investigated for proof-of-concept simulations. Probes were specifically designed for both taxonomical classification as well as direct detection. A sample containing fungi or bacteria can be tested by simultaneous measurement of a series of biosensors. It can be determined whether it contains fungi, bacteria, and specifically *Escherichia coli*, *Staphylococcus aureus*, *Bacillus subtillis*, and *Streptococcus pyogenes*. The goal of classification is to develop a more broad detection method, which can be tailored such that it can simultaneously detect not only a class of organisms but also a single

organism. Eventually all pathogens considered as threats can be detected through a series of probes transcending the taxonomical hierarchies.

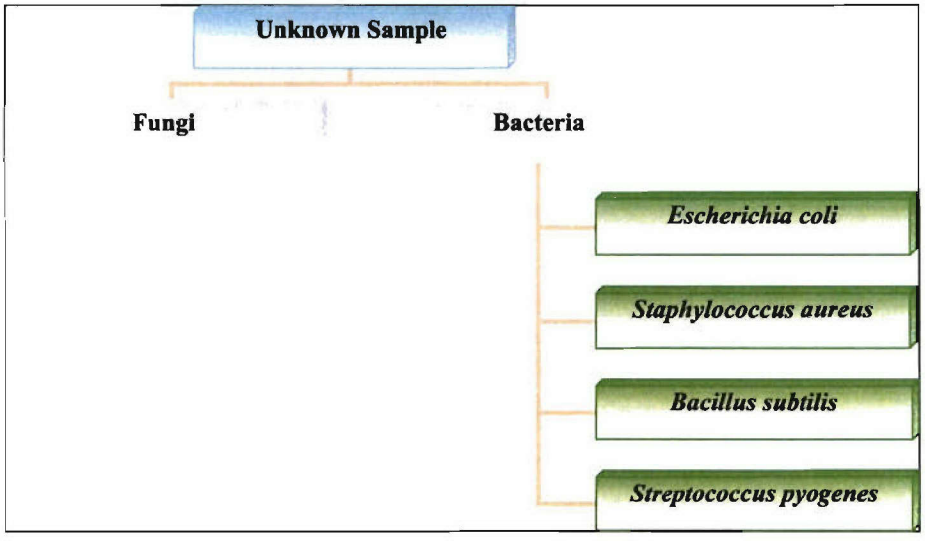

Figure 48: Illustration of a current classification method for a possible biological antigen

vi. Oligonucleotide immobilization on Au/PSA material

Fluorescent trials, using the same immobilization procedures as for the Au substrate, were conducted on the Au/PSA carbon and polymer material. The trials revealed that good oligonucleotide probe binding had occurred to the carbon and polymer material. Thiolated and non-thiolated oligonucleotides were placed on varying pre-implant thickness substrates, and the binding affinity was determined to show the feasibility of attaching the oligonucleotides onto the carbon and polymer material such that a transducer signal could be established in light of a detection event (figure 49). The oligos were bound to a low concentration of Au mixed with PSA sample and a high concentration of Au mixed with PSA. As seen in figure 49 binding of thiolated oligos did occur to the Au/PSA materials, where as the unthiolated oligos did not show any binding.

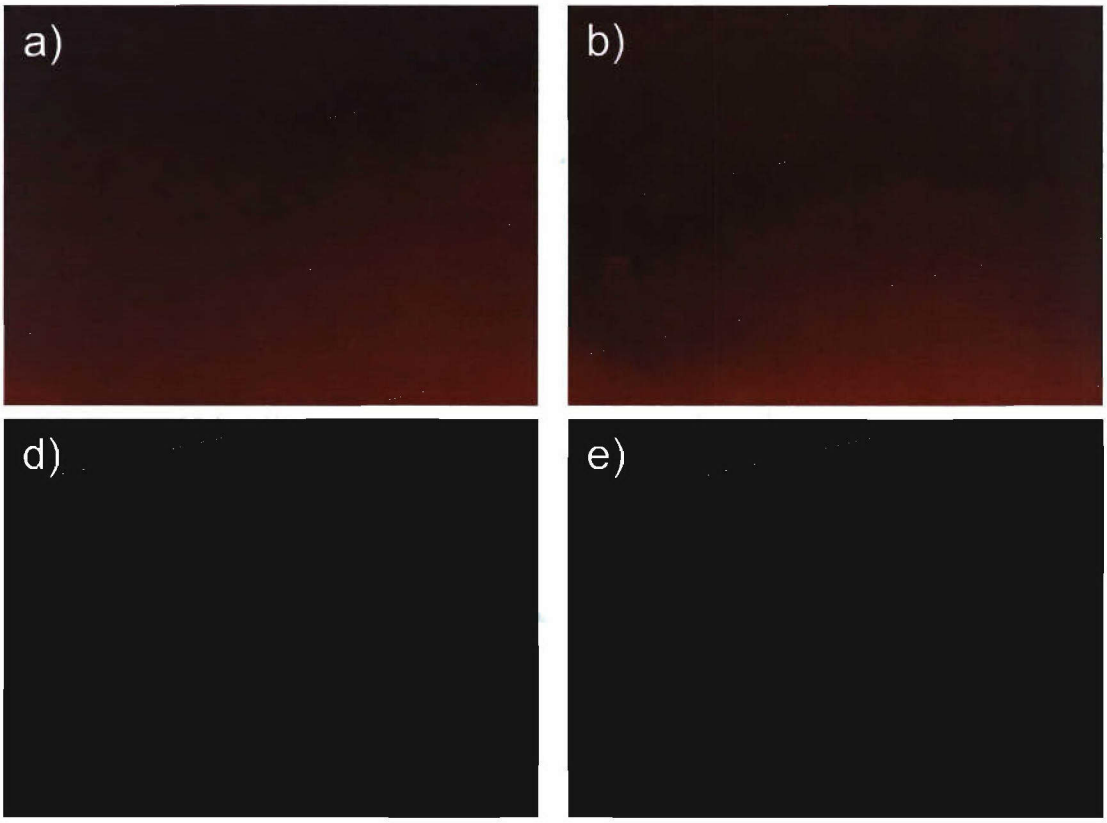

Figure 49: Fluorescently-tagged oligonucleotides bound to different Au/PSA substrates, all incubated for 20 min @ 37°C. a) Cy3 thiolated probe oligo on 25Å Au/PSA. b) Cy3 thiolated probe oligo on 75Å Au/PSA. c) Cy5 non-thiolated oligo on 25Å Au/PSA. d) Cy5 non-thiolated oligo on 75Å Au/PSA.

1.3.2.4 Unique Sense & Release Technology

Crosslink, one of the subcontractors on this project investigated the development of active sense and release experiments for incorporation into the broadband platform. The unique sense and release technology was developed such that it could be integrated into the broadband platform with the capability of releasing specific agents that would interact with antigens for the purpose of conducting multi-component platform experiments. The release of these agents is controlled by an electroactive polymer delivery system, which is composed of release materials that could sense environmental changes and result in stimuli-sensitive agent delivery. The delivery system is utilizes inherently conductive polymers (ICP), due to their ability to deliver ionic agent species through their redox properties.

In these studies a polypyrrole/ poly(styrene sulfonate) (PP/PSS) host polymer system as shown in figure 50 was used to load and release cationic biomolecules such as dopamine, epinephrine, and metaproterenol; while a polypyrrole/ adenosine triphosphate (PP/ ATP) system and a polypyrrole/ salicylate system were used to study anionic biomolecule loading and release. Polypyrole can exist in either an oxidized or natural form, and it is this conversion between the two forms oxidation and reduction that allows for electrical addressability by an electrode or MEMS pixel. The counter ions can be either loaded or released from PP on the pixel, which helps to maintain charge neutrality when it undergoes electrochemical switching. A small anionic agent molecule can be imbedded in the polypyrrole (PP) matrix through electro-polymerization and released through the electrochemistry reduction of the oxidized PP.

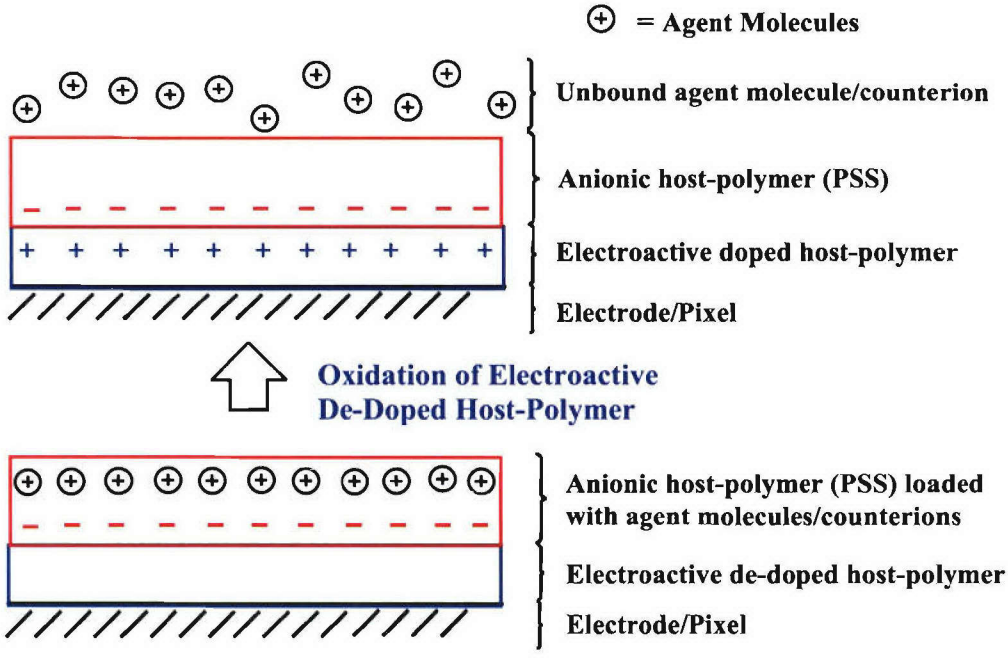

Figure 50: Cationic agent delivery system

The major part of this research and development plan was to build upon the above technology and extend it to target large molecules that have antibiotic and antibacterial activity. These electroactive polymer-agent systems would be synthesized either chemically or electrochemically. Utilizing microlithography the electroactive polymer-agent systems would then be patterned onto the CPMEMS platform so they may be electronically addressable.

The MEMS delivery devices shown in Figure 51 were fabricated using microlithography to conduct agent/antigen reaction experiments on the broadband platform. This would allow the platform to perform active experiments where feedback from a release event could be used to further improve antigen analysis or detection. The sense and release pixel configuration is shown in Figure 52. In response to a given recognition event (i.e. antigen-antibody detection or DNA-DNA hybridization), an agent molecule can be released through the functionalized conducting PP or PEDOT-OH is patterned on a gold working electrode pillar. A nearby Au counter electrode pillar can be used to produce the electric field necessary for release once a recognition event has been detected.

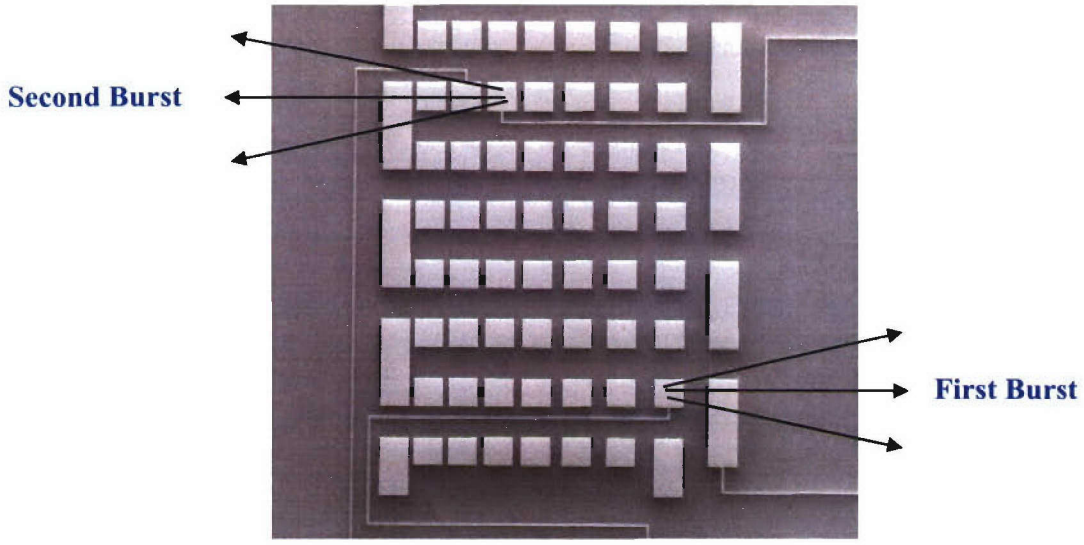

Figure 51: CPR burst release agent delivery system will be placed on the Au electrode pillars

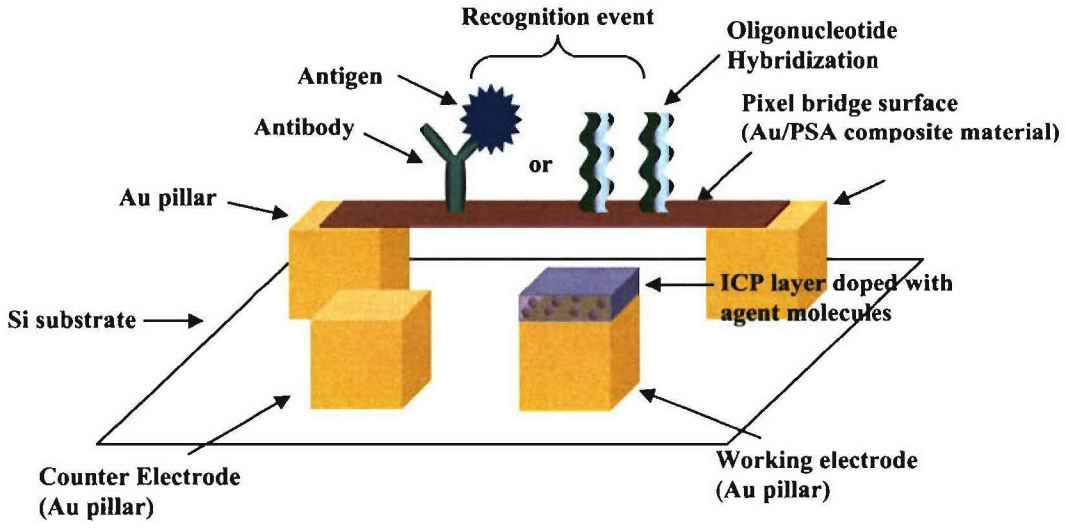

Figure 52: Sense and release pixel configuration where a release pixel is triggered in light of a recognition event.

a. Developing active sense and release experiments

The primary objective was to develop active sense and release experiments for incorporation into the broadband platform. Polypyrrole, a conducting polymer was chosen due to its redox switching property. Phenol red was selected for the initial study to prove the release concept. Carbon or Gold electrodes were deposited on a polycarbonate substrate. Initially, a Polypyrrole based film was prepared on the surface of the electrode through an electro-polymerization method. Electrode sizes were varied to determine design implications and feasibility for eventual incorporation into the MEMS platform. Figure 53 also shows a design of the multi electrodes where four single working electrodes and one counter electrode were combined to make 4 devices on one substrate.

The method to deposit polypyrrole/phenol red based films on the surface of the electrode was developed. The film properties can be determined mainly by (1) the amount of the current passing through the electrodes, (2) the concentration of a pyrrole monomer in the reaction media, (3) the reaction time, (4) the type of the dopant molecule, and (5) the concentrations of both pyrrole and the dopant. The film thickness was simply determined by the reaction time and the type of the dopant employed. After each reaction, a smooth green film formed on the surface of the electrode. If the size of the electrode is further reduced, the experimental conditions for making an ideal film will be impacted.

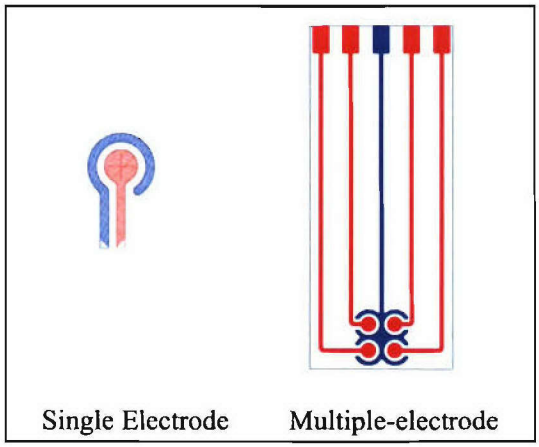

Figure 53: Configurations of both single and multi electrodes

It was reported in previous interim reports that an analytical method for measuring the concentration of phenol red released from an electrode was developed. With the use of a UV-Vis spectrometer it was determined that for a series of trial runs, that phenol red at 537 nm in Tris buffered solution was measured at different concentrations which included $5x10^{-5}$M, $1x10^{-5}$M, $5x10^{-6}$M, $1x10^{-6}$M, and $5x10^{-7}$M. As shown in figure 54, the working curve that a plot of absorbance versus concentration allowed for the calculation of the concentration, as well as the amount of the released phenol red. In principle, this method can detect any released absorbing molecules in solution.

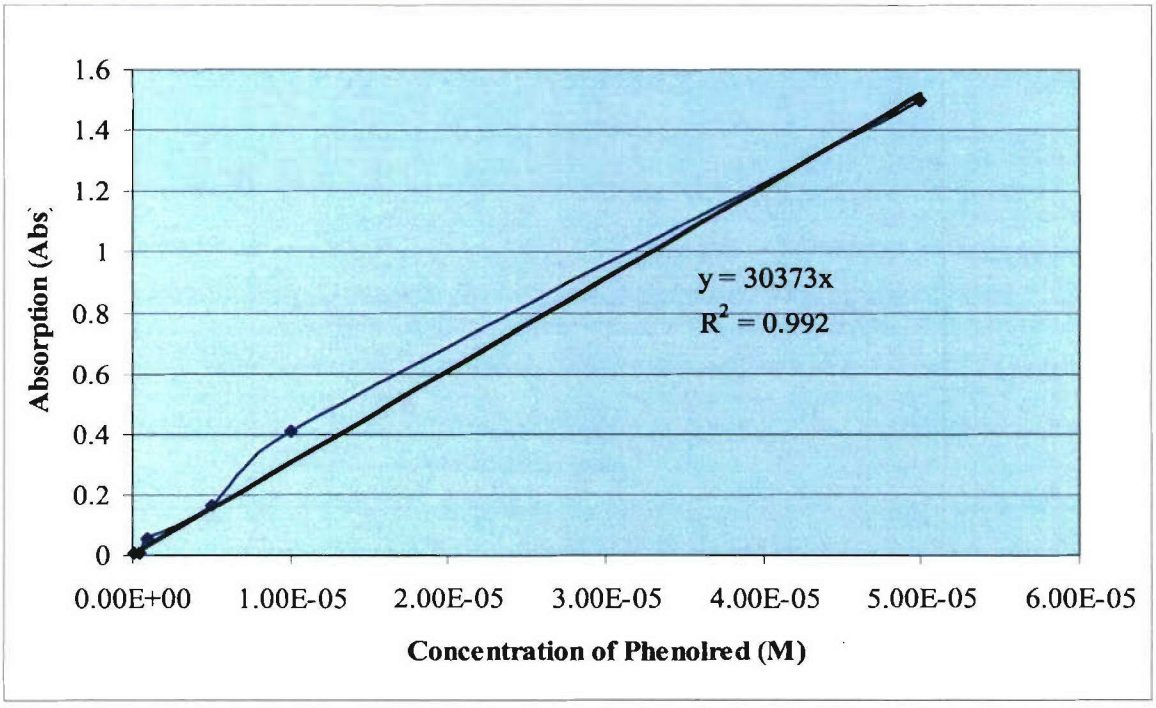

Figure 54: The working curve for phenol red in Tris-Buffered Saline

The thickness of PPY/phenol red films increases from sample (2) to (5). Curve (1) for sample (1) in figure 55 shows that phenol red was not released when the circuit was open. However, phenol red (see curve (2)-(5) for sample (2)-(5)) was released when a voltage (-2V) was applied with the release profile depending on the film thickness. As one can see, curve (2) for the thinnest PPY/phenol red film shown solely in figure 56 demonstrated that 70% of the releasable phenol red was released in 20 minutes. This is considered a burst release.

However, the release behavior changed with the thicker film and the burst release profile disappeared as indicated by curves (3) to (5) in Figure (4). As discussed in the proposal, a negative voltage applied to a PPY/Phenol red film will reduce the PPY film from a positive stage to a natural stage where phenol red, the negative counter ion, will be expelled from the PPY film by the negative voltage. For the thin film, phenol red was released into the solution immediately and a burst release was observed. For the thick film, most of the phenol red within the polymer film in principle has to migrate to the film surface and then get released. This migration will take a much longer time, which explains why the burst release disappears and a diffusion controlled release is observed.

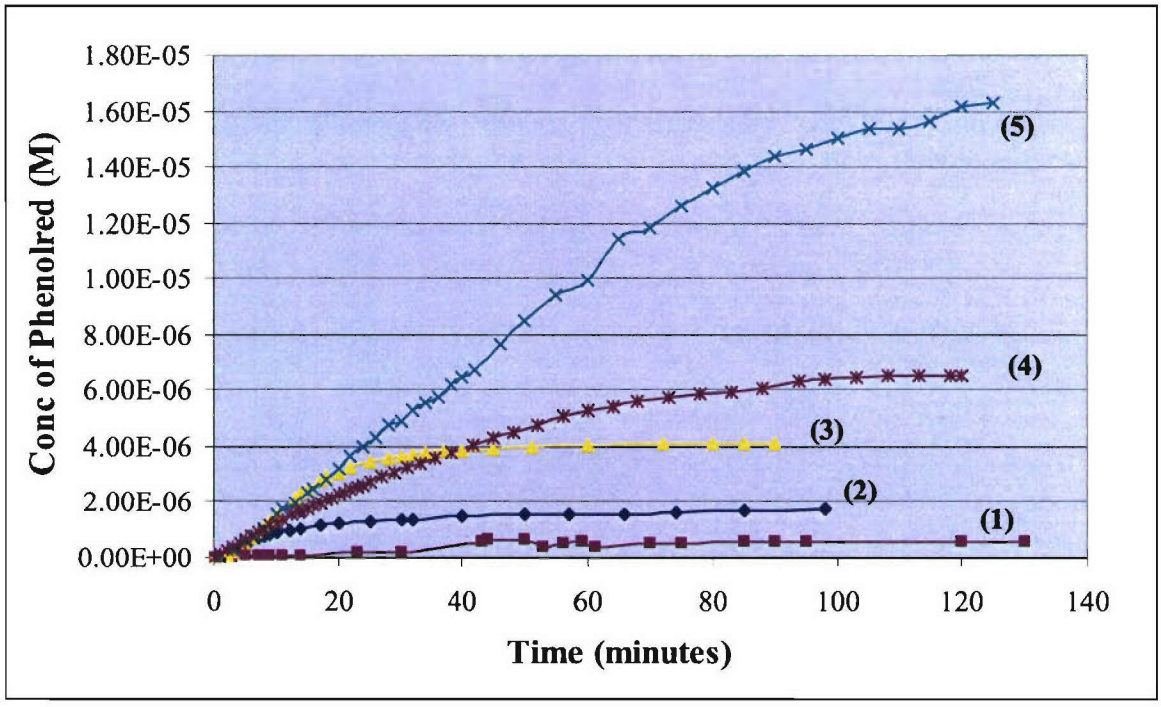

Figure 55: Release profiles of phenol red from PPY in Tris-Buffered Saline

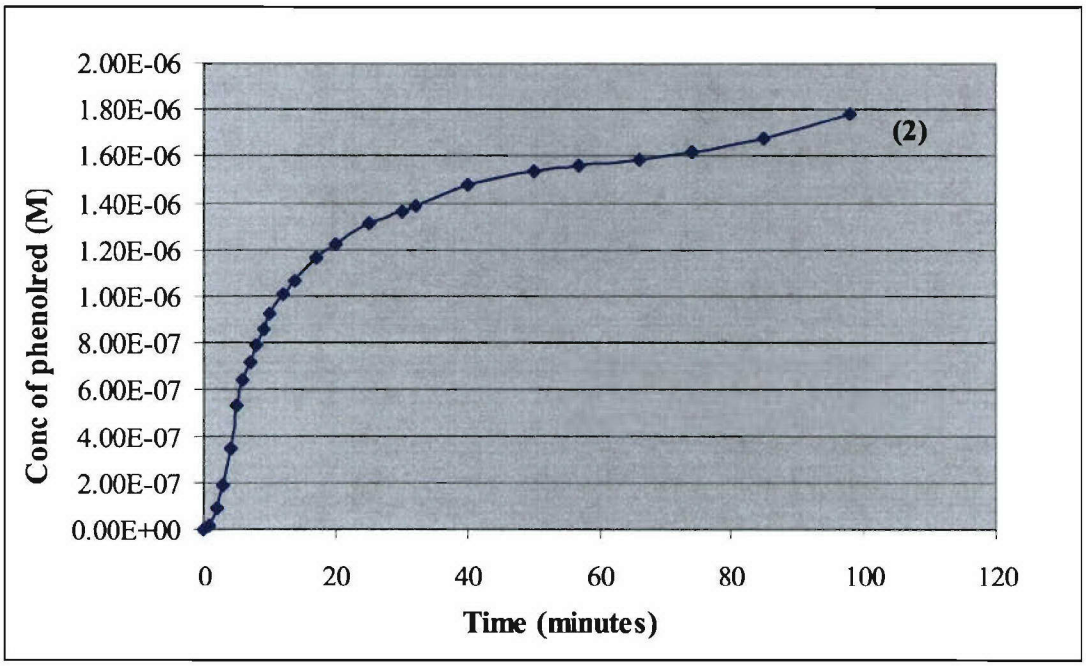

Figure 56: Release profile of phenol red from thin PPY film in Tris-Buffered Saline

This new result has not been discussed in any related literature and is also critical to the design of our triggered release device. For example, if the burst release is required for our device, the film has to be thin enough to achieve the goal. Further experiments are required to fully understand this result.

The depositions of Polypyrrole/Phenol red or Ampicillin films on the carbon electrode have been established and films with different thickness have been made via an electro-polymerization method. The analytical method for measuring the released dopant such as phenol red was developed. The measured absorbance of the released dopant by a UV-Vis spectrometer in solution was used to determine the amount of the released dopant. The release profiles of PPY/Phenol red in solution at different conditions were obtained with the developed analytical method. The results showed the release mechanism under the applied voltage is associated with the film thickness and the burst release changed to the diffusion controlled release when the film thickness increased. A small multi-carbon electrode device was designed and prepared where the deposition of PPY/dopant film on each electrode is underway.

b. Polymer based release system on a CPMEMS platform

Once the procedure to deposit polypyrrole/phenol red on the carbon electrodes with films of different thicknesses was established, it was then necessary to develop a method to deposit PPY/phenol red based films on the surface of the MEMS devices. Figure 57 shows a schematic diagram of the experimental setup. A PPY/Dopant film was deposited on the surface of the MEMS devices that were prepared via photolithography. A bi-potentiostat was employed for the

electro-polymerization experiments using either chronoamperometry or cyclic voltammetry. The MEMS electrodes made with Au were fabricated on a silicon wafer via photolithography. There are over 120 microelectrodes on each silicon chip and each square microelectrode has a size of 125 μm^2. The reference electrode was a silver wire and a gold wire served as the counter electrode. The polymerization process was visually inspected in situ, using an optical microscope.

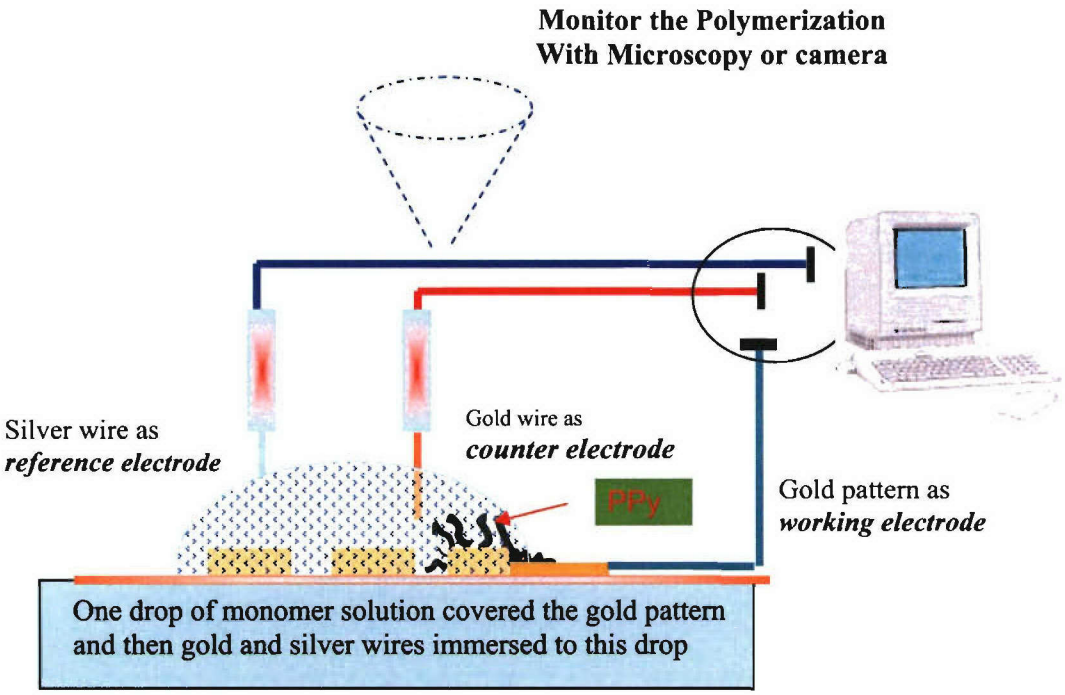

Figure 57: Electrochemical polymerization to deposit PPY/phenol red on microelectrode

The microelectrodes used for the release experiments allowed for only a small volume of the solution to be utilized in the reaction. In a typical polymerization experiment, a drop of solution (less than 0.2 ml) containing pyrrole (0.1 M) and dopant molecule (0.1 M) was added to the surface with a syringe to cover a selected electrode. The tips of the reference and the counter electrodes were then immersed into the solution. A constant voltage of 0.8 V was applied (chronoamperometry) to the electrode. When the polymerization stopped, any unreacted solution was removed and the deposited polymer was then rinsed with water 3 times to remove the unreacted monomer and any dopant molecule on the surface. After air drying, the coated microelectrodes were examined by either scanning electron microscopy (SEM) or optical microscopy. In these studies, the phenol red dopant molecule was released to demonstrate a proof of concept.

SEM allows the observation of the deposition of PPY/dopant film on the microelectrode. Figure 58 shows a PPY/chloride film only formed on the surface of those two selected microelectrodes whereas other microelectrodes remained intact. No film grew in the gap between the two adjacent microelectrodes. The electro-polymerization time for the second microelectrode

was 4800 seconds, compared to 3600 seconds for the first microelectrode. Identical polymerization conditions were used to make PPY/phenol red on the microelectrodes.

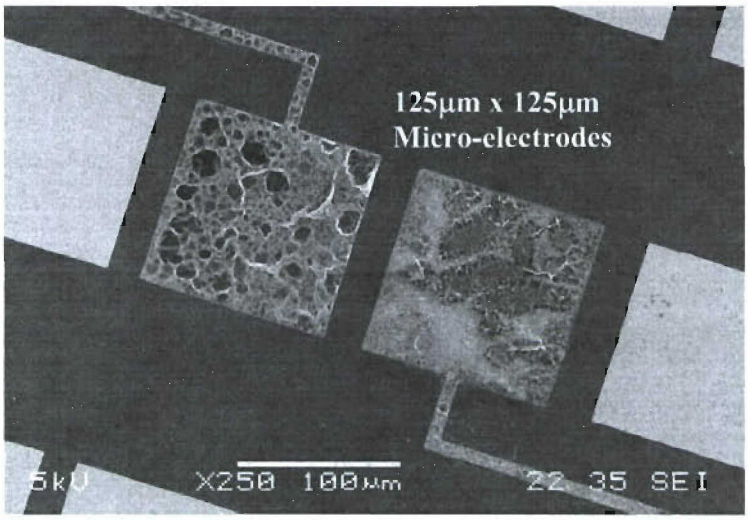

Figure 58: SEM images of the deposition of PPY/chloride on the surface of two microelectrodes

Figure 59(a-d) shows the images of the growth of PPY/phenol red on two microelectrodes. As shown in the center of cycle in Figure 59b, the red spot indicates the growth of PPY/phenol red film on the first microelectrode. As the polymerization proceeds, PPY/phenol red film grew on the second microelectrode as indicated by the appearance of the second red spot in Figure 59c and 59d.

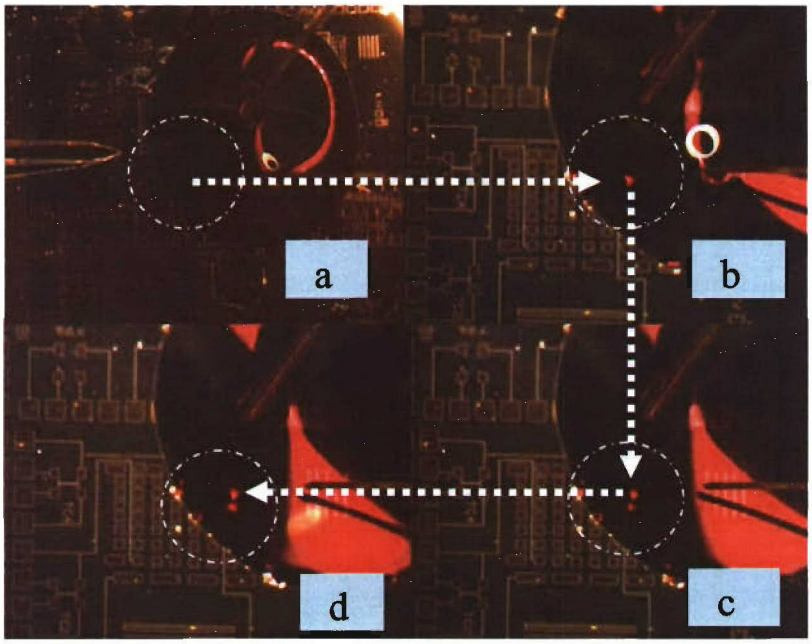

Figure 59: Growth progression of PPY/phenol red on the surface of two microelectrodes

In another typical experiment, phenol red was again employed as a dopant molecule replacing chronoamperometry with cyclic voltammetry (CV) to polymerize pyrrole. The "cell" was scanned in a cycle from -0.5V to 0.98V to -0.5V with a scan rate of 100mV/s. In theory, each CV scan polymerizes a thin layer of PPY/Phenol red film on the working electrode. The number of scan cycles controls the thickness of the film. Using SEM, the film surface morphology was then monitored. Figure 60 shows PPY/phenol red film formation on the microelectrodes. With an increase of the scan number increased from 16 to 72, the film thickness increased accordingly. The optimal scan number was determined to be between 16 and 32. In brief, PPY/phenol red films made from the CV method appeared smoother than those made from either the chronopotentiometry or the chronoamperometry method.

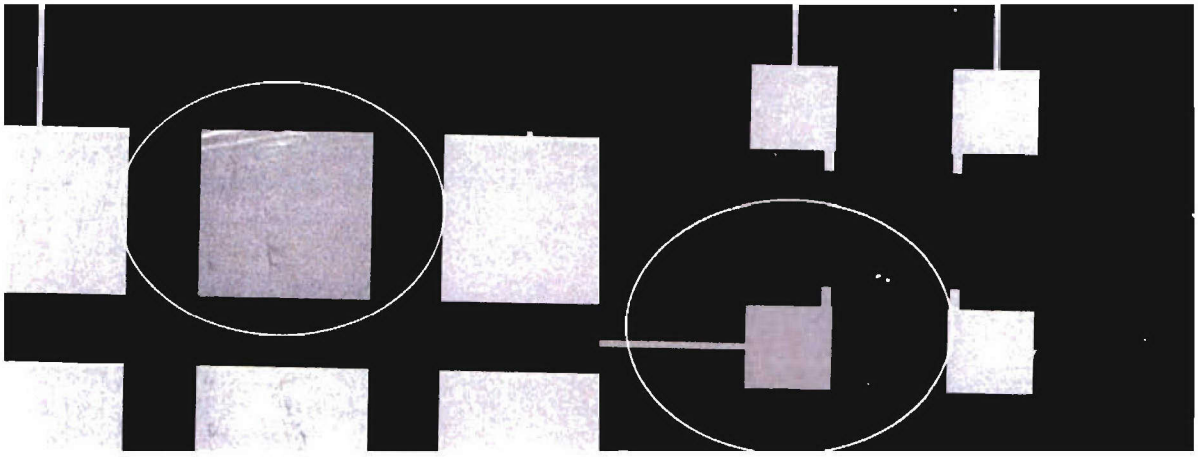

Figure 60: SEM images of smoother PPy/ phenol red films due to the use of cyclic voltammetry

The release of phenol red in solution from PPY/phenol red coated on these microelectrodes was the next study. Initially, a PPy/phenol red film was coated on 100 μm diameter gold wire using chronoamperometry. Figure 61 shows the electrochemical apparatus for measuring the release of phenol red. As shown in Figure 61 (a – d), a pink color associated with the released phenol red was observed after -1v was applied to the electrode. Work was then conducted on applying a similar system to observe the release of phenol red from the microelectrodes. More phenol red could be released by increasing the thickness of PPY/phenol red film.

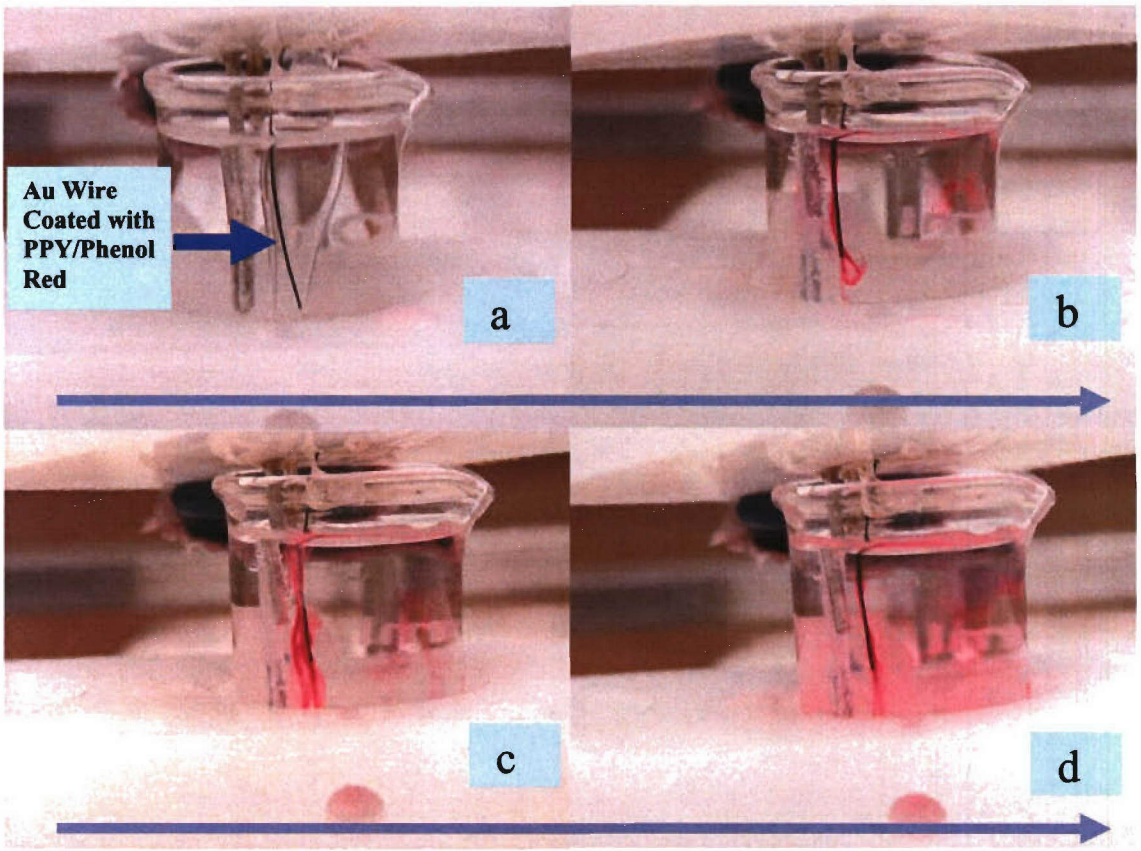

Figure 61: The release of phenol red from PPY/phenol red on a Au wire in a solution

Figure 62 displays a schematic diagram of the microelectrode test chip similar to ones that were developed using the microlithography process. This design allows for quick fabrication, and subsequently quick testing of the release experiments. Each microelectrode (1-8 or a-h) can be coated with a PPY/dopant film via our electro-polymerization method and ideally the dopant from each microelectrode can be released individually when a voltage is applied. The design for controlled release devices on a chip contains 16 microelectrodes with four different sizes fabricated on any given substrate. The size of the microelectrode varies as follows: 250μm ×250μm, 500μm ×500μm, 750μm ×750μm and 1000μm ×1000μm. Gold is used as the electrode material and the microelectrodes are patterned on the substrate via thermal vapor deposition using a mask design. Figure 63 is a photograph of an actual device before (63a) and after (63b) it was deposited with PPY/Dopant. 14 of 16 microelectrodes in Figure (63b) were coated with PPY/Phenol red on the surface. A bi-potentiostat was employed for the electro-polymerization experiments and the release study. Figure 64 shows an SEM micrograph of one of the electrodes that was electro-polymerized with PPY/phenol red.

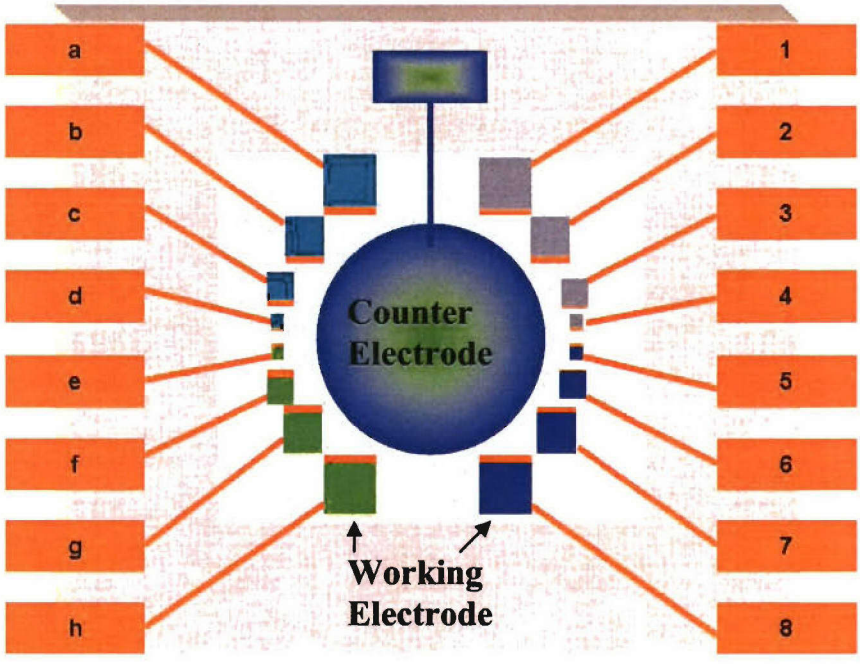

Figure 62: A configuration of multi-microelectrodes on a chip

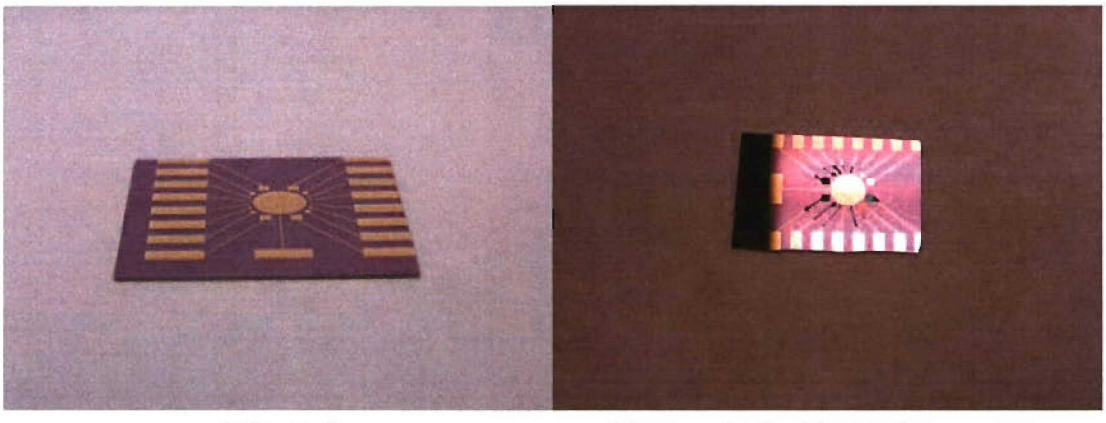

a) Control

b) Deposited with PPY/Dye on 14 microelectrodes

Figure 63: A chip with 16 Au microelectrodes on a silicon wafer

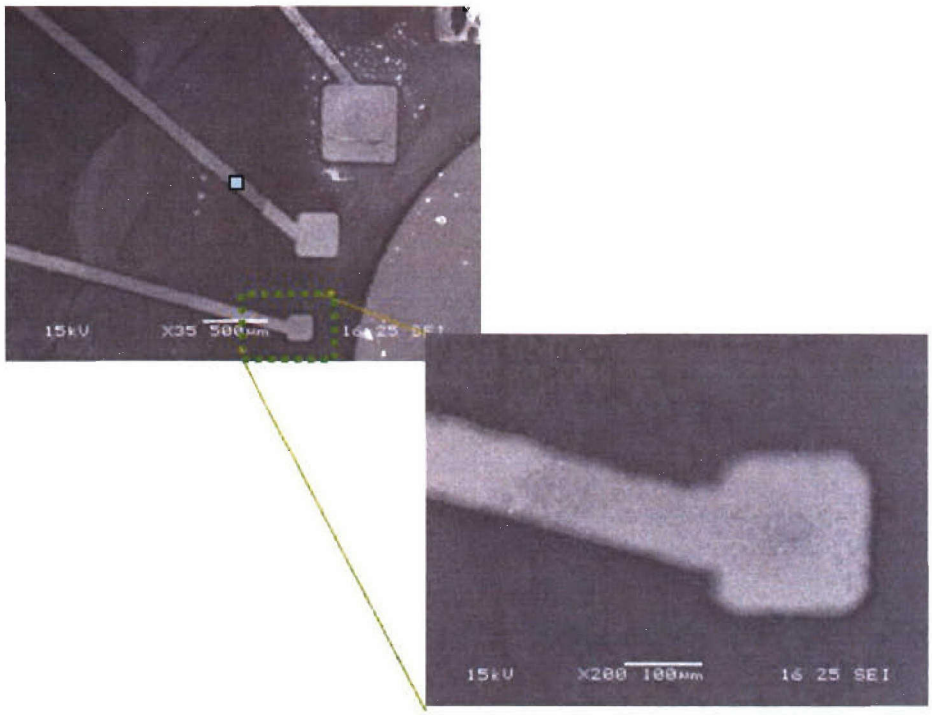

Figure 64: SEM micrographs of the deposition of PPY/dye on the surface of a microelectrode

Figure 65 shows the subsequent release of phenol red after -1.0 V is applied to the electrode, which confirms release at the microelectrode level. Notice also that when the same voltage is applied to a second electrode which is covered with PPy/tetrabromo phenol blue, the same release phenomenon is also observed, thus demonstrating the ability to release two different release agents that are electro-polymerized on the same microelectrode test device.

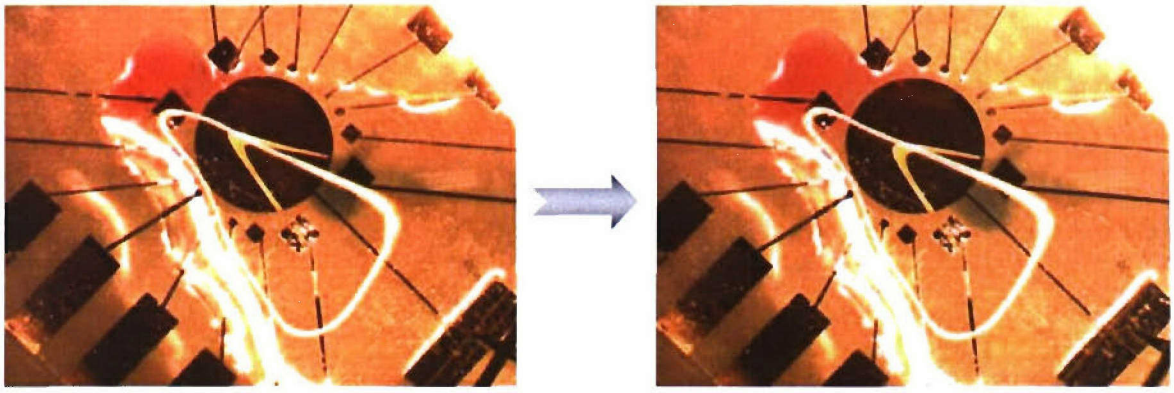

Figure 65: The simultaneous release of phenol red and blue

A study was conducted to determine the amount of the released dye molecules in a solution. PPY/phenol red was deposited on the surface of the microelectrodes and the charges (Q) passed through the electrode during the polymerization was measured. Figure 66 shows the current-time curves obtained from electro-polymerization on four microelectrodes with the electrode area varying from 250μm ×250μm to 500μm ×500μm to 750μm ×750μm to 1000μm ×1000μm. Since other factors were kept constant during polymerization, the current passing through each microelectrode is proportional to the microelectrode area. The charge that passes through each of the micro-electrodes can be determined by integrating the current-time (i-t) curve.

Phenol red from the film was released into a tris-buffered solution for 60 minutes when a potential (-1.2v) was applied to the device and the amount of the released phenol red was obtained from a UV vis spectrometer. When the amount of the released phenol red is plotted against the charges (Q) passed through the electrode during the polymerization, a linear correlation was obtained as shown in figure 67. This correlation can be used to estimate how much of the phenol red can be released. The ratio of actual/theoretical released phenol red is between 0.12 and 0.25, indicated that up to 25% incorporated phenol red can be released from the PPy within 60 minutes.

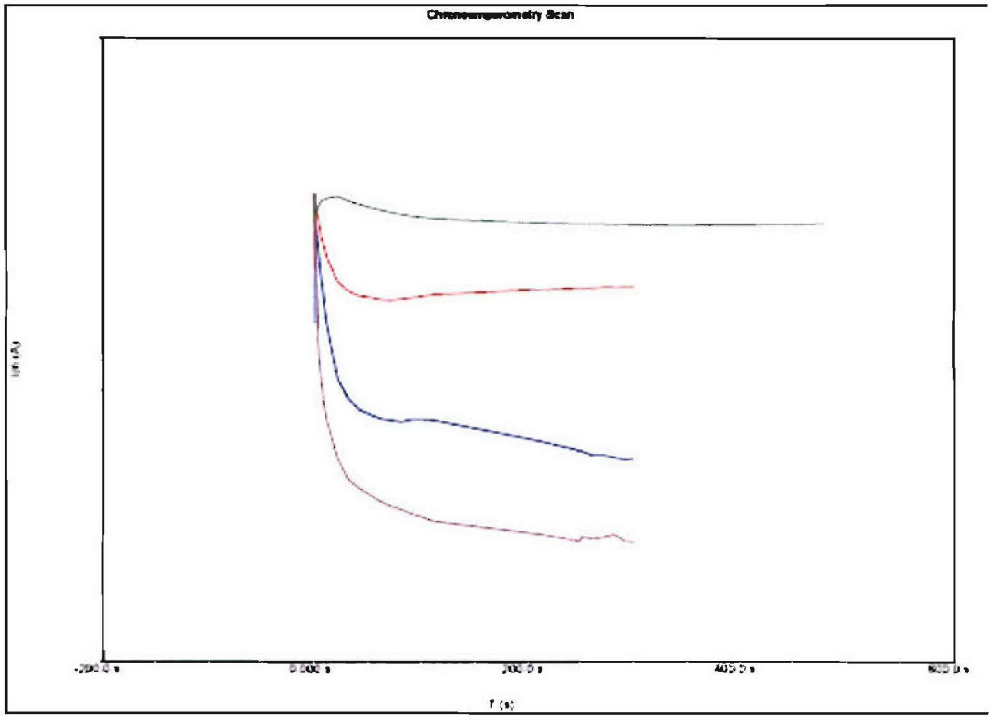

Figure 66: The Current~Time Curves of the Chronoamperometry in electro-polymerization of PY where green curve is for 250x250 μm^2, red curve is for 500x500 μm^2, blue curve is for 750x750 μm^2, and purple curve is for 1000x1000 μm^2

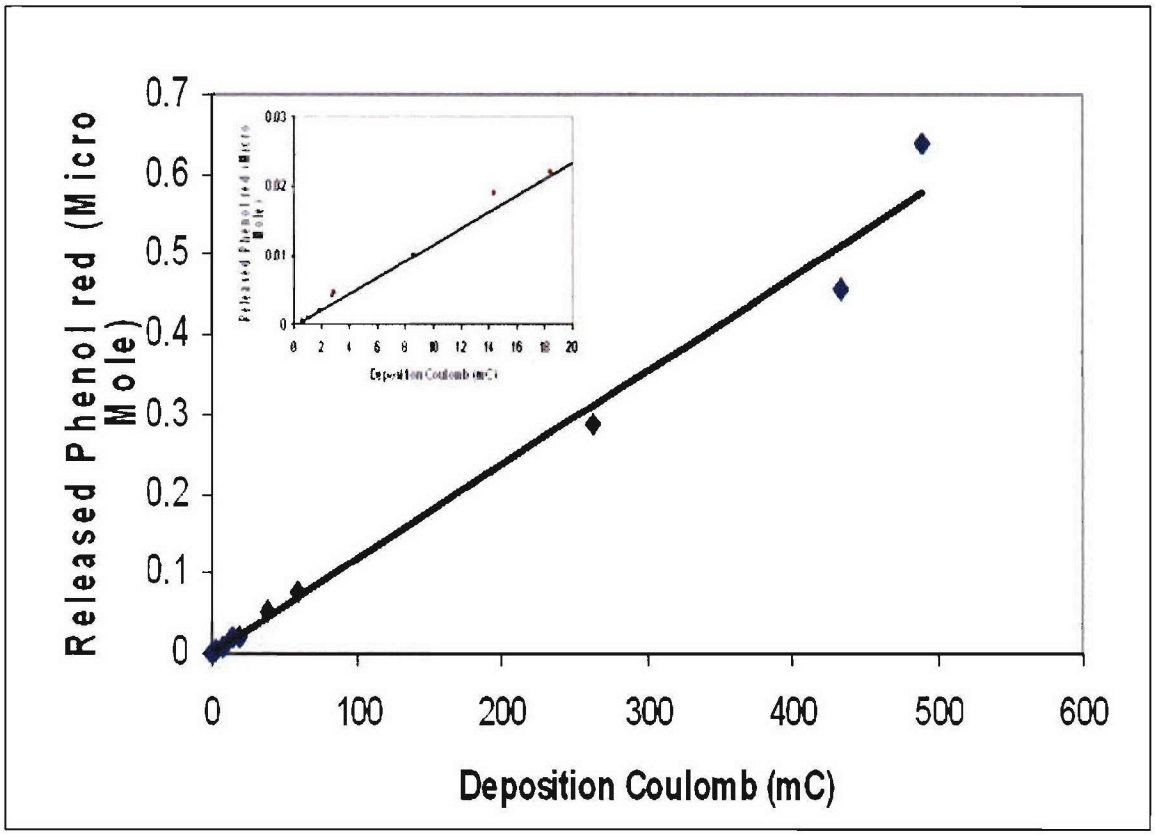

Figure 67: The linear correlation between the charges (coulomb) in electro-polymerization and the amount of phenol red released in the solution

c. Fabrication of a gel layer and release of dye molecules

Previous release experiments have focused on the release of dopant in aqueous solution. Although the release of phenolred as well as other dopants has been demonstrated earlier in this report, the release of the dopants in other media is unknown but may have potential applications in many fields. Many hydrogel materials are commercially available. To demonstrate release in a gel layer, an alginate based hydrogel was used because an electrolyte is already present in the hydrogel. In a typical experiment, the hydrogel layer of alginate is prepared by adding 0.1M Calcium chloride solution onto wet coating of sodium alginate, followed by cooling it at -4°C for 30 minutes.

In our initial study, the PPY/Phenol red layer was deposited onto the surface of both small carbon electrodes as well as the Au microelectrodes on the test chip via electro-polymerization. Then alginate hydrogel was fabricated onto the surface of the device to cover both the working and counter electrodes and the device was then ready for the release experiment. A bipotentiostat was used with a two or three electrode system in the release study

and different potentials ranging from -1.0 to -2.5 V were applied to the device to initiate release of the dye molecule, which was monitored with a digital camera.

As shown in Figure 68, the appearance of red color in the gel between the center carbon working electrode and the ring carbon counter electrode indicated that phenolred was released into the gel after a potential was applied to the device for 1 hour. Similar release of phenolred from PPY/phenol red on four of the Au microelectrodes into the gel was also demonstrated as shown in figure 69 after the potential was applied to the device. Compared with the released process in aqueous solution, the release process within the gel layer is slower and all released molecules remain within a small area. This is because the diffusion of released dye molecules within the gel layer is slower than that in aqueous solution.

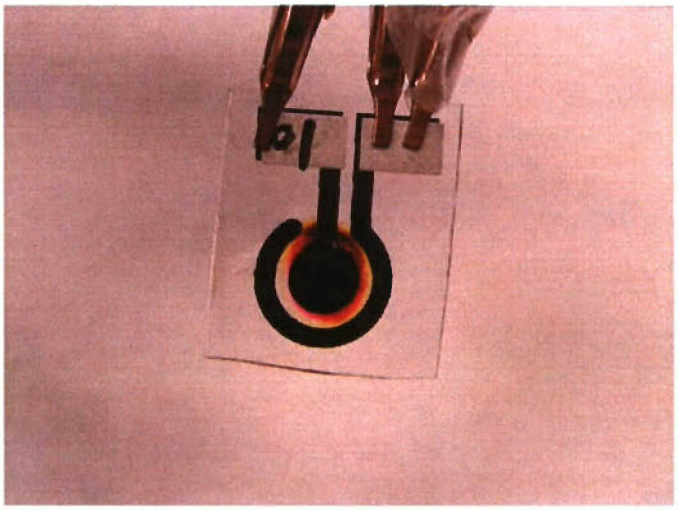

Figure 68: Release of phenol red from PPY on a single carbon electrode into the gel

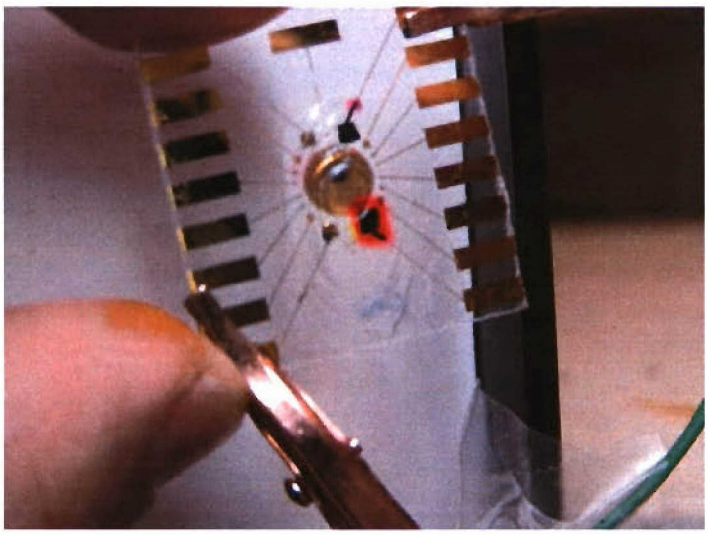

Figure 69: The release of phenol red from PPY on the multi-electrodes into the gel

d. Drug release study

In the initial study, ampicillin (amp), an antibiotic, was incorporated into the PPY film on our small carbon electrode via the chronopotentiometry method where the current was kept constant. Although previous results showed that amp can be released into the buffer solution when a potential is applied to the PPY/AMP coated electrode, a number of difficulties were faced which included (1) deposition of smooth films on the electrode, (2) the loading of amp in PPY/amp film, (3) the stability of ampicillin in PPY, and (4) the release of amp in a controlled manner. Several methods including chronopotentiometry, chronoamperometry, and cyclic voltammatry were employed to prepare PPY/amp on the surface of small carbon electrodes. Results showed that none of the above mentioned methods provided a smooth PPY/amp film on the surface of the carbon electrode.

The effort to establish a protocol to well detect the released ampicilin in a buffered solution was also continued. Initially, tris-buffered solution was to be used for the experiment, however it was found from literature that ampicillin in solution is not very stable at a pH above 7. Since the pH of tri-buffered solution is about 7.4, it was decided to switch to phosphate buffered solution where the pH can be controlled from acidic to basic. High Performance Liquid Chromatography (HPLC) was used for detecting ampicillin in the buffered solution and the working curve at a pH equal to 4.3 was established by monitoring the absorbance of ampicilin at 204 nm.

e. Release of biologically active molecules from polypyrrole

Cyclic voltammetry (CV) was used to determine whether the drug dopant of interest would be electroactive or not during the electro-polymerization process of PPY/drug dopant. Several molecules were tested including sulfacetamide sodium salt, naproxen sodium salt. Sodium acetate, sodium chloride, and sodium nitrate were employed as controls. CV or chronoamperometry was used to electro-polymerize pyrrole in the presence of the dopant drug anion.

i. Sulfacetamide

As shown in figure 70, a significant current increase starts at approximately 0.7 V and peaks at about 1.1 V. Upon the second scan an oxidation peak at 0.45 V and a reduction peak at about -0.2 V was observed. This implies that sulfacetamide is electroactive in the potential window for electro-polymerization. As shown in figure 71, an oxidation peak associated with pyrrole during the first scan was observed. However, subsequent scans show a dramatic decrease in peak current, which suggests further polymerization either stops or the polymerization rate reduces rapidly. After carefully examining the surface of the electrode, formation of a PPY/Sulfacetamide film was not produced.

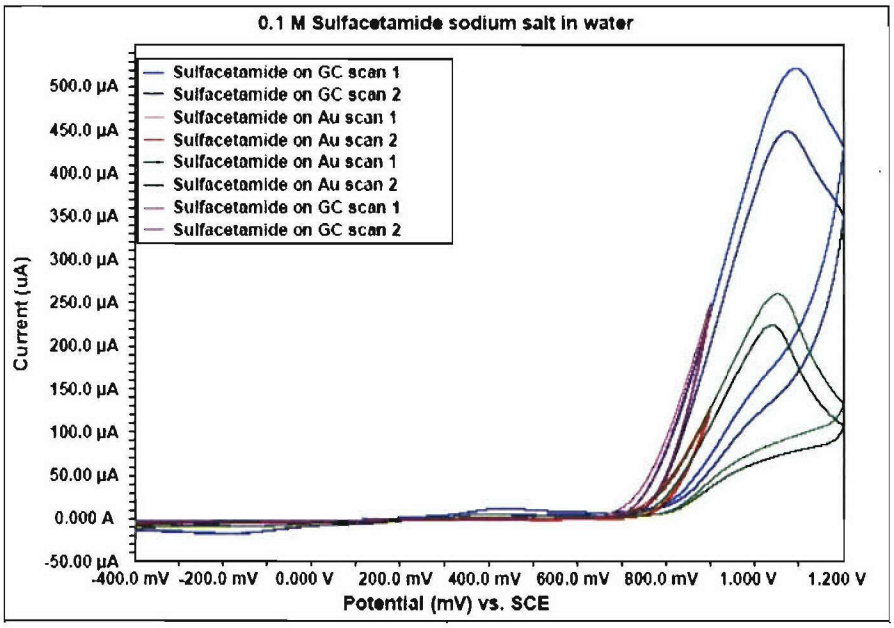

Figure 70: Cyclic voltammograms of sulfacetamide in water

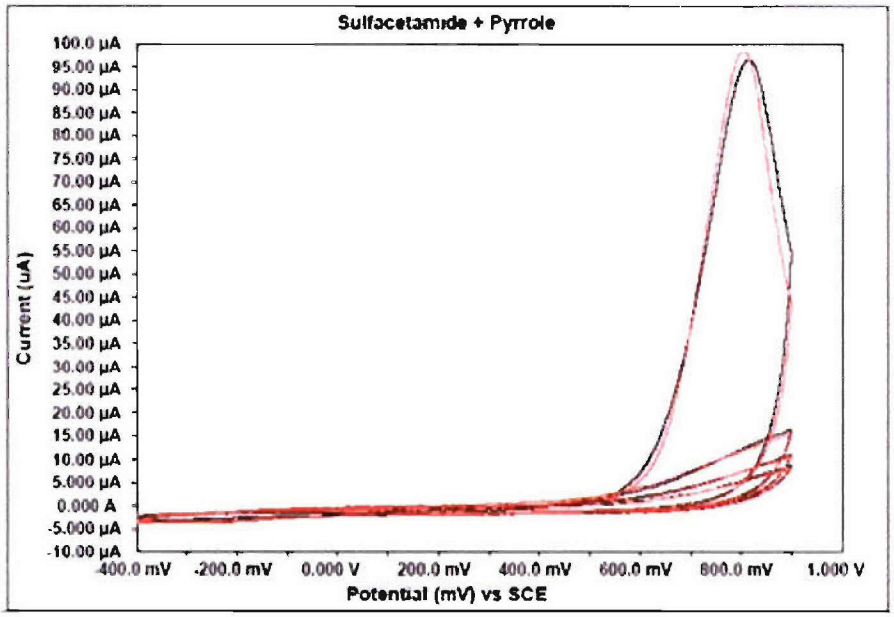

Figure 71: Cyclic voltammograms of sulfacetamide sodium salt in pyrrole aqueous solution

ii. Naproxen

Naproxen sodium salt was the second drug molecule that was tested. The pH of the naproxen salt solution was 10.15 and the pH of naproxen/pyrrole solution was 9.97. An attempt was made to adjust the pH of the solution (8.6, 7.68 and 7.5). However, at a pH lower than 9.0 it was observed that the naproxen salt precipitated out of solution and more of the drug precipitated out as the pH decreased further. Figure 72 shows the CV of naproxen itself in an aqueous solution. Clearly an oxidation peak at 0.8 V was noticed; the same potential was used for pyrrole polymerization. This result certainly suggests that there are problems with trying to incorporate naproxen as the dopant into PPY.

The amperometry method was also attempted to try to prepare PPY/naproxen on the electrode surface, but again no polymer formation was observed. By switching to the chronopotentiometry method, a white material did form on the electrode surface. The white material is thought to be naproxen coming out of solution and depositing on the surface of the electrode and it was again observed that no PPY was deposited on the electrode surface.

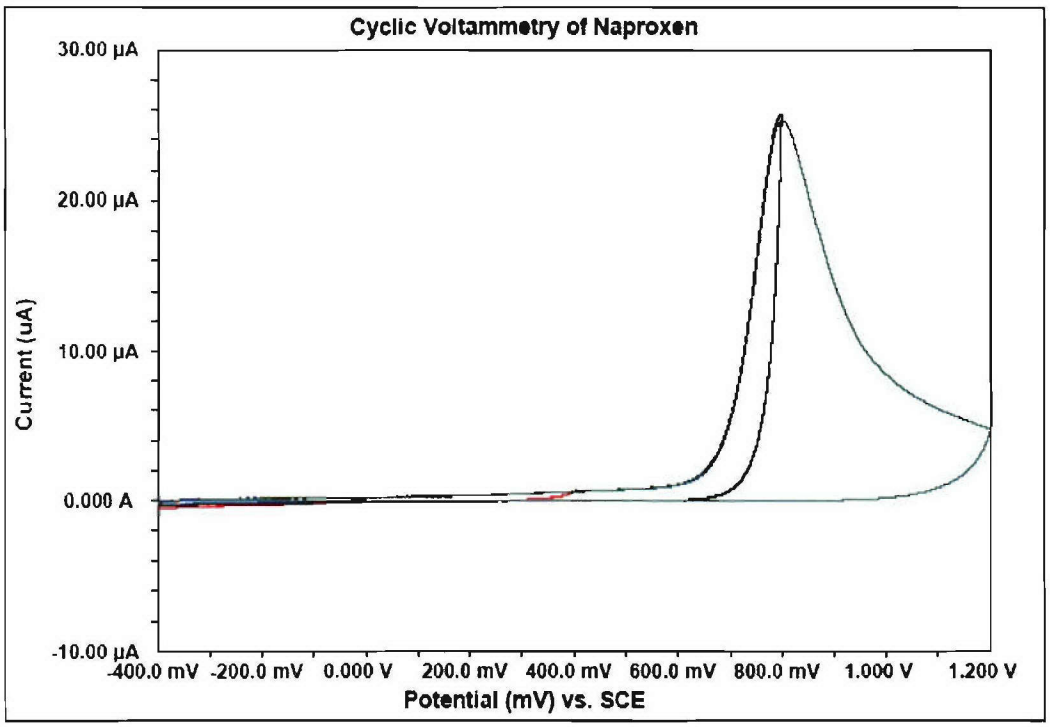

Figure 72: Cyclic voltammograms of naproxen in water

iii. Acetate

Acetic acid was neutralized with 0.1 M sodium hydroxide aqueous solution to a pH of 7.01, 6.01, and 3.05. Figure 73 shows CV of acetic acid at pH 7.01 and the current increased at 0.8 V. This suggested that acetate is electroactive at 0.8 V and again it would be difficult to

introduce acetate into PPY as the dopant. It was thought that changing the pH of the solution may change the oxidation potential, but it was determined that the CV of acetic acid at pH 6.01 and 3.05 showed the similar curves to that at pH 7.01.

Despite of the observance of acetate being electroactive at 0.8 V, a PPY/acetate film was still prepared using the CV method. Figures 74a and 74b show cyclic votammograms of electro-polymerization of pyrrole in the presence of acetate. In Figure 73a a pyrrole oxidation peak was observed when the oxidation potential increased to 0.8 V or above. In figure 74b, an oxidation peak associated with pyrrole during the first scan was observed. However, subsequent scans show a dramatic decrease in peak current, which suggests that further polymerization either stops or the polymerization rate reduces rapidly. After carefully examining the surface of the electrode, it was again evident that there was no formation of PPY/acetate on the electrode surface.

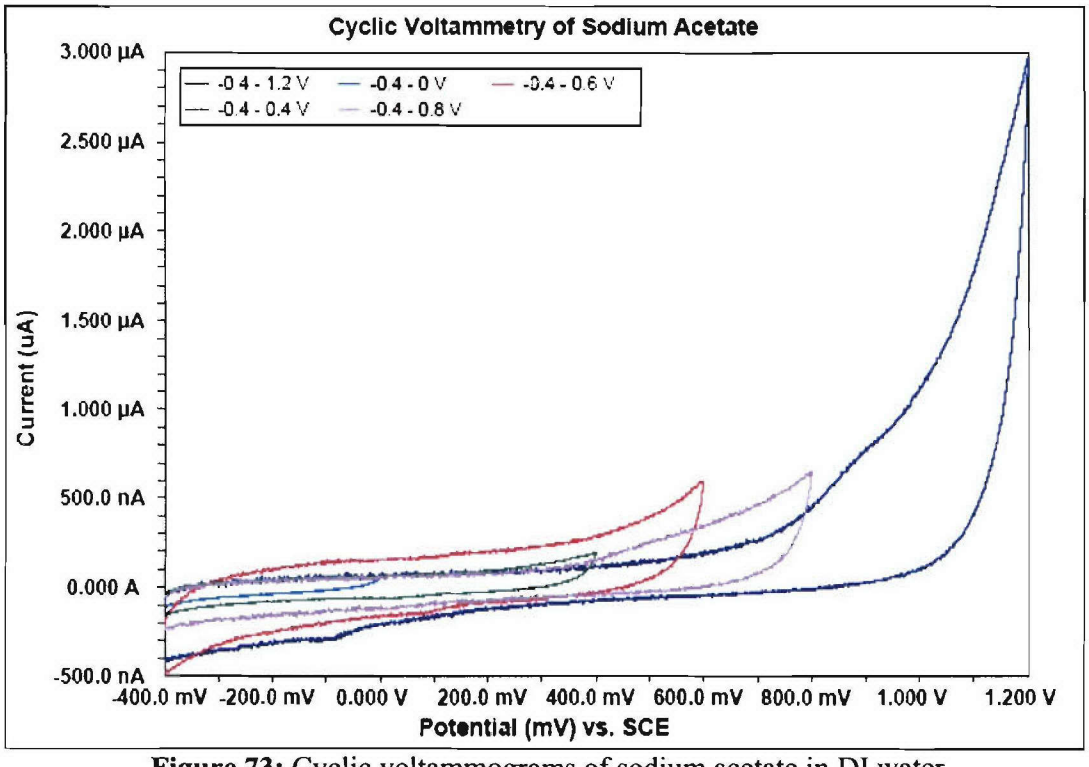

Figure 73: Cyclic voltammograms of sodium acetate in DI water

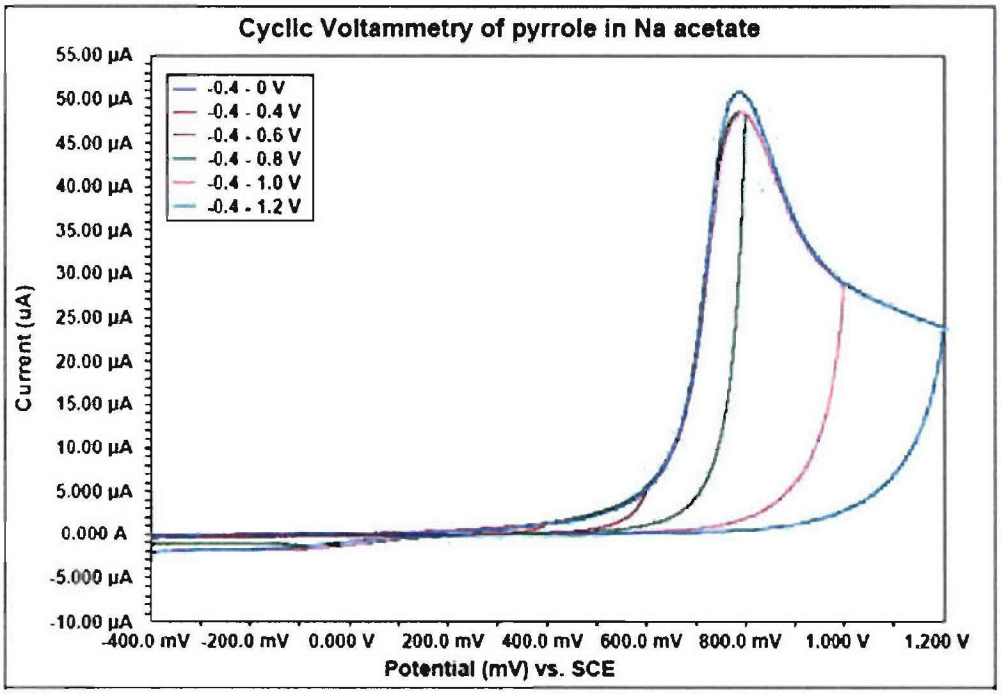

Figure 74a: Cyclic voltammograms of electro-polymerization of pyrrole in the presence of 0.1 M sodium acetate with different scan ranges

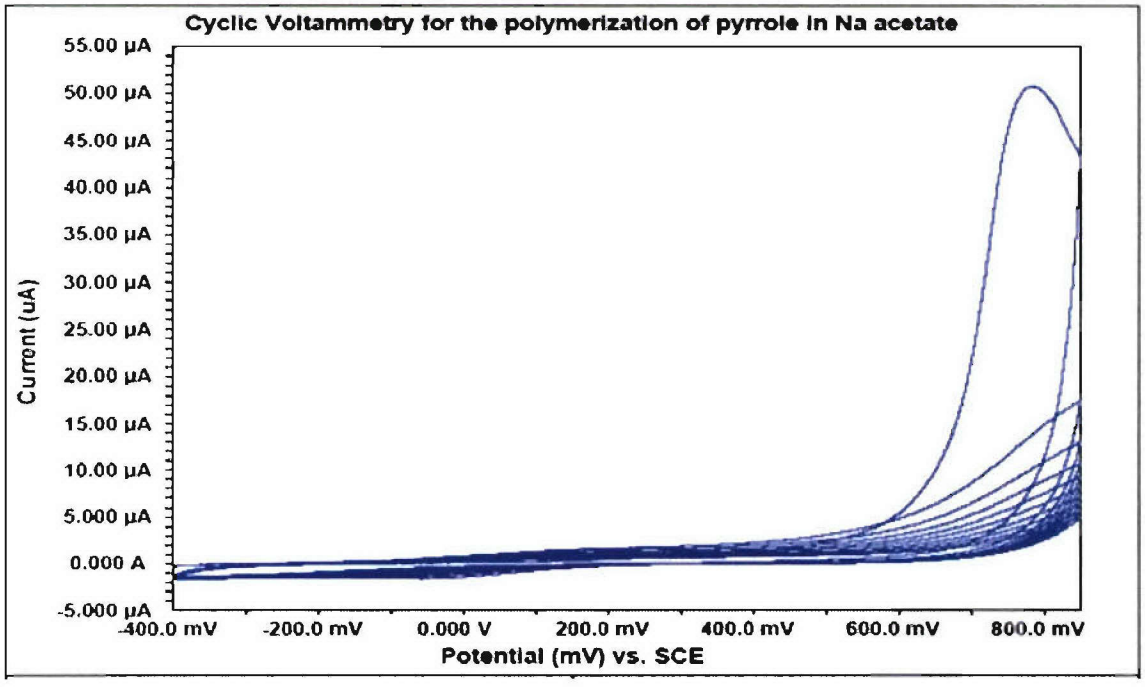

Figure 74b: Cyclic voltammograms of electro-polymerization of pyrrole in the presence of 0.1 M sodium acetate with 10 scans

iv. Ampicillin

In previous reports polymerization of pyrrole in the presence of ampicillin was studied via the chronopotentiometry method where the current was kept around 0.1 to 0.05 mA. Other methods to electro-polymerize pyrrole in the presence of ampicillin were also evaluated. With the chronoamperometry method 0.8 V was applied to the electrode to polymerize pyrrole for various amounts of time. The formation of a PPY/ampicillin film was not observed on the surface of the electrode. Figure 75 shows the current changing during the polymerization. One can see that the current decreased from 5 to less than 0.5 μÅ after 100 seconds. The initial current decay certainly suggests that a non-conducting or less conducting layer formed on the surface of the electrode, which hindered the further growth of the film.

The CV method was also evaluated, with a scan potential from -0.4 V to 0.9 V and scan rate of 50 mV/s for 50 cycles to deposit PPY/ampicillin on the electrode surface. Again, it was observed that there was no formation of PPY/ampicillin on the surface of the electrode. As shown in Figure 76 the initial CV exhibits a peak for the oxidation of pyrrole. However, subsequent CVs were representative of the formation of a less conducting passive layer on the electrode surface. This observation agrees with the result from the chronoamperometry method.

The chronopotentiometry method was also conducted with a constant current of 0.1 mA applied to an electrode that was immersed in a solution of equimolar pyrrole and Amp as before. Ampicillin (Amp) salt was used in the reaction and the pH of the Amp/pyrrole solution (equimolar) was 9.3. Although, a film growth was observed on the surface of the electrode as well as the release of ampicillin, the data indicated that PPY/ampicillin does not behave like PPY/phenol red. PPY/ampicillin may over-oxidized during the polymerization.

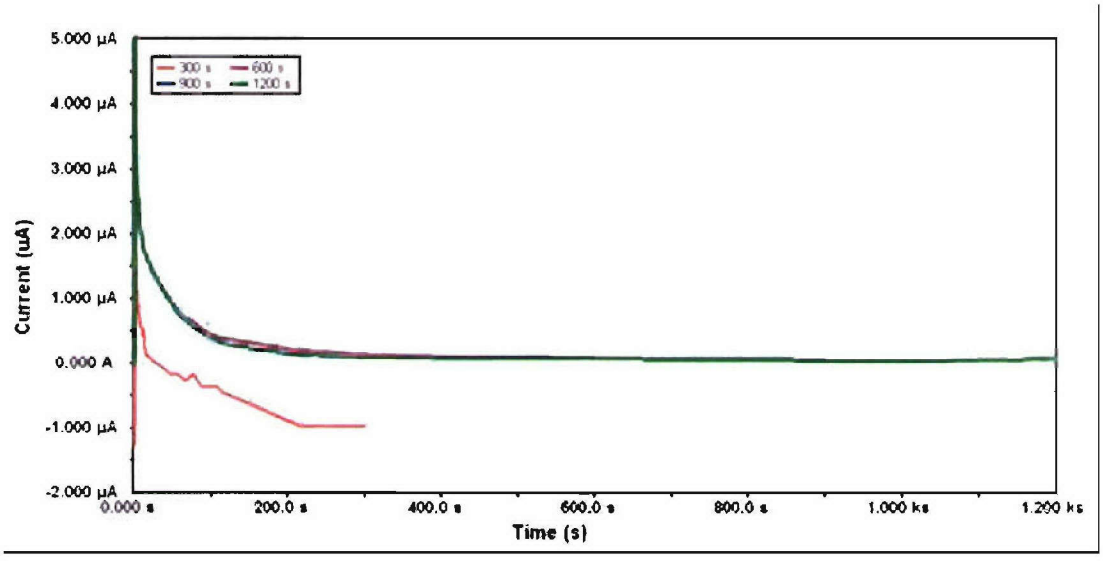

Figure 75: Current vs. time during the polymerization when a potential of 0.8 V was applied

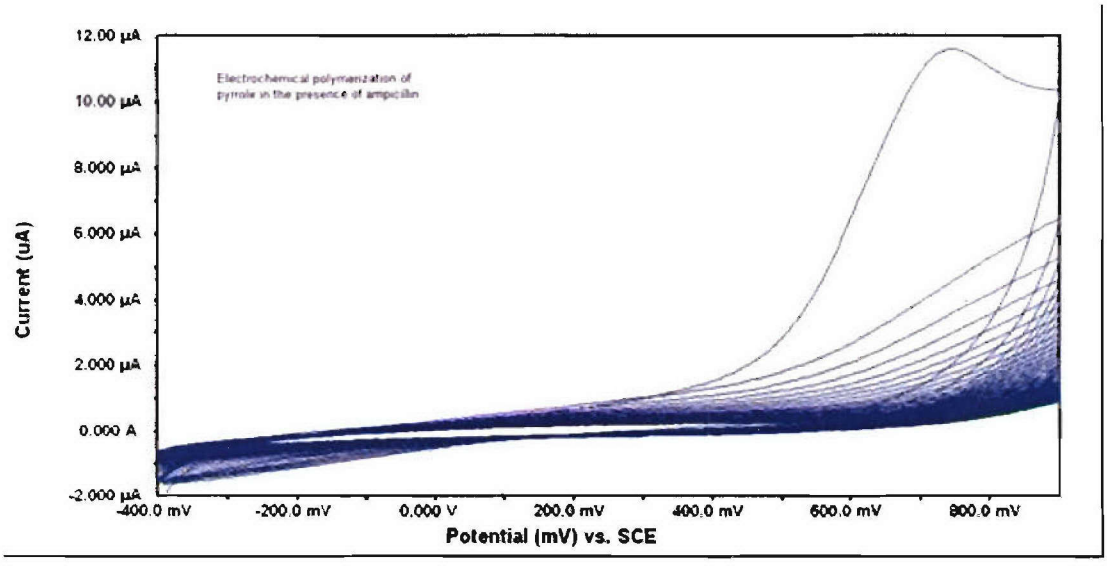

Figure 76: Cyclic voltammograms of electropolymerization of pyrrole in the presence of 0.1 M ampicillin sodium salt

v. Trichloroacetic acid

For tricholoracetic acid the CV method was used to initially test the electroactivity of trichloroacetic acid in DI water. The scan potential window ranged from -0.4 V to 0.9 V with a scan rate of 50 mV/S and the result didn't show a significant current change at 0.8 V. This suggests that TAA is not an electroactive molecule in the potential range used and therefore can potentially be used as a dopant for polypyrrole. A PPY/TAA film did form on the surface of the electrode.

Based on the results discussed above, a summary of the results is provided in Table 1. One can see that both sodium salicylate and trichloroacetic acid are not electroactive, and consequently PPY/dopant films were formed on the surface of the electrode. Sodium acetate, naproxen, and sulfacetamide sodium salt are electroactive and therefore hinder electro-polymerization of pyrrole. For sodium acetate and Naproxen, either CH_3 or CH attached to carboxylic acid in the dopant may be oxidized into a radical during the CV screen and the resulting radical may quench electro-polymerization of pyrrole. This is probably why it is observed that there is a rapid current decrease after a short period when using chronoamperometry or that the oxidation peak decreases after the first cycle when using cyclic voltammetry.

Formation of PPY/dopant on the surface of the electrode was not observed, but it is suggested that the pKa value for carboxylic acids plays a decisive role in PPY film growth. When carboxylates whose conjugate acids have pKa values greater than that of p-nitrobenzoic acid (pKa = 3.40) were used as dopants, no appreciable film growth of PPY was observed. The absence of PPY film growth in the presence of a carboxylate whose conjugate acid pKa is greater

than 3.40 can be explained by assuming that the electrostatic interaction is too strong for the deposited film to possess any appreciable conductivity. The finding that the very thin films prepared in such environments did not show any redox activity provides further indirect evidence for the insulating properties of PPY films prepared in this manner. Unfortunately, most of the possible drug candidates for that were studied for this application contains carboxylic acid groups whose pKa is greater than 3.4; therefore this PPY/dopant approach as a drug release device is limited to only a few drug molecules.

Table 1: Summary of the Dopants

No	Name of the Dopant	Electrochemical activity between 0.4 and 0.9V	Polymer formation in the presence of Pyrrole via constant current	pKa of the acid
1	Sodium Salicylate	No	Yes	2.4
2	Trichloroacetic acid	No	Yes	1.2
3	Sodium acetate	Yes	No	4.74
4	Naproxen	Yes	No	4.8
5	Ampicillin sodium salt	Unknown	No	2.5 (-COOH) 7.3 (-NH2)
6	Sulfacetamide sodium salt	Yes	No	5.4

1.3.2.5 Biological Sample Collection Technology

a. Generic prototype Instrument and collection strategies

All bio-aerosol collection systems follow a similar chronology during the course of their operation: (1) air intake, (2) capturing interface, and (3) sample transport to detector [10,11]. In order to design the most efficient collection system, the parameters of these three stages were optimized. The air intake should be large enough to ensure that if antigens are present in the air they will be collected. The interface area must be sufficient so that every antigen present has an opportunity to be captured. The collected material must be transported quickly to the detector and in a concentrated medium for quick and easy detection.

Figure 77 shows a block diagram of a generic antigen collection system. This portion of the project entailed the investigation of different biological collection systems, which would further allow for the design and construction of a novel collection system. Macroscopic volumes of air or water are passed into a cell where a buffer solution is atomized to keep a thin mist film of buffer over the two CPMEMS devices at all times. The air or water to be tested is mixed with this buffer solution. The major advantage of using an ultrasonic transducer to atomize the buffer solution is that all the constituents of the buffer solution as well as the test air and liquid are produced in vapor form [12].

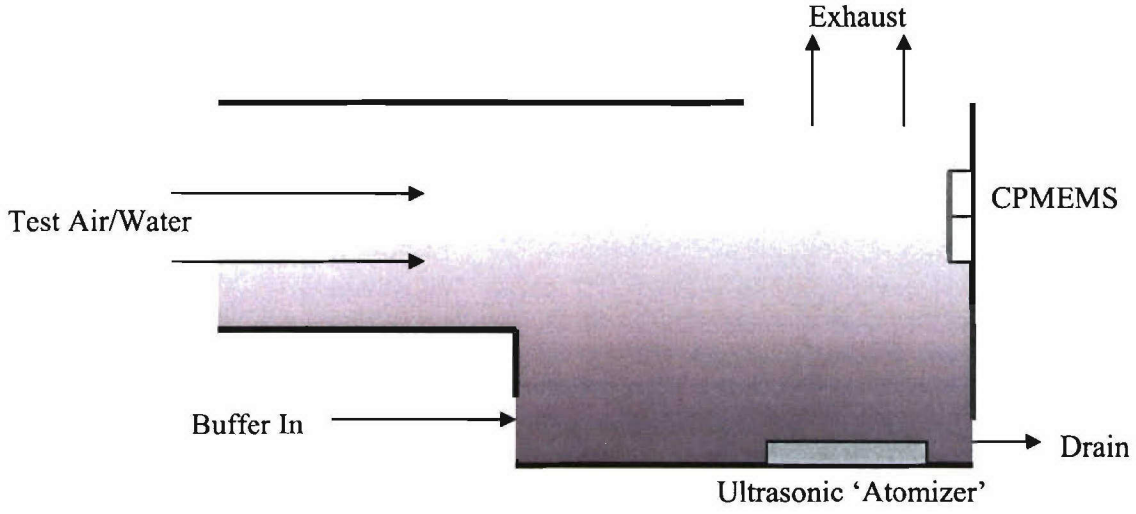

Figure 77: The antigen collection cell must provide a constant film of buffer solution over the CPMEMS bio-detectors. This is done with an ultrasonic 'atomizer' or mist generator. The test air or water is mixed with the buffer solution then turned into a mist by the ultrasonic transducer. Unlike a boiling process, the mist generator creates a composite mixture of the chemicals and biologicals present in the buffer solution.

In developing a biosensor, autonomous operation and continuous sampling are two issues that were considered when dealing with "real world" applications. In developing a biosensor

that can perform autonomously, it is necessary to develop a biological sample collection system that can sample a relatively large area continuously. Collection of finite volumes of analyte at any given time would lead to a statistical probability that the sample will not have a sufficient concentration of antigen. It is also possible that if sample collection is not continuous, events of interest that may occur in a window of time could be missed. Therefore, a system that allows for continuous automatic collection of biologics in air or water would increase the reliability of the biosensor.

b. ISAVAC collection system

A couple of variations of a collection system schemes were investigated, as was reported in previous interim reports. All investigated variations still have promise of being viable collection systems with further engineering, but it was the ISAVAC system which had the most promise for a continuous, autonomous collector of biologics from the air. Originally designed as an air purification system for commercial applications (i.e. homes, offices, hospitals, etc.), the system was modified to collect biological material from the air.

A particle separation system was also investigated to work in conjunction with the main collection system. Once an analyte was captured from an arbitrary environment, there would a wide range of particles that would be collected (i.e. dirt, pollen, bacteria, viruses, etc). An ultrasonic "cracking" technique that was capable of mass separation of the collected particles into groups was reported in previous interim reports. A system that would allow for particle separation of the collected analyte would serve as an initial particle-type analysis system. Separating the particles into groups of different sizes and/or masses would make it easier to detect the antigens of interest.

Again, as with the other collection systems that were investigated, this type of particle separation based on mass has promise with further engineering. The design of the final collection system in part depended on the analyte being detected. With a number of variations that were investigated, a wide range of analytes could be collected. However, since the study on the self assembled protein layer for biological event detection showed that the most feasible detection method would be the use of oligonucleotides rather than the protein antibody approach, a need for mass separation would not be required.

The ISAVAC was purchased form ISAVAC Ideal Atmospheres, Inc., and was modified such that it could be tested to function as a means for bio-collection. The ISAVAC is a filter-less, self-cleaning system that uses a liquid sub-micron particle collection medium. Water is introduced into the system and then accelerated by an impeller onto an anvil which aerosolizes it while simultaneously mixed with the intake air from the environment. This creates a dynamic particle removal system where the tiny particles form the environmental air are entrapped in the water droplets and then discharged to a drain. The purified air is then sent back into the environment.

Figure 78 below shows an image of the modified air purification system along with a schematic diagram of the process of collecting biological particulates from the environment. Figure 78 a) is the actual picture of the ISAVAC system with a closed system attachment and

HEPA filter. Figure 78 b) is the schematic diagram of the ISAVAC system with the closed system attachment HEPA filter and arrows showing the flow of air (red indicating contaminated incoming air and green indicating clean outgoing air).

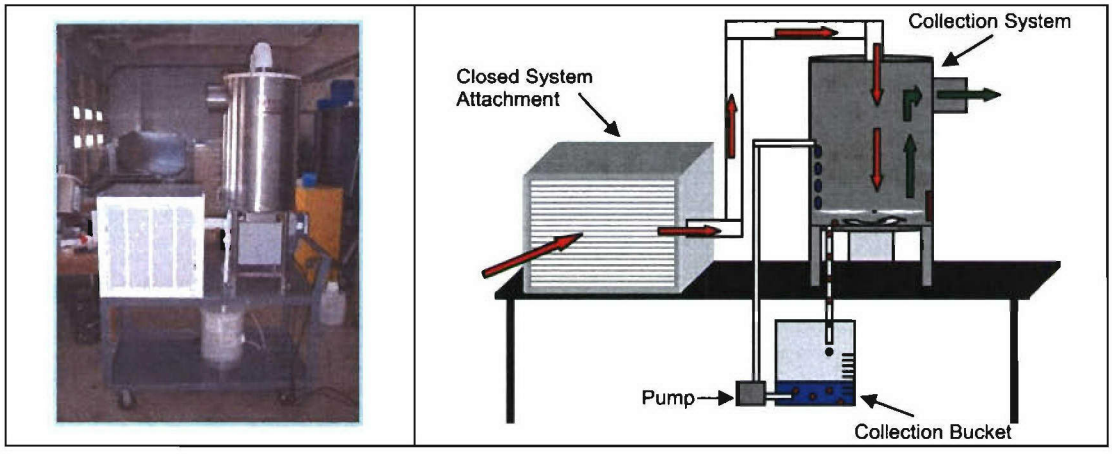

Figure 78: a) Actual image of the ISAVAC system b) Schematic of the ISAVAC system

The water that is discharged to the drain is collected in a collection bucket, where it is then recycled by being pumped back up into the system, therefore concentrating the collected solution over time. The square box with the vent and HEPA filter is called the closed system attachment. The attachment is connected to the input opening of the ISAVAC system by a series of piping that is connected to a clear acrylic box with a 2 micron HEPA filter and a vent. The air is drawn in the vent and passes through the HEPA filter into the box and on through the piping to the ISAVAC's main compartment. This attachment can be easily removed from the collection system based on the type of study being conducted. The importance of this attachment is that particles 2 micron and larger cannot pass through the filter, and thus the air that enters the box is for the most part contaminant free. We can then only collect nonpathogenic bacteria that we purposely introduce into the system to create a control collection study. For real world applications, the Closed System Attachment would simply be taken off, and the inlet could be connected to any building air handling system that would allow for collection of biologics.

A number of studies were conducted to determine the viability of the ISAVAC system to operate as a bio-collection system. These studies included evaporation rate of the liquid medium used to capture particulates, particle collection of known analytes, as well as the size distribution of particulates that the system would be able to capture. It was noted that as the system ran over a period of time, even with recycling of the liquid medium into the collection chamber to concentrate the solution, that the volume of the liquid medium decreased. Therefore, a study was conducted to determine the evaporation rate of the liquid medium. Autoclaved deionized water was used as the liquid medium because the desired source of analyte being captured would be strictly collected from the air environment for a controlled study. It was noted that the humidity at the exit of the system was rather high and therefore autoclaved deionized water used to collect

the airborne particulates evaporated at a certain rate. 10.25 L of the autoclaved deionized water was added to the collection bucket, and the system ran for 4 hours. The environment humidity, exhaust humidity, temperature, and amount of water in the collection bucket were monitored every 30 minutes.

The rate of evaporation was determined by finding the slope of the volume of water versus time graph in figure 79, which was determined to be -2.085 L/hr. A high rate of evaporation meant that the particulates that were being captured were evaporating at a large rate and therefore the concentration of the final collected solution was not very effective. We determined that a large amount of the water used to collect the particulates was evaporating due to the humidity caused at the exit of the system. It was determined after further review that an isothermal condenser would need to be installed on the output of the system to decrease the rate of evaporation.

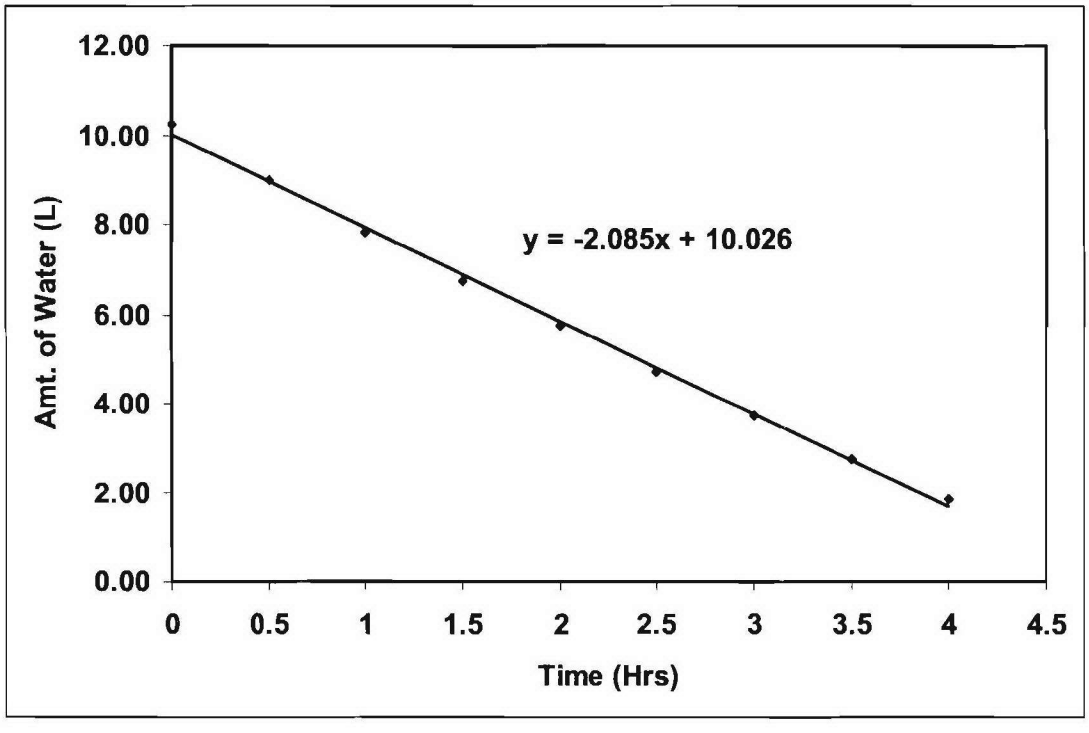

Figure 79: Evaporation rate of the system collection solution

For the study that was conducted in a closed environment to determine collection of known bacteria, 4.25 L of autoclaved deionized water was added to the collection bucket and kept constant throughout the study. The system ran for 6 hours with a 5 ml sample collected every hour including at time 0. After collection, 60 µL of each sample was plated on an LB agar. The remaining samples in the vials were then centrifuged for 5 minutes at 3000 rpm at 4°C where all but 100 µL of the supernatant was removed and the pellet was re-suspended, and 60 µL

was spread onto new LB plates. All plates were incubated overnight at 37.5°C and colony forming units were then counted.

This study was done to determine the number of colonies that could be grown from the collected solution after a 6 hour run. Each sample was plated on an LB agar and the remaining sample solution was centrifuged then plated to determine if centrifuging the samples would obtain a higher number of colonies per plate to get a more accurate count. Figure 80 shows bacteria collected by the system over time, and the growth of colonies on the LB agar showed that the system did in fact collect some form of bacteria. The graph also shows that the concentration of biological material in the collected solution decreased over time. This decrease in concentration is directly correlated to the loss of solution due to humidity issues with the system. The plates that contained the centrifuged samples had many more colonies than the plates with the non-centrifuged samples. Also, no colonies appeared at time "0" where the samples taken were of the autoclaved deionized water that had ran through the system for a short interval of time, which signified that at time "0" the system was clean prior to collection, and all microorganisms that were collected after time "0" had been collected by the system.

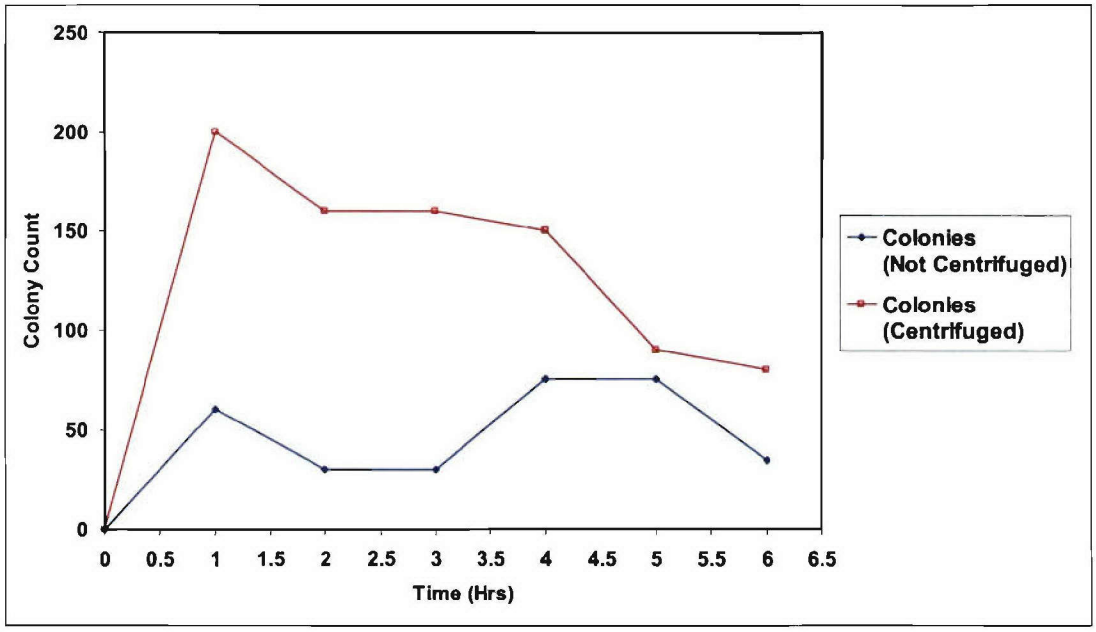

Figure 80: Bacteria collected by the system over time

Another similar study was conducted outdoors where 5.0 L of autoclaved deionized water was added to the collection bucket and kept constant throughout the study. To measure the effectiveness of the system, seven uncovered LB plates were set outside on a table next to the system as it was running. A comparison was made to determine the amount of growth of microorganisms on each plate that sat in an ambient outdoor environment compared to the rate of growth for plates that contained solution that was collected by the system. The system ran for 3 hours with a 10 ml sample collected every 30 minutes. After every 30 minutes that a sample was

collected, one LB plate that was placed out in ambient air was covered and refrigerated. After collection, the samples were centrifuged for 5 minutes at 3000 rpm at 4°C where all but 150 μL of the supernatant was removed and the pellet was re-suspended, and 60 μL was spread onto new LB plates for the collected solutions. All plates, including the plates set outside during collection, were incubated overnight at 37.5°C and colony forming units were then counted.

The number of colony forming units counted on the LB plates after incubating overnight at 37.5°C for both the plates that sat outside in ambient air and the plates that had the collected solution is shown in figure 81. It was noted that the number of colonies on each plate that had the collected solution was larger by a multiplied factor of approximately 830 compared the number of colonies on each of the time correspondent plates left out in ambient air. This clearly confirms that this system is far more effective in collecting microorganisms rather than trying to collect them without any sort of collection device.

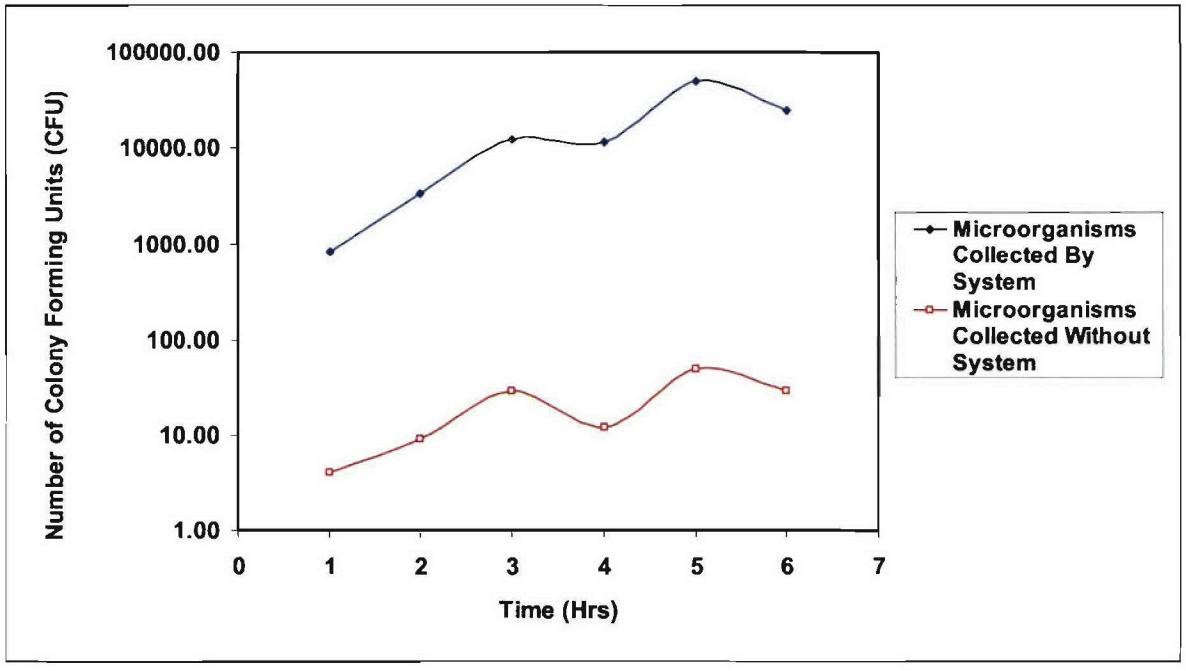

Figure 81: Number of colony forming units counted

The last study that was conducted was the controlled collection experiments, where Escherichia coli HB101 K-12 was used as a test microorganism. This strain of E. coli is classified as enteric meaning it is naturally found in the body's intestinal tract where it helps provide a source for Vitamin K and B-complex vitamins. This microorganism was chosen because its doubling time is about 20 minutes in ideal conditions, making it is easy to get large amounts of bacteria that we need, it is nonpathogenic, and its genome is well understood and easily modified.

For this study, 4.0 L of autoclaved deionized water was initially added to the collection bucket and kept constant throughout the study. The closed system attachment with a 2 micron HEPA filter was connected to the system and 140 μL of Escherichia coli in an LB solution at a concentration of 3.0 x 10^9 bacteria/ml was added to a small ultrasonic humidifier, which was placed inside the closed system attachment box. The ultrasonic humidifier was then turned on, allowing the bacteria to be aerosolized such that the collection system could collect the bacteria. This was also done to determine whether or not a biological particle of known size can be collected. Initially, 15 ml of water from the collection bucket was removed with a new disposable syringe and stored in a sterile 15mL conical vial. The system ran for 3 hours with a 15 ml sample collected every 20 minutes. After every sample was collected, the humidity and temperature of the room was recorded and autoclaved deionized water was added to the collection bucket to maintain a constant volume of 4.0 L. The samples were centrifuged for 5 minutes at 3000 rpm at 4°C where all but 100 μL of the supernatant was removed and the pellet was re-suspended, and 60 μL was spread onto LB plates. Plates were incubated overnight at 37.5°C and colony forming units were then counted.

Figure 82 does show that nonpathogenic E coli was captured by the system. It was determined that the lack of linearity from the graph of the collection can be attributed to the high rate of evaporation of the solution in the system. Some of the collected bacteria is re-aerosolized and then expelled from the system lowering the concentration of bacteria in the solution. Prior to conducting these experiments it was known that adding autoclaved deionized water to maintain a constant volume in the system would dilute the solution, which in turn would lower the concentration of bacteria. This study as well as the preceding studies confirmed this by showing that for longer time periods that the system ran, the lower the concentration of microorganisms in solution. As was stated earlier, installing an isothermal condenser on the output of the system and draining the condensed liquid back into the collection bucket.

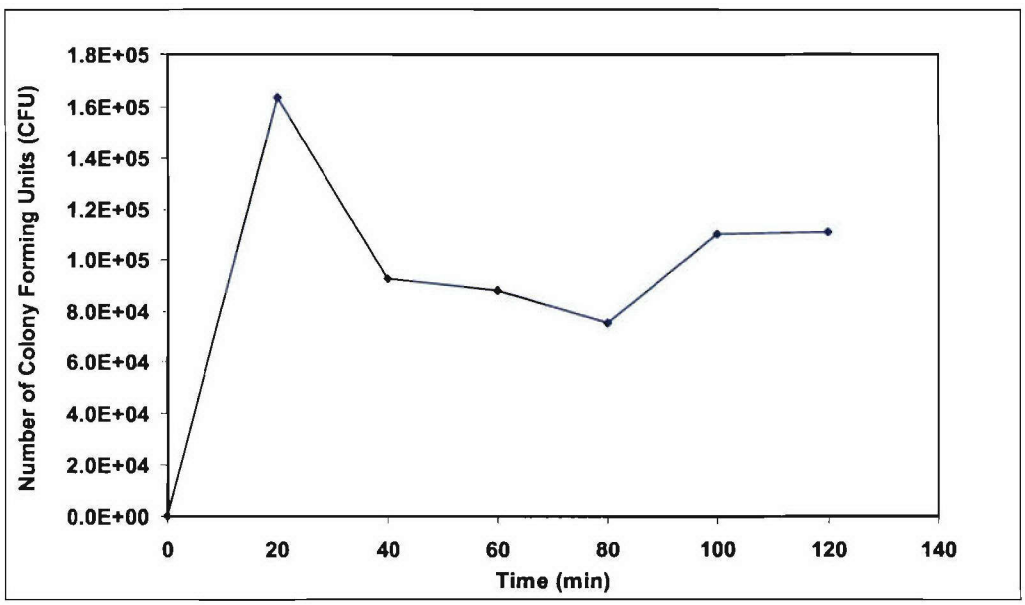

Figure 82: Number of E. Coli (CFU) per plate in the controlled collection experiment

As was mentioned earlier, the ISAVAC system is designed to be attached to the air handling system of building, but in the interest of collection in areas where a more portable collection system is required, work on a scaled down version of the ISAVAC was designed and built by ISAVAC Ideal Atmospheres, Inc. As shown in figure 83 below, a scaled down version approximately a third of the size of the original ISAVAC system was completed. Initial testing included mechanical, vibrational, and wear testing to ensure the performance of the system. Further studies to determine its viability as a collection system are yet to be conducted.

Figure 83: Scaled down version of ISAVAC system on tabletop

1.3.1 Conclusions

The intent of this project was to investigate the development of a broadband bio-detection platform. A number of technologies were investigated to create a bio-detection system that would have the ability to go from sample collection, to sample preparation, to detection, and finally analysis. To add, this entire process would be done autonomously. The bio-detection system was based on its unique nature of being bio-compatible. In order to develop a transducer output signal based on a biological detection event, a link needed to be created between the Au/PSA carbon and polymer material, and a number of different biological detection elements. It was demonstrated that a two biological sensing elements could be immobilized onto the carbon and polymer material; the first being antibodies, and the second being oligonucleotides. A new novel detection method based on a capacitor model to measure impedance as a function of oligonucleotide hybridization was also established.

The fabrication of the CPMEMS devices was also accomplished in this study, which would serve as the eventual broadband transducer that would bridge the biological sensing world to the electrical signaling world. These devices were fabricated in collaboration with BSI who worked on alternative methods of fabricating the CPMEMS devices. A unique sense and release technology was also investigated by Crosslink who worked with a conductive polymer (polypyrrole) to embed different molecules for release purposes. It was demonstrated through the release of dyes that this technology has the potential of being integrated into the broadband CPMEMS detection platform to serve as a second detection signal or as an analysis tool in the event of bio-detection. Lastly, a bio-collection system was developed to capture biological particles from air and concentrate them in solution for detection.

1.4 References

1. J. Thaysen, "BioMEMS Materials and Fabrication Materials", 3rd Annual BioMEMS & Biomedical NANO Tech; Official meeting for the International Society for BioMEMS and Biomedical Nanotechnology (ISBBN), Sep. 6-8, 2002.

2. V. Svorcik, V. Rybka, V.Hnatowicz, L. Bacakova, V. Lisa, and F. Kocourek, "Surface Properties and Biocompatibility of Ion-Implanted Polymers", J. Mater. Chem., 1995, 5(1), 27-30.

3. Y.Q. Wang, D.S. Robey, M.G. Moss and R.E. Giedd, "Piezoresistivity in Ion Implanted Polymer Films", Mat. Res. Soc. Symp. Proc., 316, (1994), pg. 349-354.

4. M. Baszun, and D. Grzda, "Applications of shear horizontal surface acoustic waves to thin film evaluation", Journal of Materials Processing Technology, Volume 133, Issues 1-2, 1 February 2003, Pages 34-38

5. Y.Q. Wang, D.S. Robey, M.G. Moss and R.E. Giedd, "Piezoresistivity in Ion Implanted Polymer Films", Mat. Res. Soc. Symp. Proc., 316, (1994), pg. 349-354.

6. M. Baszun, and D. Grzda, "Applications of shear horizontal surface acoustic waves to thin film evaluation", Journal of Materials Processing Technology, Volume 133, Issues 1-2, 1 February 2003, Pages 34-38

7. Y.Q. Wang, D.S. Robey, M.G. Moss and R.E. Giedd, "Piezoresistivity in Ion Implanted Polymer Films", Mat. Res. Soc. Symp. Proc.Vol. 316, pg. 349-354, 1994.

8. M. Baszun, and D. Grzda, "Applications of Shear Horizontal Surface Acoustic Waves to Thin Film Evaluation", Journal of Materials Processing Technology Vol. 133, pg. 34-38, 2003.

9. Peterson, A., Heaton, R., Georgiadis, R., " The effect of surface probe density on DNA hybridization", Nucleic Acids Research 29 (24), 5163-5168, 2001.

10. J. Hone, B. Batlog, Z. Benes, A. T. Johnson, J. E. Fischer, "Quantized Phonon Spectrum of Single-Wall Carbon Nanotubes", Science Vol. 289, pg. 1730, 2000.

11. R.H. Baughman, A.A. Zakhidov, and W.A. de Heer, "Carbon Nanotubes-The Route Toward Applications", Science Vol. 29, pg. 787-792, Aug 2002.

12. S. Ramesha, E. Sominskab and A. Gedanken, "Synthesis and characterization of submicrospherical silica particles uniformly coated with nanocrystalline yttria stabilized zirconia", Ultrasonics Sonochemistry, Volume 9, Issue 2, Pages 61-64, March 2002.